University of Szeged

Faculty of Pharmacy

Department of Pharmaceutical Technology

Head: Prof. Dr. Piroska Szabó-Révész D.Sc.

Ph.D. thesis

APPLICATION OF WET MILLING TECHNIQUES TO PRODUCE MICRONIZED AND NANONIZED DRUG PRE-DISPERSIONS FOR THE DEVELOPMENT OF INTRANASAL FORMULATIONS

By

Csilla Bartos

Pharmacist

Supervisors:

Prof. Dr. Piroska Szabó-Révész D.Sc.

and

Dr. Habil. Rita Ambrus

SZEGED

2016

CONTENTS

PUBLICATIONS RELATED TO THE SUBJECT OF THE THESIS

1. Csilla Bartos, Rita Ambrus, Péter Sipos, Mária Budai-Szűcs, Erzsébet Csányi, Róbert Gáspár, Árpád Márki, Adrienn B. Seres, Anita Sztojkov-Ivanov, Tamás Horváth, Piroska Szabó-Révész

Study of sodium hyaluronate-based intranasal formulations containing micro- or nanosized meloxicam particles

Int. J. Pharm. 491 198-207 (2015) IF: 3.650

2. Csilla Bartos, Ákos Kukovecz, Rita Ambrus, Gabriella Farkas, Norbert Radacsi, Piroska Szabó-Révész

Comparison of static and dynamic sonication as process intensification for particle size reduction using a factorial design

Chem. Eng. Process. 87 26–34 (2015) IF: 2.071

3. Bartos Csilla, Ambrus Rita, Szabóné Révész Piroska

Szonikus kavitáció alkalmazása hatóanyag szemcseméretének csökkentésére

Acta Pharm. Hung. 84 131-137 (2014) IF: -

4. Cs. Bartos, P. Szabó-Révész, R. Ambrus

Optimization of technological parameters by acoustic cavitation to achieve particle size reduction

Farmacia Nr.1, 2014 IF: 1.005

5. Levente Kürti, Róbert Gáspár, Árpád Márki, Emese Kápolna, Alexandra Bocsik, Szilvia Veszelka, **Csilla Bartos**, Rita Ambrus, Monika Vastag, Mária A. Deli, Piroska Szabó-Révész

In vitro and *in vivo* characterization of meloxicam nanoparticles designed for nasal administration

Eur. J. Pharm. Sci. 50 86-92 (2013) IF: 3.350

6. Ambrus R., **Bartos Cs**., Szabóné Révész P.

Eljárási paraméterek optimalizálása szónikus kavitáció alkalmazásával hatóanyag szemcseméret csökkentése céljából

Acta Pharm. Hung. 81 51-58 (2011) IF: -

OTHER PUBLICATIONS

1. Tamás Horváth, **Csilla Bartos**, Alexandra Bocsik et al.

Cytotoxicity of different excipients on RPMI 2650 human nasal epithelial cells

Acta Chim. Slov. (under revision)

2. Bartos Csilla, Kata Mihály

Szabadkai gyógyszertárak története, 1780-2011

Bácsország, 2013.

ABBREVIATIONS

API	active pharmaceutical ingredient
AUC	area under the (time–concentration) curve
C_d	drug concentration
C_{VR}	constant characteristic of the material
D	milling chamber diameter
D10	particle diameter below which 10% of the sample volume exists
D50	particle diameter below which 50% of the sample volume exists
D90	particle diameter below which 90% of the sample volume exists
DSC	differential scanning calorimetry
E	energy
$E_{1\text{-}2}$	specific energy
η_b	bioadhesive viscosity component
FT-IR	Fourier transform infrared spectroscopy
G'	storage modulus
G"	loss modulus
HA	sodium hyaluronate
HPLC	high-performance liquid chromatography
IBU	ibuprofen
IS	internal standard
J	API flux
K_p	permeability coefficient
m/v (%)	mass/volume percentage concentration
MEL Dyn.	meloxicam sonicated by dynamic process
MEL Stat.	meloxicam sonicated by static process
MEL	meloxicam
MEL-PVA PM	meloxicam–poly(vinyl alcohol) physical mixture
MeOH	methanol
micro MEL spray	nasal spray containing micronized meloxicam
micro MEL	micronized meloxicam, prepared by a combined technique
nano MEL spray	nasal spray containing nanonized meloxicam
nano MEL	nanonized meloxicam, prepared by a combined technique
NSAID	non-steroidal anti-inflammatory drug

P	power output
PBS	phosphate buffer solution
Poloxamer	Poloxamer 188, poly(ethylene)–poly(propylene glycol)
PS	particle size
PSA	particle size analysis
PSD	particle size distribution
PVA	poly(vinyl alcohol)
PVP	poly(vinylpyrrolidone)
raw MEL spray	nasal spray containing raw meloxicam
SEM	scanning electron microscopy
Solutol	Solutol HS 15, poly(ethylene glycol 15-hydroxystearate)
SPE	solid-phase extraction
SSA	specific surface area
t	exposure time
T_g	glass transition temperature
Tween	Tween 80, poly(oxyethylenesorbitan monooleate)
V_p	processed volume
w/v (%)	weight/volume percentage concentration
x	uniform particle diameter
XRPD	X-ray powder diffraction
ZrO_2	zirconia

1. INTRODUCTION

Particle design techniques are widely used to modify the physico-chemical and biopharmaceutical properties of active pharmaceutical ingredients (**API**s) (Maghsoodi et al., 2008). Particle engineering techniques that control the crystal size distribution and morphology and make use of different additives can offer improvements as concerns the solubility, rate of dissolution and permeability of poorly water-soluble drugs and can open up new, alternative administration routes (Pomázi et al., 2011, Ghosh et al., 2012, Maggi et al., 2013).

The various size reduction techniques include bottom-up approaches, where micro- or nanoparticles are built up from dissolved drug molecules, and top-down methods, where the raw material is subsequently broken down by using milling methods until micro- or nanosized particles are produced (Ambrus et al., 2009). Milling belongs among the disintegration procedures. Dry and wet milling can be distinguished. Microparticles may be produced by dry or wet milling, with or without the use of excipients. For the preparation of nanoparticles (in either dry or wet milling), the usage of additives is required, because the processes are controlled by surface forces and, if the particles are not stabilized, they may coagulate because of the high particle mobility (Paltonen and Hirvonen, 2010). For wet milling, additives are essential, independently of the preparation of micro- or nanoparticles. Through wet milling, the preparation of pre-dispersions is possible, while intermediate solid-state products (powders) can be prepared by means of drying, and the development of liquid or semi-solid formulations (sprays and gels) is feasible directly from pre-dispersions.

Intranasal administration is a possible route for the delivery of drugs to reach the systemic circulation (Prommer and Thompson, 2011). It offers certain advantages, including rapid absorption, avoidance of the hepatic first-pass metabolism and gastrointestinal side-effects, and painless application, with sterility not a requirement (Meng et al., 2014). In the case of intranasally administered formulations containing a suspended drug, particle size (**PS**) distribution (**PSD**) is a determining factor. In order to achieve a systemic effect, intranasal compounds can be mixed with different additives so as to ensure a longer residence time, better mucoadhesion (Horvát et al., 2009) and increased permeability (Chunga et al., 2010). Pharmaceutical formulations delivered intranasally may be liquid (spray) (Baumann et al., 2012), gel (Osth et al., 2002) or powder forms.

It is a major challenge in pharmaceutical technology to find organic solvent-free, cost-effective, time-saving PS reduction techniques which are suitable for preparation of the products (pre-dispersions) of the same quality, built into the process of production of

pharmaceutical formulations. This thesis reports the development of two wet milling techniques with the aim of decreasing the PSs of poorly water-soluble drugs to the micro or nano range (in the presence of polymer as aggregation inhibitor).

2. THEORETICAL BACKGROUND

2.1. Milling techniques

Milling is a technique commonly applied to produce micro- or nanosized drug crystals in order to increase the dissolution rate and absorption, and hence the bioavailability of poorly-soluble materials. According to the Noyes–Whitney equation, reduction of the PSs of drug crystals increases the specific surface area (**SSA**), which can improve the rate of dissolution of a drug (Noyes and Whitney, 1897). There are many different types of milling techniques; dry and wet milling can be distinguished.

2.1.1. Dry milling

Dry milling is carried out at low moisture contents of the drug. A number of dry milling possibilities are known; the survey of these in Table 1 is non-exhaustive. Techniques for dry milling are usually used for micronization (Boudriche et al., 2014). In this case, the Rittinger theory describes the PS reduction produced relative to the energy (*E*) input of milling: the new surface area generated is directly proportional to the *E* required for the PS reduction. As the surface area of a quantity of particles of uniform diameter *x* is proportional to 1/*x*, the *E* required for PS reduction is therefore also proportional:

$$E_{1\text{-}2} = C_{VR}\left(\frac{1}{x_2}\right) - \left(\frac{1}{x_1}\right)$$

where $E_{1\text{-}2}$ is the specific energy, and C_{VR} is a constant characteristic of the material (Temmerman et al., 2013). In general, additives are not required for micronization (Liu et al., 2014). Nanonization can be achieved on the use of an additive and a long milling time, but in this case changes may occur in the physico-chemical structure of the drug. The dry milling process has both advantages and disadvantages (Table 2).

Table 1 Dry milling techniques (Sushant and Archana, 2013)

Milling techniques	Milling device	PS (μm)
Cutting machine	Cutter mill	100-80 000
Milling based on compression	Roller mill	50-10 000
Ball milling	Planetary ball mill	1-2 000

Table 2 Advantages and disadvantages of dry milling (Manfredini & Schianchi, web reference 1)

Advantages	Disadvantages
Total recovery of production wastes	Dust production
Minor consumption of water	Adhesion
Practical to run and service	Electrostatic charge
Elimination of the additional costs needed for the appropriate management of slurries	
Stability of the API	

Ball milling

Ball milling is usually used for the dry micronization of drugs, in order to enhance their rates of dissolution. Apart from its comminution function, ball milling also serves as an intensive mixing technique capable of producing co-ground drug–excipient mixtures (Loh et al., 2015). Furthermore, the preparation of nanosized particles is also possible through ball milling. Our research group has reported results on dry nanonization through the application of a planetary ball mill in the presence of additives with a long milling time (2 h). The presence of additives and the increase of their amount reduced the collision energy required for the nanonization of meloxicam (**MEL**) (Table 3) (Kürti et al., 2011, Kürti et al., 2013).

Table 3 Milling energetic map of the experiments performed

Cumulative collision energy transferred (kJ/g) in the cases of different MEL to additive ratios					
Rotation speed (rpm)	**Collision frequency (1/s)**	**No additive**	**1:0.5**	**1:1**	**1:2**
200	240	8.56	5.71	4.28	2.85
300	360	28.89	19.27	14.45	9.63
400	480	68.50	45.67	34.25	22.83

The ball mill consists of a chamber filled with balls constructed from ceramic, agate, silicon nitride, zirconia (**ZrO_2**), etc. The drug to be milled is put into the chamber, which is made to rotate, vibrate or perform planetary motion. The movements of the chamber result in

the balls cascading or moving in a pattern, colliding with each other and with the inner walls of the chamber. The reduction in PS of the drug particles results from the impact they receive from the balls and attractive forces arising from the movement of the balls relative to each other. The quantities of the balls and drugs to be milled are the determining factor as concerns the effectiveness of the milling. The total volume of the chamber is usually one-third filled by balls and one-third by drug materials (Figure 1). In the case of a rotating chamber, rotation is usually carried out at 55-75% of the critical speed at which the balls adhere to the walls of the milling chamber as a result of the centrifugal force. The critical speed may be estimated via the following equation:

critical speed = $42.3/\sqrt{D}$ (King, web reference 2)

where D is the diameter of the milling chamber (Juhnke et al., 2012).

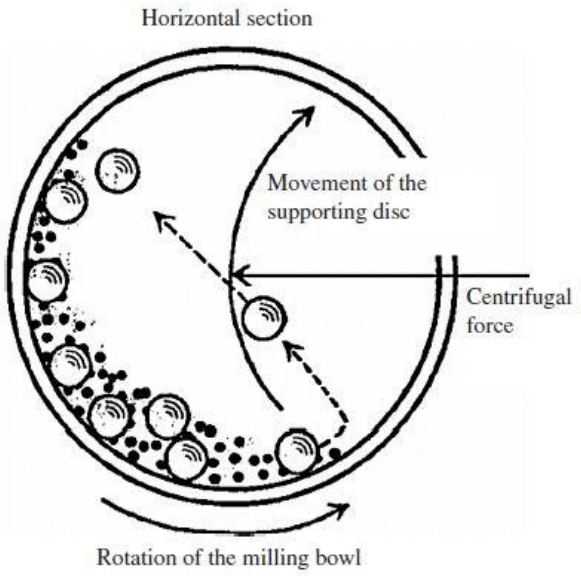

Figure 1 Schematic view of the ball mill (W. Cao, web reference 3)

2.1.2. Wet milling

In many cases, wet milling is required to reach the expected PS of a drug. In the wet milling procedure, a sufficiently concentrated dispersion of drug particles in an aqueous or non-aqueous liquid medium is treated. Some wet milling opportunities are presented in Table 4. Wet milling is applicable for micronization (Pomázi et al., 2013), but is usually used for nanonization (Hou et al., 2007, Bujňáková et al., 2015). For wet milling, the usage of additives is required to prevent the aggregation of the milled drug particles and to inhibit particle growth (ripening) during milling/storage (Niwa et al., 2011). Drug suspensions produced by wet milling can be transferred into the related drug products, such as capsules, granules, tablets, injectables, sprays

and gels (Wang et al., 2013, Junyaprasert and Morakul, 2015). Table 5 lists some advantages and disadvantages of wet milling (Swarbrick, 2013). Certain scaling-up techniques are detailed below.

Table 4 Wet milling techniques (Fan et al., 2009, Pomázi et al., 2013, Swarbrick, 2013, Pawar et al., 2014)

Milling techniques	Milling device	PS (μm)
”Rotor/stator” milling	Colloid mill Toothed high-shear inline mixers Cone mill	1-50
Milling based on cavitation	High-pressure homogeniztaion	1-20
Pearl milling	Pearl mill	0.02-200

Table 5 Advantages and disadvantages of wet milling

Advantages	Disadvantages
Increased mill capacity	Increased wear of the grinding medium
Lower energy consumption	Drying stage after milling
Closed system (without dust production)	Hazards of corrosion
Easier handling of materials	Extra water needs
Intermediate product	Stability of API

Acoustic cavitation

During the sonication process, the ultrasound waves that form in the liquid media result in alternating high-pressure and low-pressure cycles, with rates depending on the frequency. In the low-pressure cycle, the high-intensity ultrasound waves evolve small gas- or vapour-filled bubbles (cavities) in the liquid. When the bubbles reach a volume at which they can no longer absorb energy, they collapse violently during a high-pressure cycle. This phenomenon is called ultrasonic cavitation (Figure 2). It has been proven that, when ultrasound technology is applied in the frequency range 20–100 kHz, the implosion of vacuum bubbles can induce a PS reduction (Suslick, 1998). The use of ultrasound is a common technique to promote chemical reactions (Patil et al., 2013). As regards pharmaceutics, power ultrasound can be applied for emulsification and to investigate the sedimentation of emulsions and suspensions (Benes et al., 1998, Behrend and Schubert, 2000). Supercritical, solvent diffusion (Hatkar and Gogate, 2012) and melt emulsification are well-known bottom-up methods in the field of sonocrystallization

for solving problems of drug solubility (Ambrus et al., 2012). The application of ultrasound can readily be scaled up; as an example, sonification is successfully applied at an industrial level for the preparation of metal nanoparticles (Li et al., 2013). The disintegration of drug particles (top-down approach) has not been widely investigated so far with the aim of improving the properties of drugs, and acoustic cavitation is therefore a new possibility for controlling the crystal size distribution and morphology of drugs, primarily with the intent of PS reduction (Patil and Pandit, 2007, Raman and Abbas, 2008). It has the ability to erode and break down particles and to increase the SSA of crystals (Sandilya and Kannan, 2010).

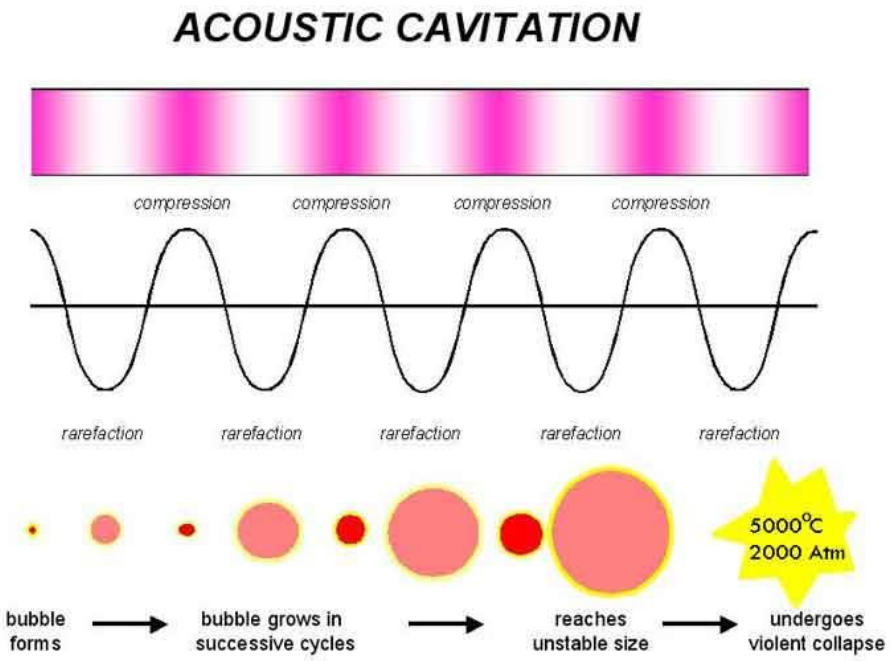

Figure 2 Schematic illustration of acoustic cavitation (Electrowave Ultrasonics Corporation, web reference 4)

Ultrasonic liquid processing is influenced by a number of parameters (amplitude, pressure, temperature and concentrations of compounds). The effect of the process may be determined as a function of the E per processed volume (V_p):

$$\text{effect} = f\,(E/V_p)$$

where E is the product of the power output (P) and the exposure time (t):

$$E\,[Ws] = P\,[W] * t\,[s]$$

Additionally, the value of *P* per surface area of the sonotrode of an ultrasonic unit depends on the parameters as described by Hielscher (web reference 5). There are two sonication routes for wet grinding to achieve a PS reduction: the static method, which means that a sample at rest is sonicated, and the dynamic method, which allows continuous circulation of the sample by means of a pump during the sonication. These two methods are appropriate for the PS reduction of materials with different physico-chemical properties (Bartos et al., 2014). The production of intermediates (as pre-dispersions) and powder products (after drying) is carried out by applying a short-term ultrasound *E* input.

Media milling

Wet stirred media milling has proven to be a robust process for the production of nanoparticle suspensions of poorly water-soluble drugs (Afolabi et al., 2014). In this method the nanosuspensions are produced through the use of high-shear media mills or pearl mills (Figure 3). Media mills consist of a milling chamber, a milling shaft and a recirculation chamber. Media milling is a continuous process wherein the drug suspension is pumped through the milling chamber to effect PS reduction of the suspended material. The milling chamber is charged with the milling media, dispersant medium, drug and stabilizer, and the milling media or pearls are then rotated at a very high shear rate. The milling medium consists of glass, zirconium oxide or highly cross-linked polystyrene resin (Patravale et al., 2004). The physical characteristics of the resulting nanocrystals depend on the number of milling pearls, the amounts of drug and stabilizer, and the milling time, speed and temperature (Chen et al., 2011).

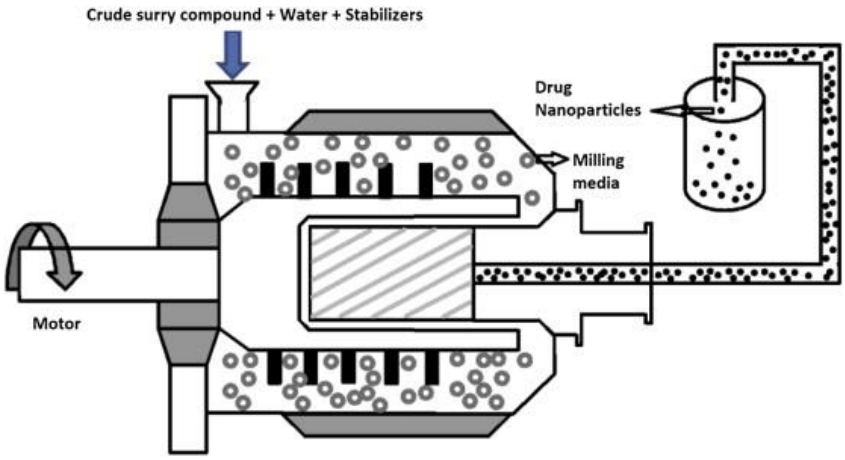

Figure 3 Schematic representation of the pearl milling process (Loh et al., 2015)

2.1.3. Combination milling techniques

To overcome the limitations of the conventional PS reduction technologies for poorly-soluble drugs, new combinational methods have been developed for the production of ultrafine suspensions. Combinative technologies are a relatively new approach to improve the effectiveness of PS reduction and to reduce the process times. In general, they can be described as a combination of a bottom-up process (the building-up of particles) (Blagden et al., 2007, Bund and Pandit, 2007, Bakar et al., 2009) followed by a top-down technology (disintegration) (Salazar et al., 2012, Möschwitzer, 2013, Vivek et al., 2014). This method involves two steps of PS reduction. There is also a possibility for the combination of dry and wet milling in one step, but literature data relating to the application of this combined method are lacking. Retsch GmbH has made a recommendation for the combination of planetary ball milling, as dry milling, and pearl milling, as wet milling (Retsch®, web reference 6).

2.2. The role of additives in wet milling

In dry nanonization, and wet micronization and nanonization, the application of additives is required in order to retain the individuality of the particles. Micro- and nanoparticles with high SSA and high free *E* are controlled by surface forces and, if the particles are not stabilized, they may coagulate because of the high particle mobility (Friedrich et al., 2006). Stabilizers are added to compensate the extra free *E* of the newly created surfaces, thereby preventing the aggregation of milled drug particles and inhibiting particle growth (ripening) during milling/storage (Bilgili and Afolabi, 2012). The degree of compensation required is related to the interactions between the drugs and stabilizers. For effective stabilization and a reasonable processing time, strong and fairly fast adsorption is necessary, with full coverage and slow desorption. If the amount of the stabilizer is too low, particles tend to aggregate, while concentrations that are too high promote Ostwald ripening (Peltonen and Hirvonen, 2010).

The choice of stabilizer is specific for each drug candidate and each formulation procedure. Polymers and surfactants are commonly used as stabilizers to impart physical stability to the suspensions produced by the wet milling of poorly water-soluble drugs, which singly or in combination help to minimize the agglomeration of suspended particles via electrostatic and steric mechanisms. In these processes, aqueous suspensions containing drug particles and dissolved stabilizers (polymer and/or surfactant) are treated. Different additives are used to stabilize these particles: poly(vinylpyrrolidone) (PVP), Poloxamer^R (Poloxamer 188 = poly(ethylene)–poly(propylene glycol), polysorbate (Tween 80^R = poly(oxyethylenesorbitan monooleate)), Solutol^R (Solutol HS 15 = poly(ethylene glycol 15-hydroxystearate)), PVA

(poly(vinyl alcohol)), etc. (Paltonen and Hirvonen, 2010). Some of them are listed in Table 6. The application of additives allows the preparation of stable pre-dispersions with optimum drug PS, which can be used for the development of further pharmaceutical formulations.

Table 6 Stabilizers (Friedrich et al., 2006, Ghosh et al., 2011)

Name	Feature
PVP K-25	protective layer-forming polymer
Poloxamer 188	non-ionic surfactant
Tween 80	emulsifier and solubilizer
Solutol HS 15	non-ionic solubilizer
PVA	protective layer-forming polymer

2.3. Formulation of nasal dosage forms

Intranasal administration is a potential way to deliver drugs into the systemic circulation as an alternative route for some therapeutic agents (Fortuna et al., 2014). The development of nasal formulations has opened up new areas of indication and many delivery problems can be solved. The main reasons for this are the high permeability, wide absorption area, and porous and thin endothelial basement membrane of the nasal epithelium. Pharmaceutical formulations delivered intranasally may be powder (Kaye et al., 2009), gel (Osth et al., 2002) or liquid (drops and sprays) (Baumann et al., 2012) forms. The advantages of a nasal spray include the ease of use for the patients and the possibility of self-administration without the assistance of a physician (Marttin et al., 2000). In the case of spray formulations, drugs in dissolved form can achieve the fastest therapeutic effect, and they have to be in dissolved form for the absorption of drugs (dissolution of drug on the mucosa in the case of suspensions) (Sosnik et al., 2014). However, low aqueous solubility is a common characteristic in current biopharmaceutics, and over 40% of new chemical entities exhibit poor solubility (Beig et al., 2012). Difficulties are therefore liable to occur in the event of the preparation of drug solution-containing formulations. This problem may be solved through the preparation of a pre-dispersion of a poorly-soluble drug with a suitable technique so as to reach the optimum PS for high bioavailability and, following this, the development of a liquid formulation.

For the preparation of intranasal formulations in order to achieve a systemic effect, intranasal compounds can be mixed with different additives in order to ensure the pH (compliance with the nasal cavity), viscosity (Furubayashi et al., 2007), a longer residence time, better mucoadhesion (Horvát et al., 2009), increased permeability (Chunga et al., 2010), and in

some cases controlled release of a drug. Because of the rapid mucociliary clearance in the nasal cavity, viscous, mucoadhesive formulations are needed in order to prolong the contact time with the nasal mucosa, thereby enhancing the delivery of the drugs (Hasçiçek et al., 2003). Different agents are used to increase the viscosity (cellulose derivates) and the mucoadhesive strength (carbomers, chitosans, lectins, thiomers, alginate poly(ethylene glycol acrylate) or Poloxamer) in the intranasal formulation (Pathak, 2011, Anand et al., 2012). One of the most important biocompatible, mucoadhesive agents is sodium hyaluronate (**HA**). This natural anionic polysaccharide has excellent mucoadhesive capacity (Liao et al., 2005), high biocompatibility and low immunogenicity (Ding et al., 2012). Besides its mucoadhesive properties, it may enhance the absorption of drugs and proteins via the mucosal tissues (Lim et al., 2000). To ensure controlled drug delivery, responsive polymers (α-cyclodextrins, acrylic acid, hydroxyethyl acrylate, PVP, and PVA) may be used, which regulate the release of drugs (Bajpai et al., 2008).

The solubility, the rate of dissolution and the permeability of drugs are of great importance (Zelkó and Süvegh, 2005), and reduction of the PS to the micro or nano range is therefore the strategy of first choice with the aim of increasing the bioavailability of poorly-soluble drugs (Sinha et al., 2013, Anarjan et al., 2015). Nanoparticles are controlled by surface forces and, if the particles are not stabilized, they may coagulate because of the high particle mobility. Different additives are used to stabilize these particles: polysorbate, hydroxypropyl methylcellulose, Poloxamer, PVP, etc. (Paltonen and Hirvonen, 2010). PVA is frequently used as a stabilizer, coating the particles and promoting their separation from each other.

3. AIMS

The aim of my research work was to investigate new possibilities in the field of wet milling techniques through study of the PS reduction effect. Via the preparation of pre-dispersions, different organic solvent-free wet milling techniques were compared (sonication and combined wet milling) and the process parameters affecting the PS and their influence on the physico-

chemical and biopharmaceutical properties of drugs were determined. Poorly water-soluble, crystalline, non-steroidal anti-inflammatory model drugs (**NSAID**s) (MEL and ibuprofen-**IBU**) were chosen for PS reduction investigations. Intranasal formulations as sprays containing suspended drugs were developed from selected drug pre-dispersions and investigated.

The main steps in the experiments were as follows:

i. The use of acoustic cavitation, an organic solvent-free, static wet milling technique, as a new approach for PS reduction (preliminary studies with IBU and MEL).
ii. Comparisons of the PS reduction effects of static and dynamic sonication as process intensification through use of a factorial design (MEL).
iii. Application of a combination of planetary ball and pearl milling for the production of pre-dispersions of micronized and nanonized MEL.
iv. The development and investigation of intranasal formulations directly from the pre-dispersions containing micro- or nanonized MEL.
v. Creation of a proposal for the production of an innovative intranasal dosage form for pain management through controlled drug delivery.

4. MATERIALS AND METHODS

4.1. Materials

MEL was obtained from EGIS Ltd. (Budapest, Hungary), and IBU from Aldrich Chemie (Deisenhofen, Germany) (Table 7).

The milling additives: PVP K-25 was purchased from ISP Customer Service GmBH (Köln, Germany), Poloxamer and Solutol from BASF (Ludwigshafen, Germany) and Tween from Hungaropharma (Budapest, Hungary). PVA 4-98 (M_w ~ 27,000) and HA (M_w = 1,400 kDa) were gifts from Gedeon Richter Plc. (Budapest, Hungary) (Table 8). Mucin (porcine gastric mucin type II) was from Sigma Aldrich (Sigma Aldrich Co. LLC, St. Louis MO, US).

Table 7 Properties of the active agents

	Meloxicam (MEL)	**Ibuprofen (IBU)**
Chemical structure	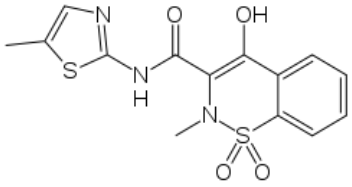	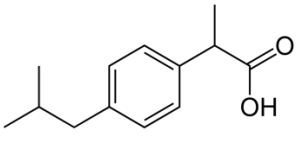

Chemical name	4-hydroxy-2-methyl-*N*-(5-methyl-2-thiazolyl)-2*H*-1,2-benzothiazine-3-carboxamide-1,1-dioxide	2-(4-(2-methylpropyl)phenyl)propanoic acid
Physical properties	a yellow powder poor solubility in water	a white crystalline powder poor solubility in water
Applications	a NSAID, a selective COX-2 inhibitor	a NSAID, a non-selective inhibitor of COX

Table 8 Milling additives and the mucoadhesive agent

	Chemical structure	**Synonyms**	**Physical properties**
PVP	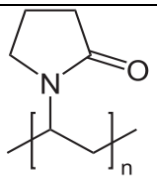	Povidone Kollidon	white-to-yellow-white powder soluble in water and polar solvents amorphous hygroscopic
Poloxamer	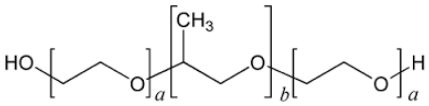	Lutrol Pluronic	white or almost white, waxy powder, microbeads or flakes very soluble in water and in alcohol
Tween	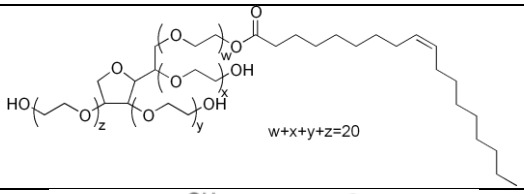	Polysorbate	viscouse yellow liquid soluble in water, ethanol, methanol, ethyl acetate
Solutol	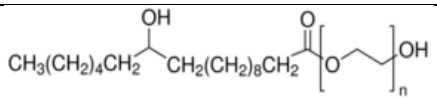	Kolliphor Macrogol(15)-hydroxystearate	Yellowish white paste soluble in water, ethanol and 2-propanol
PVA	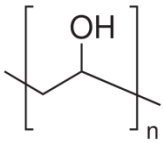	Mowiol	a white powder soluble in water, slightly soluble in ethanol semi-crystalline
HA	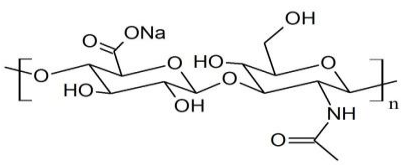		white powder soulble in water, in alcohol-water mixture

4.2. Methods

4.2.1. Preparation of formulations

4.2.1.1. Preliminary experiments of static sonication for PS reduction of IBU and MEL

A high-power ultrasound device (Hielscher UP 200 S Ultrasonic processor, Germany) operating at 200 W was applied as the *E* input in the sample preparation. The samples were sonicated at room temperature without cooling or by using an ice bath with a standardized temperature at around 18 °C. A range of ultrasonic amplitudes were tested in order to determine the optimum amplitude for 10, 20 or 30 min during the procedures (Table 9) (Figure 4). During the content optimization, different additives were applied. The effects of the concentrations of IBU and MEL on the PS decrease were also studied (Table 10) (Bartos et al., 2014).

Table 9 Parameters applied during the sonication of IBU and MEL

Temperature (°C)	room temperature, ice cooling
Amplitude (%)	30, 50, 70
Time (min)	10, 20, 30

Table 10 Applied additives; concentrations of IBU and MEL and their additives

Additives	PVP, Poloxamer, Tween, Solutol
Concentration (m/v (%)*)	1, 0.25 (IBU and MEL) 0.5, 0.25 (additive)

*m/v (%): mass/volume percentage concentration

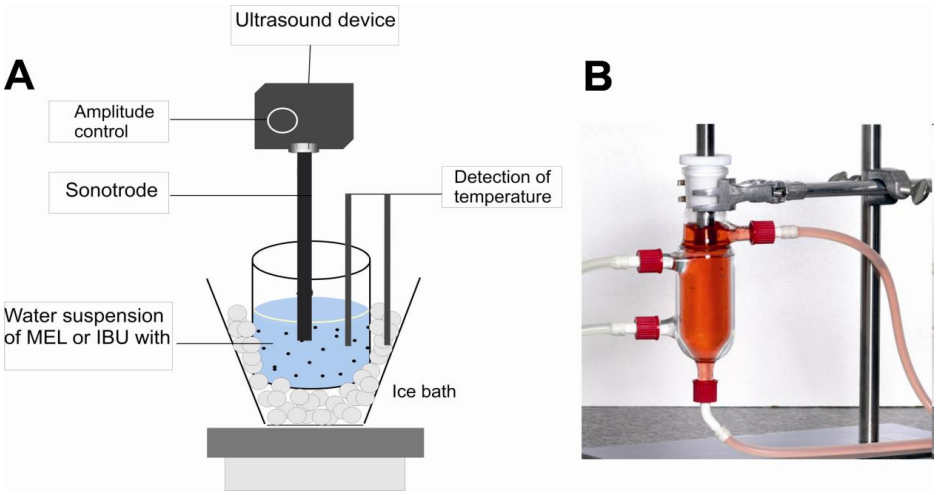

Figure 4 Scheme of PS reduction by static sonication (**A**) and double-walled flow cell for dynamic sonication (**B**)

4.2.1.2. Preparation of sonicated formulations for the comparison of static and dynamic sonication for reduction of the PS of MEL

MEL was chosen as a model drug for the comparison of static and dynamic sonication. In each sample, 0.5% of PVP was dissolved in an appropriate volume of water (Table 11). A high-power ultrasound device (200 W) was applied in the sample preparation. In the case of static sonication, samples at rest were treated. In the case of dynamic sonication, the samples were circulated continuously with a peristaltic pump (Heidolph PD 5006 Pump drive) in a double-walled flow cell (Flow Cell GD14 K) during the sonication (Figure 4). The temperature was set with a thermostat in both cases (Julabo, Germany). Through the use of different sonotrode positions, the immersed surface area of the ultrasonic horn could be changed (Bartos et al., 2015A).

Design of experiments for comparative studies of static and dynamic sonications

Six parameters were screened in the static sonication experiments, using a two-level fractional factorial design of resolution III. Here, the main effects are not confounded with each other, whereas they are confounded with two-factor interactions. This design is typically used for the rapid identification of the main effects governing the behavior of a multi-parameter system. High and low values for each parameter were set on the basis of our prior experience with similar tasks (reported in Table 11). Dynamic sonication experiments were run by screening five parameters, using the same experimental design type. High and low parameter values for the dynamic sonication experiments are presented in Table 11. All the experiments were run as triplicates.

Table 11 The applied sonication parameters

	Static sonication	**Dynamic sonication**
Volume (ml)	25; 100	100
Position*	0.25; 0.75	0.25
Pump speed (rpm)	-	50; 100
Concentration of MEL (mg/ml)	2; 18	2; 18
Temperature (ºC)	0; 36	0; 36
Amplitude (%)	30; 70	30; 70
Time (min)	10; 30	10; 30

*Position 0.25: the sonotrode was immersed to 25% of the total depth of the liquid
Position 0.75: the sonotrode was immersed to 75% of the total depth of the liquid

Adiabatic experiments were carried out to reveal the transmission efficiency of ultrasound *E* in the liquid (Figure 5). An appropriate volume of MEL-free 0.5 w/v (%) (weight/volume percentage concentration) PVP solution was used. Temperature was measured every 5 min up to 30 min during the sonication processing. The highest temperature rise (90 ºC) was observed in the small sample volume (25 ml) within 5 min. The dynamic and static methods were compared by using the following fixed parameters: 100 ml sample volume and 0.25 sonotrode position. In the case of static sonication, because of the higher *E* input, the temperature increase was higher after 10 min. When the dynamic method was used, the temperature increase was lower, due to the circulation in the vessel.

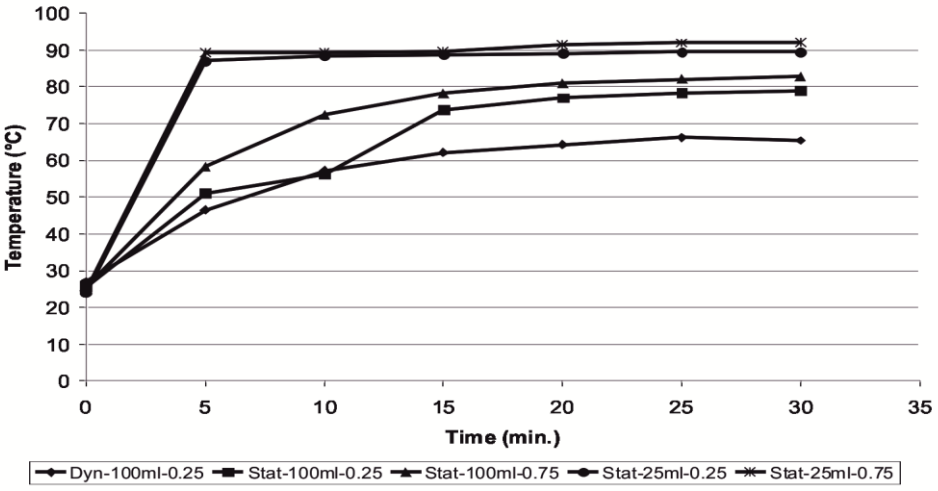

Figure 5 Results of the adiabatic investigations for an appropriate volume of MEL-free 0.5 w/v (%) PVP solution

4.2.1.3. Preparation of pre-dispersions with a combination of planetary ball and pearl milling for PS reduction

A wet milling technique (a combination of planetary ball and pearl milling) was employed. 0.5 g of PVA was dissolved in 17.5 ml of water, and the resulting solution was used as a dispersant medium in which 2.0 g of MEL was suspended. The resulting suspensions (10% drug content, 2.5% additive content) were wet-milled at 400 rpm in the milling chamber (50 ml) of a planetary ball mill (Retsch PM 100 MA, Retsch GmbH, Germany). The milling balls were 0.3 mm ZrO_2 beads. The effects of different pearl weights on the PS reduction were investigated. 10, 20, 50 and 150 g of beads were applied and milling was carried out without pearls as a benchmark. The milled suspensions were separated with a sieve with 150 µm mesh

size. Suspension sampling was carried out at milling times of 10, 20, 30, 40, 50, 60, 70, 80 and 90 (end of milling) min to perform the PS analysis (**PSA**).

4.2.1.4. Preparation of pre-dispersions for the development of an intranasal formulation

On the basis of preliminary experiments, a modified wet milling technique was employed to prepare the pre-dispersions. 0.5 g of PVA was dissolved in 17.5 ml of phosphate buffer solution (**PBS**) (pH 5.6, the pH of the nasal mucosa) and the resulting solution was used as a dispersant medium in which 2.0 g of MEL was suspended. The suspension was wet-milled in the planetary mill at 400 rpm for 10 or 50 min, using ZrO_2 beads (Table 12). The milled suspensions were separated from the beads by sieving.

Table 12 Pre-dispersions of MEL suspended in a dispersant medium containing PVA and PBS

Abbreviation in the text	Rotation speed (rpm)	Milling chamber volume (ml)	Milling time (min)
raw MEL pre-dispersion	-	-	0
micro MEL pre-dispersion*	400	50	10
nano MEL pre-dispersion**	400	50	50

*micro MEL: micronized MEL, prepared by a combined technique
**nano MEL: nanonized MEL, prepared by a combined technique

4.2.1.5. Preparation of intranasal formulations

The intranasal formulations were prepared directly from the pre-dispersions. 3.0 ml of each pre-dispersion was diluted with PBS (pH 5.6) in order to reach a concentration of 1 mg/ml MEL, and 0.15 g of HA was added; the final formulation therefore contained 5 mg/ml HA. The formulations were stored at 8 ºC in a refrigerator for 24 h. The intranasal viscous liquid formulations containing suspended MEL (referred to below as nasal sprays) were prepared and characterized according to an investigational protocol (Figure 6).

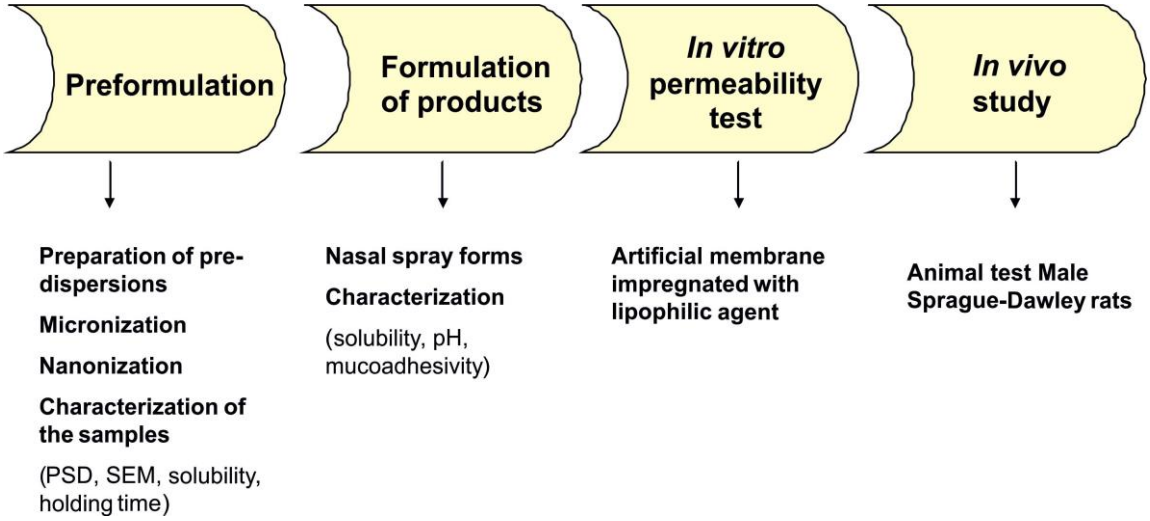

Figure 6 Protocol of the development and characterization of nasal sprays containing MEL

4.2.2. Physical-chemical investigations of solid-state products

Pre-dispersions prepared with different wet milling techniques were dried in order to obtain solid products for physical-chemical investigations.

4.2.2.1. Particle size analysis (PSA)

The volume-based PSD of drug in the samples was measured by laser diffraction (Mastersizer 2000) (Malvern Instruments Ltd, Worcestershire, UK) A dynamic laser light scattering method was used. Distilled water was applied as dispersant and the obscuration was in the range of 11-16 % for all measurements. In all cases, the volume-weighted PSD values as D10, D50 and D90 were evaluated (n = 3). The specific surface area (**SSA**) was derived from the PSD data. The assumption was made that all the particles measured were spherical.

4.2.2.2. Scanning electron microscopy (SEM)

After drying of the samples, the shape and surface characteristics of the samples were visualized by using SEM (Hitachi S4700, Hitachi Scientific Ltd., Tokyo, Japan). The samples were sputter-coated with gold–palladium under an argon atmosphere, using a gold sputter module in a high-vacuum evaporator, and the samples were examined at 15 kV and 10 μA. The air pressure was 1.3-13 MPa.

4.2.2.3. X-ray powder diffraction analysis (XRPD)

The physical state of drugs in the samples was evaluated by XRPD. The patterns were produced with an X-ray Diffractometer Miniflex II (Rigaku Co. Tokyo, Japan), where the tube anode was Cu with Ka = 1.5405 Å. The pattern was collected with a tube voltage of 30 kV and a tube current of 15 mA in step scan mode (4º / min). The instrument was calibrated by using Si. The investigated 2θ data were as follows: 13.22, 15.06, 26.46 and 26.67.

In case of combined milling, the crystallinity of the MEL in dried pre-dispersions was determined semi-kvantitatively via the mean of the decrease of the total area beneath the curve of 2 characteristic peaks (at 5.99 and 18.25 2θ) compared to the MEL-PVA physical mixture (**MEL-PVA PM**).

4.2.2.4. Differential scanning calorimetry (DSC)

DSC measurements were carried out with a Mettler Toledo DSC 821^e thermal analysis system with the STAR^e thermal analysis program V9.0 (Mettler Inc. Schwerzenbach, Switzerland). Approx. 2-5 mg of pure API or product was examined in the temperature range of 25-300 ºC. The heating rate was 5 ºC/min. Argon was used as carrier gas at a flow rate of 10 L/h.

4.2.2.5 Fourier transform infrared spectroscopy (FT-IR)

FT-IR spectra were recorded with a Bio-Rad Digilab Division FTS-65A / 896 FT-IR spectrometer (Bio-Rad Digilab Division FTS-65A/869, Philadelphia, USA) between 4000-400 1/cm, at the optical resolution of 4 1/cm (operating conditions: Harrick's Meridian SplitPea single reflection, diamond, ATR accessory). Thermo Scientific GRAMS/AI Suite software (Thermo Fisher Sciencific Inc. Waltham, USA) was used for the spectral analysis.

4.2.3. Investigation of pre-dispersions for nasal formulations

4.2.3.1. Solubility testing of MEL in the pre-dispersions

The MEL solubility in different pre-dispersions was determined. The pre-dispersions were stirred with a magnetic stirrer at 25 °C for 24 h and then filtered (0.1 μm, FilterBio PES Syringe Filter) (Labex Ltd., Budapest, Hungary), and the dissolved drug content was analysed spectrophotometrically (Unicam UV/VIS) (Thermo Fisher Scientific Inc., Waltham, MA, USA) (n = 3). The pH of each nasal spray was determined (Orion 3 star pH-meter), (Thermo Fisher Scientific Inc., Waltham, MA, USA).

4.2.3.2. Holding time determination of MEL in the pre-dispersions

For intermediate products such as pre-dispersions, the holding time was determined using PSD. Pre-dispersions were stored in sealed glass bottles at room temperature (25 ± 1 ºC) for 3 days. The PSD of the MEL in the prepared samples were analysed on the production day (day 0) and after 1, 2 or 3 days storage.

4.2.4. Investigations of nasal formulations

4.2.4.1. Rheology and mucoadhesion of samples

Rheological measurements were carried out at 37 °C with a Physica MCR101 Rheometer (Anton Paar GmbH, Graz, Austria). A concentric cylindrical measuring device with a diameter of 10.835 mm was used. Frequency sweep curves were plotted to determine the viscoelastic character of the samples. Storage modulus (G') and loss modulus (G") measurements were made over the frequency range from 0.01 to 100 Hz. The flow curves of the samples were also determined. The shear rate was increased from 0.1 to 100 1/s in controlled rate mode. The shearing time was 150 s.

In order to clarify the role of MEL PS in mucoadhesion, samples with and without mucin were also prepared (Table 13). The mucoadhesivity was determined on the basis of rheological synergism between the polymer and the mucin. The synergism parameter (bioadhesive viscosity component, η_b) was calculated (Bartos et al., 2015B).

Table 13 Samples for mucoadhesive measurements

Sample name	HA (mg/ml)	PVA (mg/ml)	MEL (mg/ml)	PSA, *D50* (µm)
HA solution	5	-	-	-
PVA solution	-	0.225	-	-
blank	5	0.225	-	-
raw MEL spray*	5	0.225	1	34.26
micro MEL spray**	5	0.225	1	1.887
nano MEL spray***	5	0.225	1	0.135

*raw MEL spray: nasal spray containing raw MEL
**micro MEL spray: nasal spray containing micronized MEL
***nano MEL spray: nasal spray containing nanonized MEL
D50: particle diameter below which 50% of the sample volume exists

4.2.4.2. In vitro permeability of MEL

In vitro permeability studies were performed on a vertical Franz diffusion cell system (Hanson Microette Topical and Transdermal Diffusion Cell and Autosampling System) (Hanson Research, Chatsworth CA, USA) ($n = 5$). The donor phase containing 300 mg of nasal formulation was placed on the polyvinylidene fluoride synthetic membrane (Durapore® Membrane Filter) (EMD Millipore, Billerica, MA, USA) impregnated with isopropyl myristate. The effective diffusion surface was 1.33 cm^2. PBS (pH 7.4, 37 ºC) was used as an acceptor phase (7 ml). The rotation speed of stir-bar was set to 450 rpm. Sampling was carried out at 5, 10, 15, 30 and 60 min diffusion time. 0.8 ml samples were taken from the acceptor phase by autosampler and were replaced with fresh receiving medium. The amount of diffused MEL was determined spectrophotometrically (Unicam UV/VIS). The API flux (**J**) was calculated from the quantity of MEL, which permeated through the membrane, divided by the insert membrane surface and the time duration [µg/cm^2/h]. The permeability coefficient (K_p) was determined from *J* and the drug concentration in the donor phase (C_d [µg/cm^3]):

$$K_p\,[cm/h] = J/C_d.$$

For residual MEL content determination in the donor phase, the vertical Franz diffusion cell system was also used to mimic the nasal cavity. Therefore the membrane was impregnated with simulated nasal fluid (8.77 g NaCl, 2.98 g KCl and 0.59 g $CaCl_2$, containing mucin, 1 %) (Jug and Bećirević-Laćan, 2007). The donor phase content was removed after 60 min diffusion time and the remaining MEL amount was determined with an Agilent 1260 RP-HLPC system (QP, DAD, ALS).

4.2.4.3. In vivo study of MEL

Intranasal administration and blood sample collection

The intranasal formulations prepared directly from the pre-dispersions contained 1 mg/ml MEL and 5 mg/ml HA. A dose of 60 µg MEL *per animal* was administered into the right nostril of 160-180 g male Sprague–Dawley rats ($n = 5$) via the pipette. Directly before the drug administration, the animals were narcotized with isoflurane. Blood samples were withdrawn from the tail vein before and at 5, 15, 30 and 60 min post-dosing. The experiments performed conformed to the European Communities "*Council directive for the care and use of laboratory animals*" and were approved by the Hungarian Ethical Committee for Animal Research (permission number: IV/198/2013).

Determination of MEL from the blood samples

The MEL contents of blood samples were quantitated with an Agilent 1260 HLPC (high-performance liquid chromatography) system. MEL and piroxicam as internal standard (**IS**) were separated on a 250 mm × 4.6 mm column packed with 5 µm Kromasil C_{18}, 100 Å (Phenomenex Inc., Torrance CA, USA). After the setting of the method (Bartos et al., 2015 B), the animal blood samples (200 µl) were diluted with 500 µl of extraction liquid and spiked with 10 µl of the working IS solution at a final plasma concentration of 1.3 µg/ml. The solid-phase extraction (**SPE**) cartridges used (Strata-X-C 33 µm Polymeric Strong Cation tubes, Phenomenex Inc., Torrance CA, USA) were conditioned with 0.5 ml of methanol (**MeOH**), followed by 0.5 ml of extraction liquid. The prepared blood samples were allowed to run through the SPE cartridge at the flow rate of 1.0 ml/min. Cartridges were rinsed with 0.5 ml of extraction liquid and 0.5 ml MeOH and dried in vacuum for 5 min. The analytes were then eluted with 0.5 ml of 5:95 (*v/v*) ammonium hydroxide- MeOH elute. The eluent liquids were dried in a vacuum oven (Binder, Germany) at 20-30 mbar and 45 °C for 2-3 h. The dried residue was reconstituted in 300 µl of mobile phase and then vortexed (30 s), sonicated (2 min) and centrifuged at 12,000 × g for 5 min. 20 µl of supernatant was injected onto the C_{18} column.

Calculations of the area under the (time–concentration) curve (AUC) and statistical analysis

Pharmacokinetic parameters were analysed by means of PK Solver 2.0 software (Zhang et al., 2010) through non-compartmental analysis of plasma data using the extravascular input model. The AUC of the time (min)–concentration (µg/ml) curves of each animal were fitted with a linear trapezoidal method. The statistical analysis was performed with Prism 5.0 software (Graphpad Software Inc., La Jolla, CA, USA). All reported data are means ± SD. Student's *unpaired t-test* was used to determine statistical significance. Changes were considered statistically significant at $p < 0.05$.

5. RESULTS

5.1. Results of preliminary static sonication experiments

5.1.1. Effects of process parameters on PSD

During the procedure, the amplitude, temperature and sonication time were varied. At room temperature, in the case of IBU (*D50* = 153.73 µm), the use of an amplitude of 30, 50 or 70%

resulted in a 50% decrease (approx. 85 μm) in the average PS. In the case of MEL (*D50* = 85.39 μm), the application of an amplitude of 30% resulted in a 50% decrease (*D50* = 41 μm) in the average PS, and higher amplitudes led to a 3-fold PS reduction (*D50* ~ 26 μm). During the procedure, the temperature of the suspension increased from 25 °C to 77-85 °C. The utilization of continuous ice cooling ($T_{\text{cooling water}}$ = 18 °C) resulted in a decrease of the temperature of the suspension to ~ 35 °C. In the case of IBU, sonication at an amplitude of 30% caused a further 50% decrease in the average PS (*D50* = 39.44 μm). In the case of MEL, cooling did not cause a further PS reduction (*D50* = 22-27 μm). The smallest particles were produced at an amplitude of 70% (the highest *E* input) with ice cooling. Although the sonication amplitude was increased (30→70%), the ice cooling prevented the temperature of the suspensions from changing significantly. Increase of the sonication time (10→20 min) had a stronger effect (a small IBU PS reduction and a considerable MEL PS reduction) than the combination of an increased amplitude and ice cooling. Further elevation of the sonication time (20→30 min) did not result in changes in the PSs of IBU and MEL. A sonication time of 20 min was therefore considered to be optimum.

5.1.2. Effects of stabilizers

The choice of stabilizer depended on the drug candidate and on the formulation procedure. When the effects of different stabilizers were investigated, the suspensions were prepared with a fixed API concentration (300 mg/ml) and fixed parameters (70%, 18 ºC and 20 min). The stabilizer type has a pronounced effect on the PS and PSD. Four different stabilizers were tested in order to check the effect of the nature of the surfactant on the PSD of the drug. In the case of IBU, the smallest PS was achieved with Poloxamer: *D50* ~ 11 μm. In the case of MEL, the most effective PS reduction was achieved with PVP (*D50* = 4 μm). The low stabilizer concentration did not cause any significant variation in the PS.

Static sonication can be applied to decrease the PS to the μm range and change the drug crystal habit. The reduction of the PS is more efficient in the presence of additives. Because of the small amount of sample, this method is recommended in pre-clinical studies.

5.2. Comparison of static and dynamic sonication methods

Following the preliminary experiments, MEL was used as API to compare static and dynamic sonication by means of a factorial design. As a result of its high melting point, MEL does not melt during sonication. Besides the other parameters, the sonication amplitude, temperature and time were examined to compare the sonication methods.

5.2.1. Static sonication

Laser diffractometry revealed considerable decreases (25-70%) in the PS of MEL in response to static sonication at the various process parameters. The *D10*, *D50* and *D90* values are reported in Table 14.

Table 14 Results of static sonication (pre-dispersion) of MEL

Volume (ml)	**Sonotrode position**	**Concentration (mg/ml)**	**Temperature (°C)**	**Amplitude (%)**	**time (min)**	**D10 (µm)**	**D50 (µm)**	**D90 (µm)**
-	-	-	-	-	-	10.82	34.03	75.81
25	0.75	2	36	70	30	1.51	10.16	19.53
100	0.75	2	0	30	30	4.81	23.07	46.88
25	0.25	2	0	70	10	2.75	18.45	42.87
100	0.25	2	36	30	10	5.92	26.52	53.39
25	0.75	18	36	30	10	3.95	19.62	41.51
100	0.75	18	0	70	10	5.19	24.16	46.98
25	0.25	18	0	30	30	3.53	17.12	29.22
100	0.25	18	36	70	30	7.19	20.83	36.62

D10: particle diameter below which 10% of the sample volume exists
D90: particle diameter below which 90% of the sample volume exists

The relationship with the sonication variables was analysed quantitatively on the basis of the *D50* data in the main effects plots (Figure 7) and interaction plots (Figure 8). The *D10* and *D90* data furnished similar results. The main effect plot for a given parameter was obtained by averaging the results of each run, where this parameter was set to low or high, and connecting these averages with a line. If the studied parameters are independent, the plot will give a clear

indication of the system response to the selected variable. The main effects plots for the MEL PSD indicated that a small sample volume, a high amplitude and a long sonication time were preferred for efficient PS reduction, whereas the PS was less influenced by the sonotrode position, the solution concentration and temperature (Figure 7). It can be seen that a small sample volume, high ultrasound amplitude and a long sonication time were preferred for efficient PS reduction.

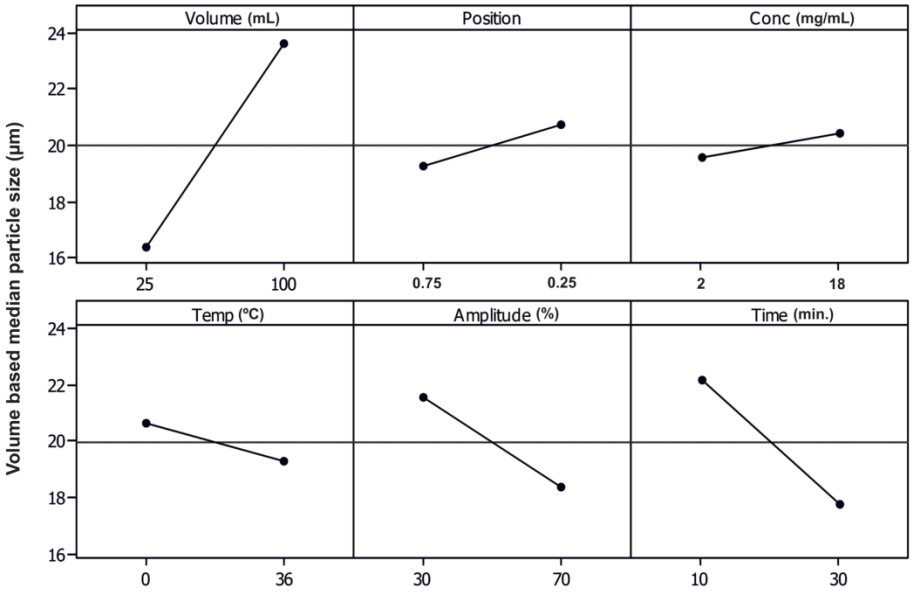

Figure 7 The main effect plots of the static sonication of MEL

Interaction plots show the effects between variables, which are not necessarily independent, by demonstrating the means of the responses, pairwise for all factors, for each level of the first and second factors involved in the study. The *D50* interaction plots (Figure 8) can be used to detect complex interactions between the sonication parameters. A longer sonication time resulted in a PS reduction, independently of the other process parameters. The connection between the physical parameters of sonication (amplitude, position and volume) was unequivocal. The high amplitude resulted in a PS decrease, independently of the sonotrode position and sample volume. The connection between concentration, temperature and amplitude demonstrated that the PS reduction effect of the increased amplitude occurred at low concentration and high temperature. The temperature–concentration and temperature–volume relationships were unidirectional, in contrast with the temperature–position relationship: increase of temperature was useful in the lower position. The upper or lower sonotrode position resulted in smaller particles at high or low MEL concentration, respectively.

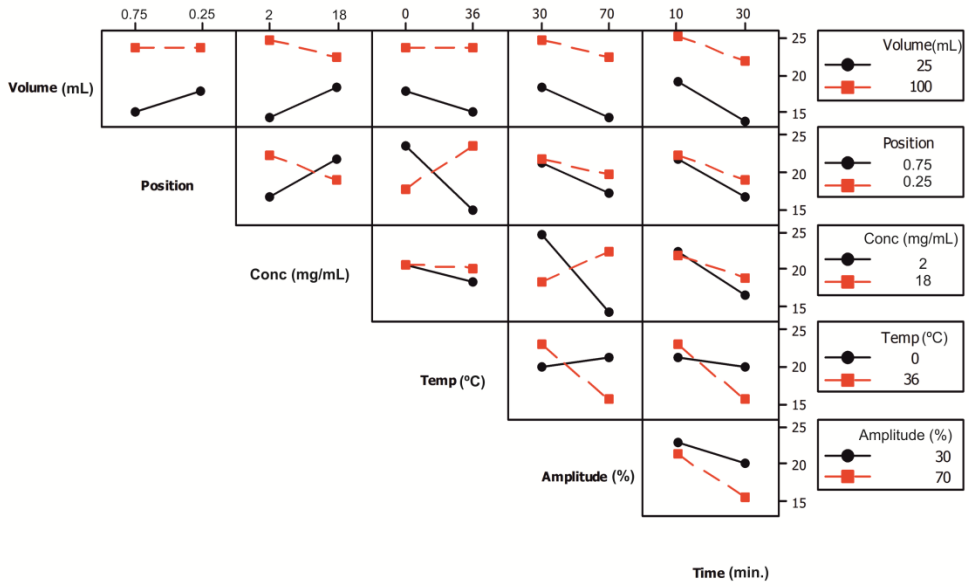

Figure 8 Interaction plots of main effects and PS for the static sonication of MEL

To summarize the results, the appropriate parameters for static sonication were a long sonication time (30 min), high amplitude (70%), a small sample volume (25 ml), high temperature (36 ºC), a lower sonotrode position (0.75) and low MEL concentration (2 mg/ml). As concerns static sonication, the ultrasound distribution was not homogeneous; the vibration was most effective surrounding the sonotrode (small volume). Because of the large energy input and long sonication time, increased amplitude was required to achieve small particles. The large energy input resulted in increased cavitation activities. When the temperature was raised, the kinetic energy of the particles increased, which affected the cohesive forces adversely. When low MEL concentration was used, the amount of energy per particle was greater.

5.2.2. Dynamic sonication

Analysis of the product MEL measured by laser diffraction revealed that dynamic sonication at the various sonication parameters resulted in a 15–60% decrease in average PS. The PSD function is reported in Table 15.

Table 15 Results of dynamic sonication (pre-dispersion) of MEL

Pump speed (rpm)	**Concentration (mg/ml)**	**Temperature (ºC)**	**Amplitude (%)**	**Time (min)**	***D10*(µm)**	***D50*(µm)**	***D90*(µm)**
-	-	-	-	-	10.82	34.03	75.81
50	2	36	70	30	2.20	14.60	35.02
50	2	0	30	30	4.56	24.22	47.05
100	2	0	70	10	5.70	26.90	51.92
100	2	36	30	10	5.90	26.15	52.20
50	18	36	30	10	4.40	22.69	53.54
50	18	0	70	10	6.27	23.54	46.77
100	18	0	30	30	9.06	29.31	45.58
100	18	36	70	30	2.87	16.73	38.03

The relationships between the sonication variables were analysed quantitatively on the basis of the *D50* data in the main effects plots (Figure 9) and interaction plots (Figure 10). The *D10* and *D90* data furnished similar results. The main effects plots for the MEL PSD indicated that the circulation of the sample at low rpm, high amplitude and long sonication time resulted in the most significant PS reduction, whereas the concentration of the suspension influenced the PS to a lesser extent. High temperature had a more significant effect on the PS under dynamic sonication than under static sonication.

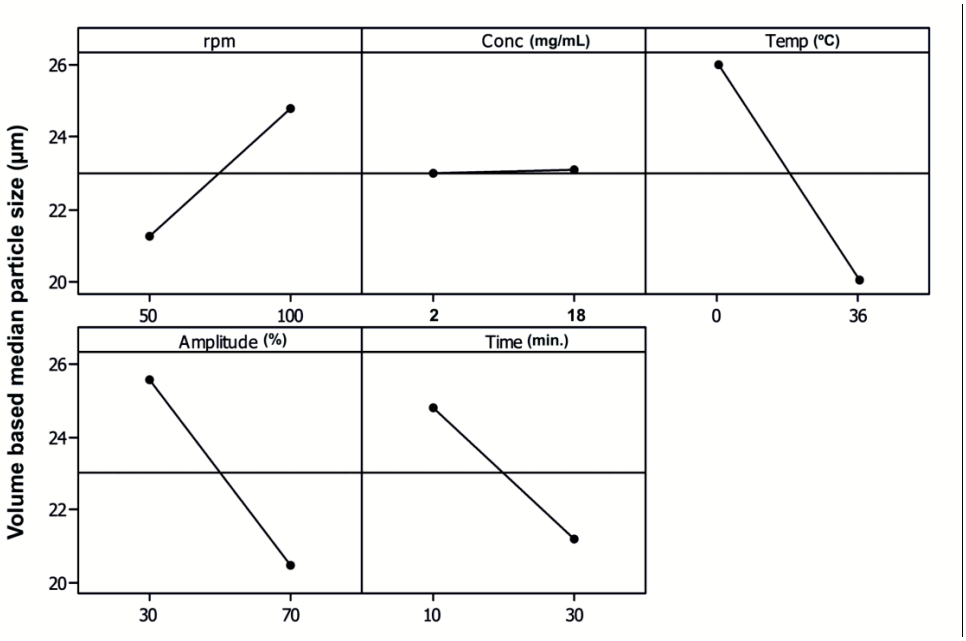

Figure 9 The main effect plots for the dynamic sonication of MEL

The interaction plots presented for *D50* in Figure 10 can be used to gain an insight into the complex interactions between the sonication parameters. The increased amplitude and the higher temperature resulted in a significant PS reduction. A longer sonication time did not have an appreciable effect in the case of low temperature and low amplitude. Increase of the concentration had an adverse effect on the PS at a low circulation rate.

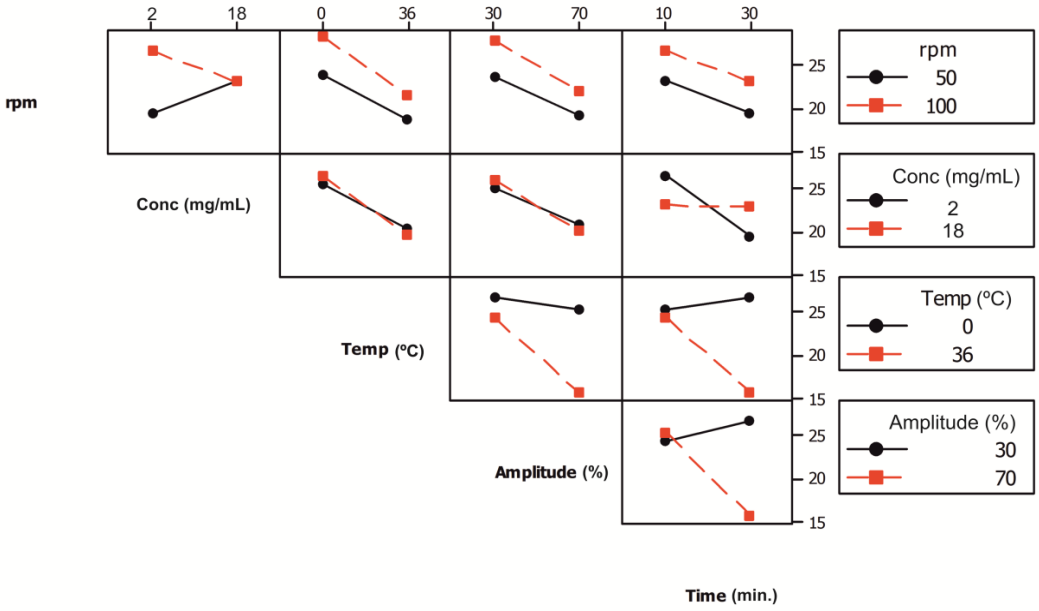

Figure 10 Interaction plots for the dynamic sonication of MEL

It was concluded that the most effective process parameters for dynamic sonication were a long sonication time (30 min), high amplitude (70%) and temperature (36 ºC), a slow rotation speed (50 rpm) and a low sample concentration (2 mg/ml). As a result of the continuous circulation of the samples, the distribution of the sonication effect was homogeneous. The PS was efficiently reduced at a low circulation rate by cavitation, because the particles were situated around the sonotrode for a longer period during one sonication cycle. The explanation of the effects of the other parameters is the same as for the static method.

5.2.3. PSA

The PSD of MEL (Figure 11) was determined in the suspensions after sonication. The raw MEL displayed a broad size distribution. The sonication methods resulted in decreased PSs. The SSA of the MEL increased as a consequence of acoustic cavitation in both sonication methods and for both suspensions relative to the raw MEL. Sonication of MEL by static process (**MEL Stat.**) led to smaller PSs compared with MEL, sonicated by dynamic process (**MEL Dyn.**) (Table 16).

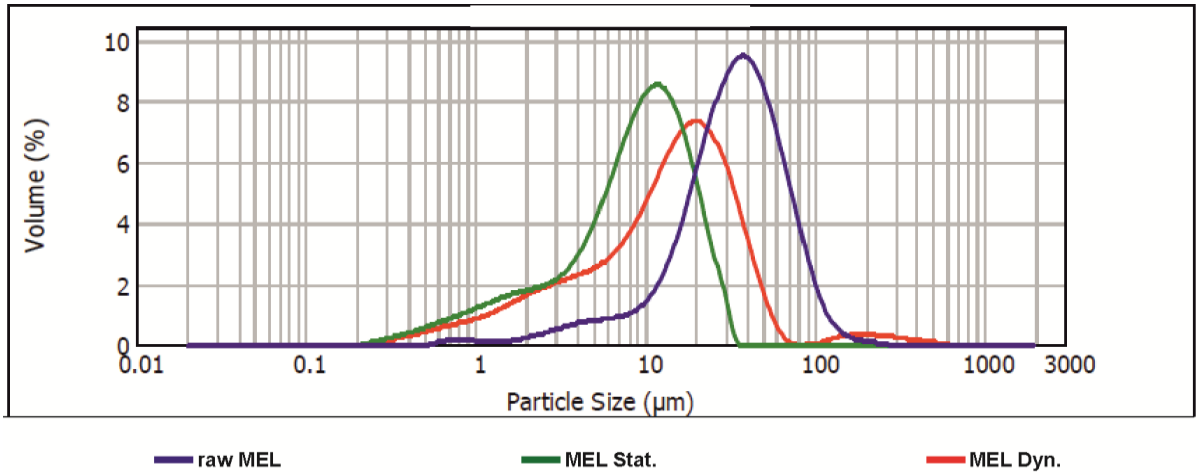

Figure 11 PSDs of raw MEL and sonicated MEL from pre-dispersions

Table 16 The SSA and PSD data on raw MEL and the sonicated pre-dispersions

	SSA (m^2/g)	***D10*** **(µm)**	***D50*** **(µm)**	***D90*** **(µm)**
raw MEL	0.340	10.82	34.03	75.81
Static sonicated sample (pre-dispersion)	2.040	1.51	10.16	19.53
Dynamic sonicated sample (pre-dispersion)	1.140	2.20	14.60	35.02

5.2.4. SEM

The SEM images (Figure 12) provided an indication of the morphology (shape and size) of the modified particles. The crystal habit of the pure MEL was changed significantly after the procedure. The raw MEL consisted mainly of angular, prismatic crystals with a broad PSD. The crystal lattice presumably demonstrated defects and cracks, along which the crystals disintegrated due to the energy input of acoustic cavitation. This factor is probably responsible for the presence of the broken pieces found on the surface of the larger particles. The drying of the samples could also cause cracks and broaden the PSD. The endurance during the treatment accounts for the roundness and smooth surfaces of the crystals. The yields of the samples by both methods were 95% at 0 ºC and 90% at 36 ºC. The average PS of the dried product was ~ 10 µm in the case of static and 15 µm in the case of dynamic sonication. Due to the high SSA of the dried product and since PVP is washed out, agglomeration might occur. Furthermore, aging or washing might also change the crystal size and shape.

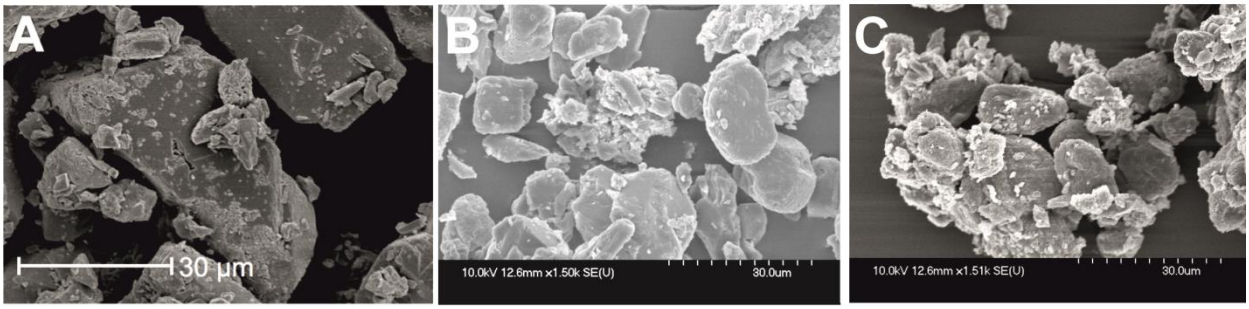

Figure 12 SEM pictures of raw MEL (**A**) and the dried products after static (**B**) and dynamic (**C**) sonication

5.2.5. XRPD

The XRPD pattern of pure MEL demonstrated the crystalline structure, as expected. The characteristic 2θ data were as follows: 13.22, 15.06, 26.46 and 26.67. The raw MEL and the sonicated dried MEL composite in both cases displayed the same XRPD patterns (Figure 13). This means that the crystalline form of the micronized MEL was not changed by the sonication and drying procedures. The intensities of the characteristic peaks were decreased in the case of the sonicated products, due to the reduced PS.

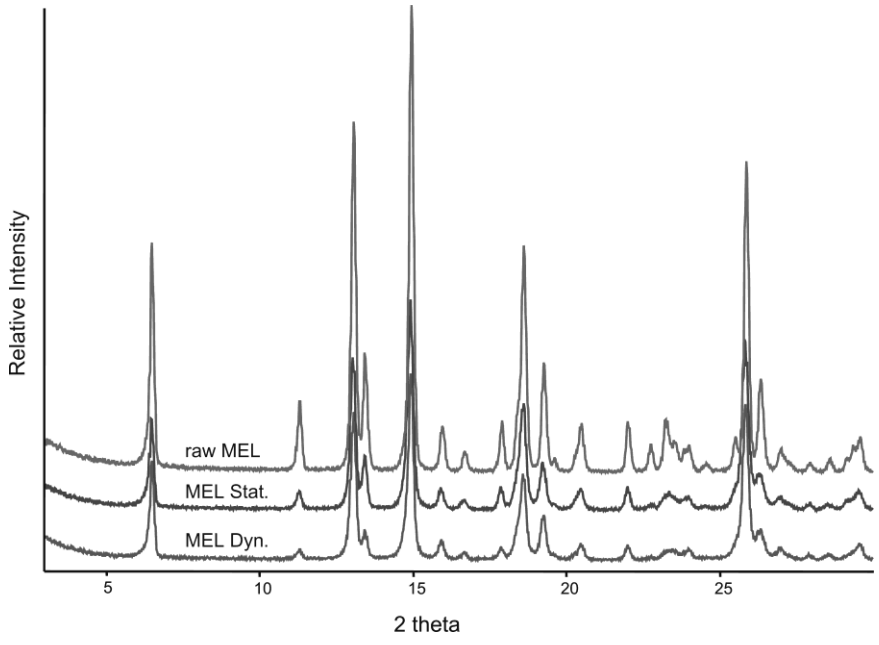

Figure 13 XRPD examination of raw MEL and dried sonicated products

5.2.6. DSC

DSC was employed to investigate the crystallinity and the melting of MEL in the pure form and in the sonicated dried products. The DSC curve (Figure 14) of the raw MEL revealed a sharp endothermic

peak at 259.11 ºC, reflecting its melting point and confirming its crystalline structure. After drying, the DSC curves exhibited the sharp endothermic peak of the MEL at 258.62 ºC in the static case, and at 259.81 ºC in the dynamic case, indicating that the crystallinity of the drug was retained. The value of the enthalpy and the onset–endset interval were not changed significantly for the sonicated products as compared with the values for raw MEL, and it can therefore be concluded that the degree of crystallinity was not decreased by the treatment.

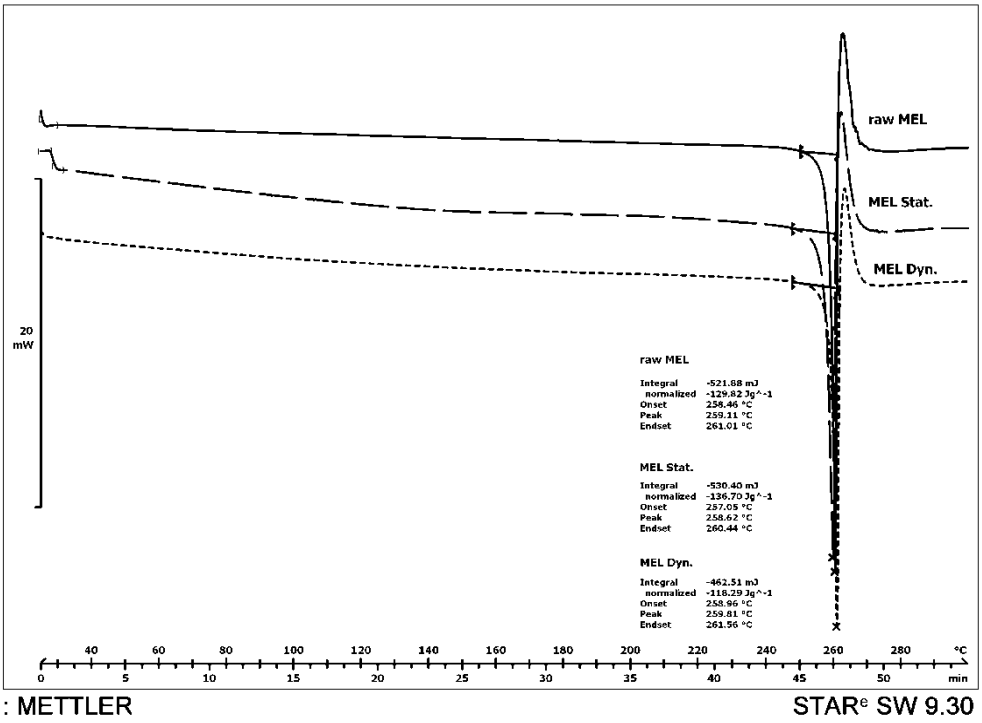

Figure 14 DSC curves of raw MEL and the dried sonicated products

5.2.7. Chemical stability (FT-IR)

To determine whether any decomposition occurred during the sonication process, FT-IR spectroscopy was carried out. This proved that no disintegration took place in the samples (Figure 15). Further, contamination of the solution with titanium particles resulting from cavitational erosion could not be detected. The E applied did not cause chemical changes in the MEL in aqueous medium during sonication (30 min) at 36 ºC. The characteristic bands of MEL were seen in all of the curves of the raw MEL and sonicated products, at 3289.76, 1550.04, 1530.36, 1346.73, 1265.88 and 1184.90 1/cm, denoting the stretching vibration of -NH, the thiazole ring (together with that at 1184.90 1/cm), the amide II band of –CO– NH–C, the

asymmetric stretching vibration of the sulfone and the amide III band of –CO–NH–C, respectively.

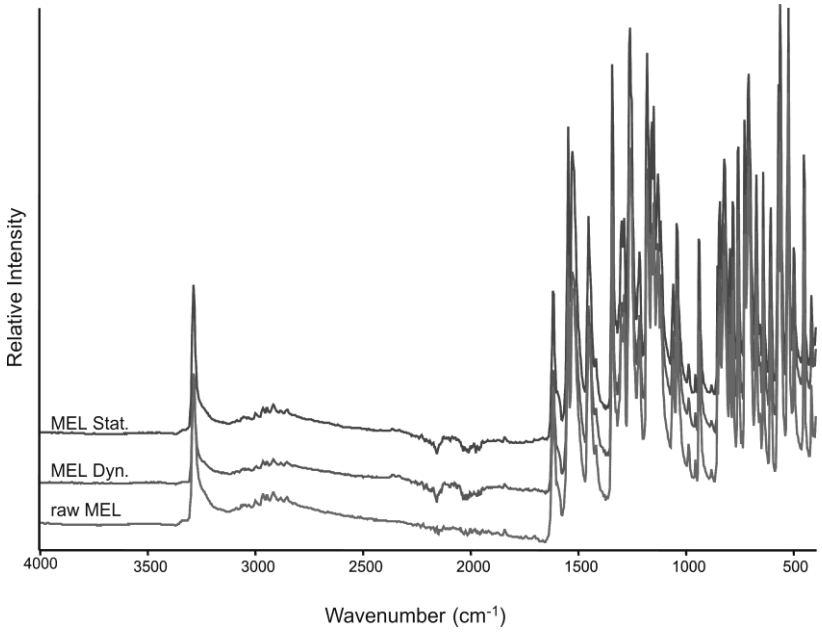

Figure 15 FT-IR curves of raw MEL and dried sonicated products

Comparative experiments revealed that dynamic sonication is also applicable for micronization. Moreover, in the case of dynamic sonication, use of a larger volume of sample is possible, as are standardization and scaling-up, which is important for industry.

Although the FT-IR investigations indicated that the process did not cause chemical degradation, metal contamination via degradation of the sonotrode could be expected. This problem should be investigated further through HPLC-MS analyses.

5.3. Results of a preliminary study of combined wet milling technique

5.3.1. Effects of milling parameters on PSD

In the course of the investigations discussed above, it could be concluded that acoustic cavitation is feasible for micronization. Our aim was to find a possibility for the production of pre-dispersed micro- and nanosized particles applicable for the development of a nasal formulation. As a novel opportunity, a combined wet milling technique (planetary ball mill and pearls, as milling media) was analysed. During the milling without pearls, the drug crystals were fractured through collision with the drug itself and also from the impact of the drug crystals with the milling chamber, which resulted in a PS reduction of 20 µm. With the progress of the milling time, aggregation of the particles could be observed. The application of 10 g of

pearls resulted in a pronounced PS reduction: *D50* values of ~ 3 μm after 10 min, and 0.150 μm after 30 min of milling, but aggregation occurred; the *D90* value was high. The most effective milling was observed when 20 g of pearls was applied. After 10 min micronized, and after 50 min nanonized particles were noted, with monodisperse PSD. Increase of the weight of pearls did not result in further PS reduction (Tables 17 and 18).

With the chosen pearl weight, the milling was performed at a lower concentration of PVA (0.5%). The use of a lower concentration of PVA led to the extensive aggregation of the MEL particles because it was less effective in overcoming the cohesive forces. After milling for 10 min, micronization could be attained, but with the advance of the milling time, the PS (primarily the *D90* value) increased (Table 19).

Table 17 MEL PSD in pre-dispersions milled with different weights of pearls (0, 10 or 20 g) containing 2.5% PVA solution as dispersant

Milling time (min)	**Without pearls**			**10 g of pearls**			**20 g of pearls**		
	D10 (μm)	**D50 (μm)**	**D90 (μm)**	**D10 (μm)**	**D50 (μm)**	**D90 (μm)**	**D10 (μm)**	**D50 (μm)**	**D90 (μm)**
0	11.40	34.26	73.59	11.40	34.26	73.59	11.40	34.26	73.59
10	10.199	26.616	52.668	0.255	2.934	10.940	0.115	1.625	5.669
20	9.239	25.285	55.202	0.108	1.254	4.775	0.070	0.151	1.951
30	11.207	28.768	54.147	0.080	0.151	2.156	0.068	0.140	1.223
40	8.585	23.848	45.489	0.069	0.146	1.667	0.070	0.135	0.729
50	7.871	24.025	50.346	0.068	0.143	1.280	0.072	0.126	0.271
60	5.203	14.269	27.548	0.068	0.141	1.082	0.069	0.129	0.295
70	5.161	15.047	29.542	0.067	0.135	0.618	0.070	0.131	0.292
80	8.966	25.478	47.930	0.067	0.135	0.538	0.068	0.127	0.288
90	5.805	17.627	34.196	0.069	0.132	0.317	0.068	0.126	0.277

Table 18 MEL PSD in pre-dispersions milled with different weights of pearls (20, 50 or 150 g) containing 2.5% PVA solution as dispersant

Milling time (min)	**20 g of pearls**			**50 g of pearls**			**150 g of pearls**		
	D10 (µm)	**D50 (µm)**	**D90 (µm)**	**D10 (µm)**	**D50 (µm)**	**D90 (µm)**	**D10 (µm)**	**D50 (µm)**	**D90 (µm)**
0	11.40	34.26	73.59	11.40	34.26	73.59	11.40	34.26	73.59
10	0.115	1.625	5.669	0.116	1.676	7.529	0.24	2.96	29.40
20	0.070	0.151	1.951	0.082	0.137	1.841	0.084	0.169	2.863
30	0.068	0.140	1.223	0.076	0.132	1.124	0.090	0.337	4.180
40	0.070	0.135	0.729	0.082	0.139	0.606	0.074	0.134	1.358
50	0.072	0.126	0.271	0.080	0.137	0.283	0.074	0.126	0.253
60	0.069	0.129	0.295	0.074	0.136	0.360	0.072	0.122	0.219
70	0.070	0.131	0.292	0.076	0.133	0.256	0.070	0.121	0.225
80	0.068	0.127	0.288	0.077	0.134	0.246	0.072	0.119	0.209
90	0.068	0.126	0.277	0.081	0.176	552.071	0.064	0.116	0.219

Table 19 PSD of MEL on milling with 20 g of pearls and different PVA contents

Milling time (min)	0.5% PVA			2.5% PVA		
	D10 (µm)	**D50 (µm)**	**D90 (µm)**	**D10 (µm)**	**D50 (µm)**	**D90 (µm)**
0	11.40	34.26	73.59	11.40	34.26	73.59
10	0.096	1.373	4.515	0.115	1.625	5.669
20	0.179	2.907	364.936	0.070	0.151	1.951
30	0.156	2.996	405.118	0.068	0.140	1.223
40	0.114	2.390	160.385	0.070	0.135	0.729
50	1.156	3.109	251.947	0.072	0.126	0.271
60	1.388	2.380	4.262	0.069	0.129	0.295
70	0.731	3.198	369.449	0.070	0.131	0.292
80	0.145	3.116	1472.283	0.068	0.127	0.288
90	1.795	135.325	336.672	0.068	0.126	0.277

5.3.2. SEM

Pre-dispersions containing micro- and nanosized MEL particles, prepared with chosen parameters (20 g of pearls, 10 or 50 min milling time and 2.5% PVA content), were dried and characterized. The SEM images (Figure 16) provided an indication of the morphology of the modified particles. The raw MEL consisted mainly of angular, prismatic crystals with a broad PSD. The micronized MEL particles (D50-1.625 μm) consisted of aggregations of nanosized particles. The nanonized MEL crystals (D50-126 nm) exhibited a regular shape and a smooth surface. The treatment accounted for the smooth surfaces of the particles.

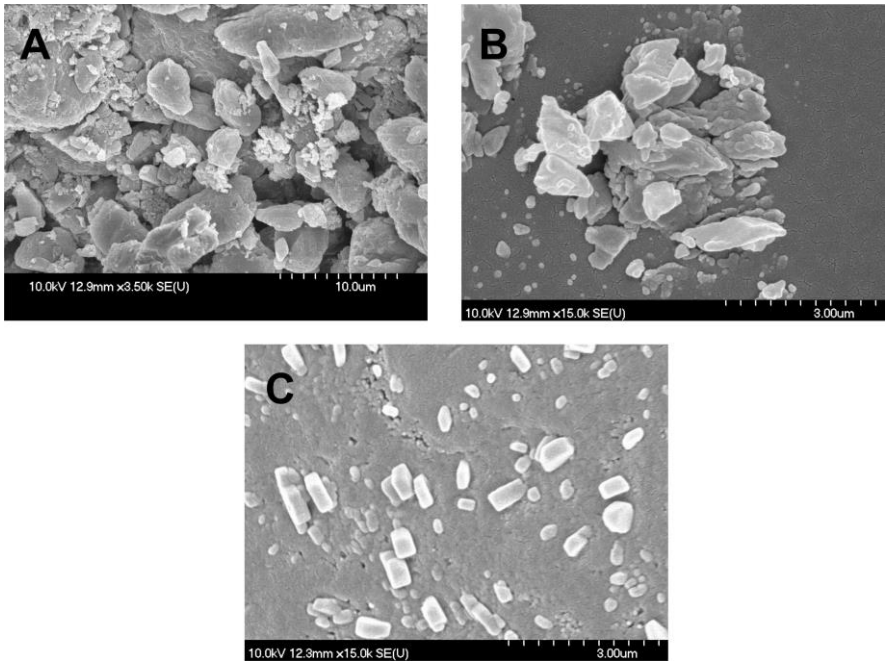

Figure 16 SEM images of raw MEL (**A**), and of MEL from microsized (**B**) and nanosized (**C**) particles containing dried pre-dispersions after milling in PVA–water solution as a dispersant medium

5.3.3. XRPD

After samples had been taken after 10 (micro MEL) and 50 (nano MEL) min of milling, the pre-dispersions in PVA–water solution as dispersant were dried and characterized. The XRPD pattern of the raw MEL demonstrated its crystalline structure, as expected. In the case of MEL-PVA PM, the intensities of the characteristic peaks were decreased due to the PVA. In the course of the milling, a decrease in crystallinity was perceptible, which was determined semi-kvantitatively via the mean of the decrease of the total area beneath the curve of 2 characteristic peaks (at 5.99 and 18.25 2θ) compared to the MEL-PVA physical mixture (**MEL-PVA PM**).

After milling for 10 min, ~ 33% of the drug remained crystalline, and this did not change subsequently (Figure 17).

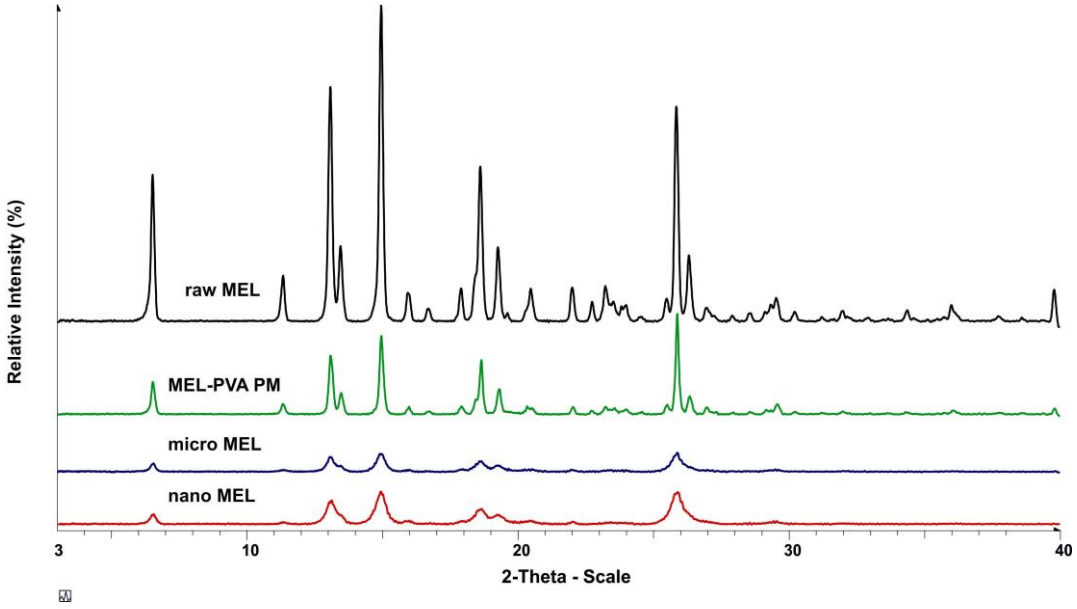

Figure 17 XRPD patterns of raw MEL, MEL-PVA PM, and of MEL from dried, microsized and nanosized particles containing pre-dispersions after milling in PVA–water solution as a dispersant medium

5.3.4. DSC

DSC was employed to investigate the crystallinity and the melting of MEL in the raw form, in the physical mixture and in the milled dried products. The DSC curves (Figure 18) of the raw MEL and of MEL in the MEL-PVA PM revealed a sharp endothermic peak at 259.11 and 256.57 ºC, reflecting the melting point of MEL and confirming its crystalline structure. After milling and drying, the DSC curves in both cases exhibited the broad endothermic peak of MEL at 239.81 ºC (10 min), and at 240.08 ºC (50 min), indicating that the crystallinity of the drug was decreased. The residual MEL crystals in the products melted at a lower temperature than the crystals of raw MEL. This process was promoted by PVA, which was softened at 85 °C as glass transition temperature (T_g) value.

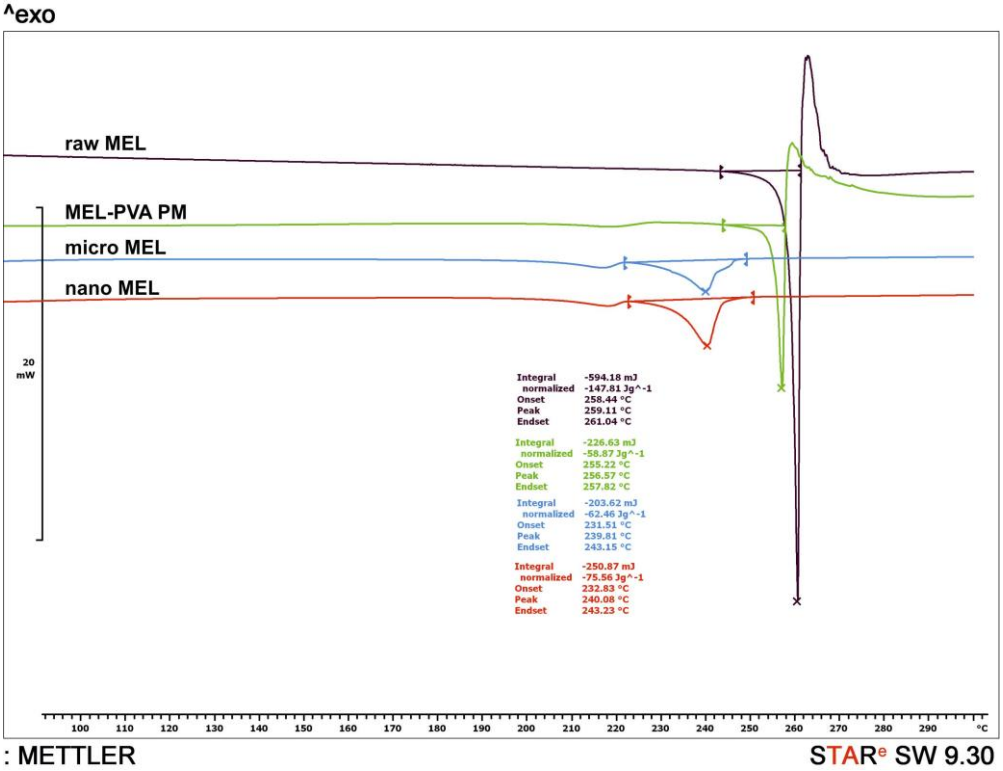

Figure 18 DSC curves of raw MEL, MEL-PVA PM, and of MEL from dried, microsized and nanosized particles containing pre-dispersions after milling in PVA–water solution as a dispersant medium

It can be concluded that a combination of planetary ball and pearl milling can be applied as a wet milling procedure to decrease the PS of MEL. Depending on the milling time, micro- and nanosized particles can be produced. In the presence of an appropriate amount of pearls and PVA as additive, this wet milling technology was suitable for the preparation of pre-dispersions which was applicable for further usage.

5.4. Characterization of the intranasal viscous liquid formulations prepared via the combined wet milling technique

For the development of intranasal formulations, micro- and nanosized MEL-containing pre-dispersions were prepared with determined parameters in PVA-PBS in order to ensure the pH, in accordance with the nasal conditions.

5.4.1. Characterization of the pre-dispersions

5.4.1.1. PSD

The MEL PS measured by laser diffraction decreased from ~ 35 µm to 1.887 µm during the 10 min (*D10* = 0.120; *D90* = 6.429) and to 0.135 µm during the 50 min milling time (*D10* = 0.077; *D90* = 0.253) (Table 20). The SSA of MEL increased 46-fold and 135-fold as a result of the micronization and the nanonization, respectively, relative to the raw MEL in the pre-dispersion. The coating effect of PVA prevented aggregation, and the stability of the system was therefore improved.

5.4.1.2. Solubility of MEL in the pre-dispersions

In order to check on the effects of PS reduction on the solubility of MEL in the pre-dispersions, solubility tests were performed at 25 ºC and pH 5.6 (Table 20). Micronization did not result in a change in the solubility of MEL. Following nanonization, a slight increase in solubility was observed, but the difference did not attain an order of magnitude.

Table 20 Solubility of MEL in the pre-dispersions

	c (µg/ml)
raw MEL pre-dispersion	6.4 ± 0.2
micro MEL pre-dispersion	6.6 ± 0.3
nano MEL pre-dispersion	9.3 ± 0.5

5.4.1.3. Holding time determination

Aggregation did not occur in the pre-dispersions during the first 24 h of storage (micro MEL pre-dispersion: *D90* = 6.462 µm; nano MEL pre-dispersion: *D90* = 0.270 µm). On the second day, however, aggregates were formed in both cases (micro MEL pre-dispersion: *D90* = 1035.340 µm; nano MEL pre-dispersion: *D90* = 695.767 µm), and the number and size of the aggregates increased still further during the third day. To avoid aggregation, the pre-dispersions should be utilized to prepare the formulations within 24 h.

5.4.2. Characterization of the nasal sprays

Nasal sprays (raw MEL, micro MEL and nano MEL sprays) were prepared directly from the pre-dispersions with MEL of different PS, using HA as a mucoadhesive polymer. The pH of

the formulations did not change significantly after the addition of HA to the systems (pH 5.5) relative to the pH of the pre-dispersions (pH 5.6).

The solubility of MEL in the nasal sprays was investigated in the freshly prepared formulations after stirring for 24 h. The solubility of the drug in the sprays was increased ~ 3-5-fold (raw MEL spray: 13.9 µg/ml; micro MEL spray: 32.1 µg/ml; nano MEL spray: 42.8 µg/ml). This can be explained by the interaction between the HA and MEL, which resulted in formation of a complex between the carboxylic groups in HA and the protonable groups in MEL (Battistini et al., 2013).

5.4.2.1. Rheology and mucoadhesion

The viscoelastic characters of the sprays were determined by frequency sweep measurements in the range from 0.01 Hz to 100 Hz. *G'* corresponds to the elastic (storage) and *G"* to the viscous (loss) modulus. Figure 19 presents frequency sweep curves of samples with different PSs (blank = MEL-free spray, raw MEL spray, micro MEL spray and nano MEL spray). The cross-over points of these curves, which are typical for gel-containing hyaluronans, could not be seen (Berkó et al., 2013). The ratio of *G'* and *G"* indicates the sol state of the samples. The findings can be explained by the pH of the formulations (pH = 5.6) and the low concentration of HA.

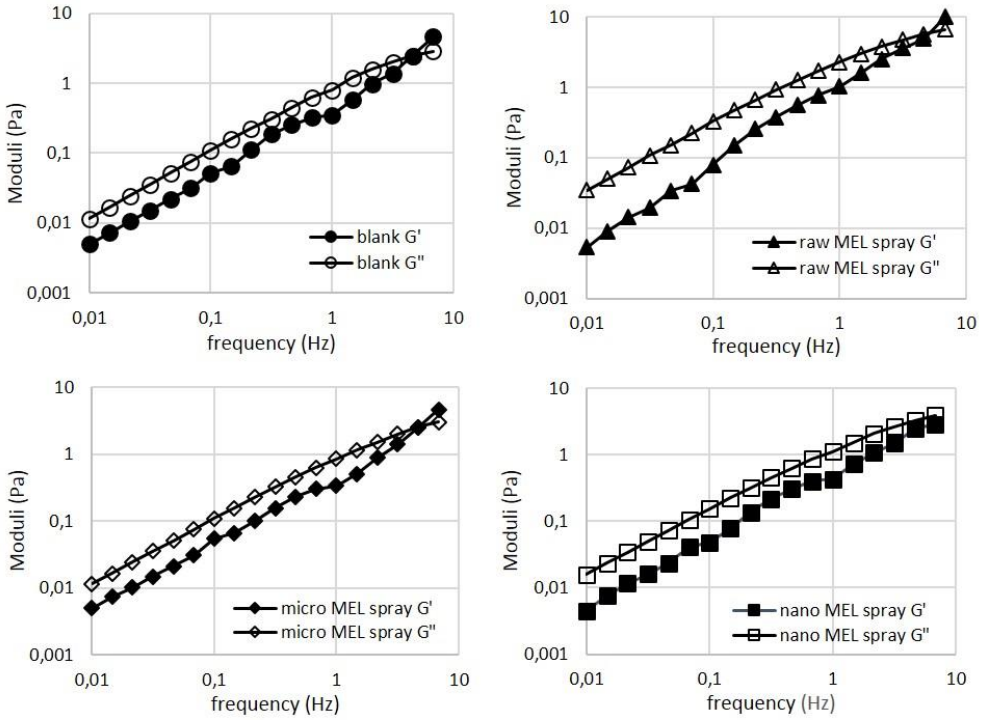

Figure 19 Frequency sweep curves of the sprays with different MEL PSs

The intranasal formulations containing MEL displayed shear-thinning behaviour, i.e. the shear viscosity depended on the degree of the shear load and the flow curve displayed a decreasing slope, which is typical for polymer solutions. The different formulations did not indicate changes in the flow characters (Figure 20). The presence of MEL and variation of its PS did not affect the viscosity of the samples, and this HA-containing drug carrier system is therefore suitable for the formulation of drugs with different PS without alteration of the flow behaviour.

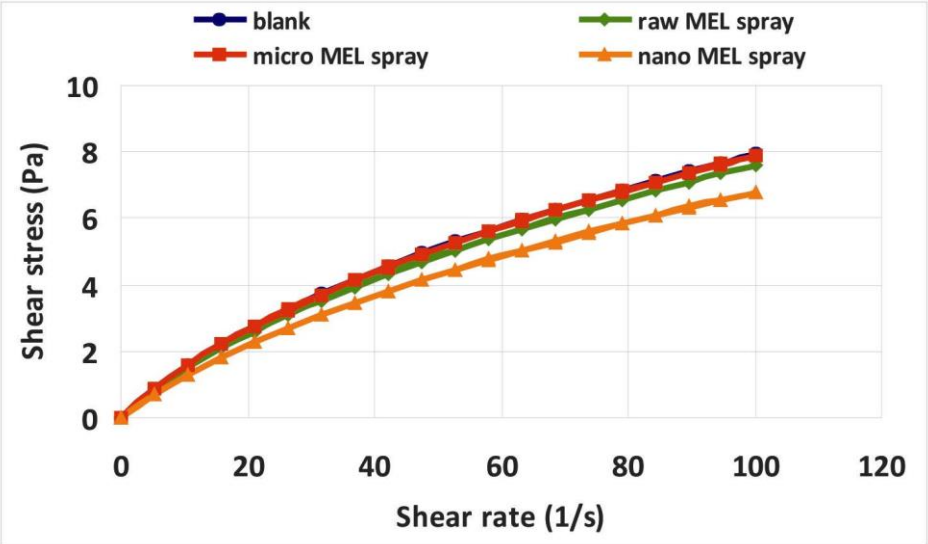

Figure 20 Flow curves of sprays with different MEL PSs

For the rheological determination of mucoadhesivity, the samples were mixed with mucin (final mucin concentration 5%) and the synergism parameter (η_b) was calculated. The mucoadhesivity values of the HA solution in PBS (pH 5.6) without PVA, of the PVA solution without HA, of the blank and of the three sprays with different MEL PSs were investigated.

The synergism parameter indicated the mucoadhesivity of the samples, with interaction between the HA and the mucin (Figure 21). PVA did not reveal mucoadhesive features, and it even broke down the mucin–HA interactions, and accordingly the mucoadhesivity of the blank was lower than that of the HA solution without PVA. Addition of MEL to the blank increased the mucoadhesivity of the formulation relative to the HA solution without PVA. This can be explained by the interactions between the mucin and the dispersed particles, and significant differences were observed between the calculated synergism data for the raw, micro and nano MEL samples ($p < 0.05$). The highest synergism was observed between the nasal spray containing nanonized MEL and mucin; the mucoadhesivity increased 2-fold as compared with that of the MEL-free blank, and hence the longest residence time could be attained. This could

be explained by the PS of the MEL: the nanosized particles possess an increased adhesiveness to surfaces (Müller et al., 2011). On the other hand, nano MEL has a PS similar to those of polymeric molecules such as HA, PVA and mucin chains, which can result in a well-structured complex, and better interactions among the components and it therefore displays more pronounced mucoadhesivity.

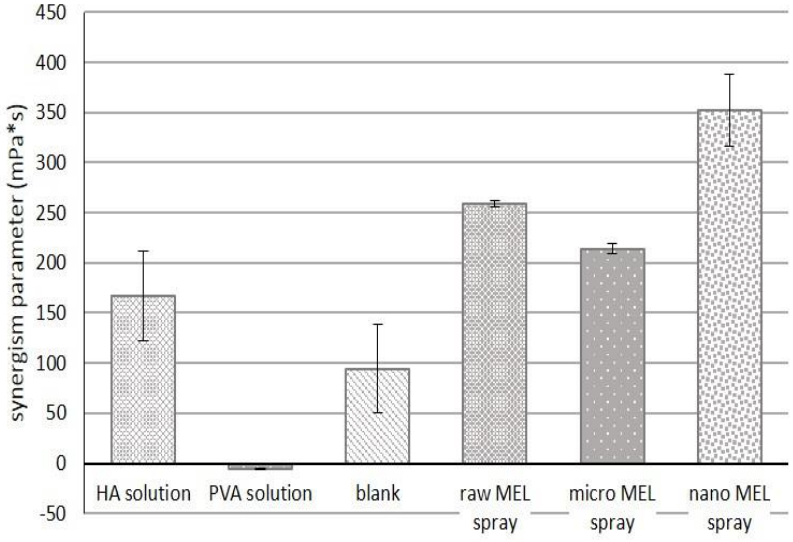

Figure 21 Calculated synergism parameters at a shear rate of 100 1/s of samples

5.4.2.2. In vitro permeability of MEL

The cumulative amount of MEL that diffused through a synthetic membrane from a nasal spray was measured against time with a Franz diffusion cell system. The diffusion from the formulation containing MEL nanoparticles was quickest, due to the rapid dissolution of the drug. The diffusion from the nanonized MEL-containing spray started in the first 5 min (Figure 22). As concerns the fastest diffusion, the question arose as to whether it was influenced by the PS or some other factor. It should be excluded that the nanosized MEL particles (*D50* = 0.135 µm) passed through the membrane without dissolving (they dissolved in the acceptor phase). Since the PS was larger than the membrane pore size (100 nm) and the membrane was impregnated with isopropyl myristate, this phenomenon was not observed. In this case, therefore, the PS and the resulting surface area had significant effects on the rate of passive diffusion.

The flux, which shows the amount of MEL that permeates through 1 cm^2 of the membrane within 1 h, was significantly higher in the case of the nasal formulation which contained nanoparticles as compared with the sprays containing micronized or raw MEL. The

permeability coefficient calculated from the flux data for the nanonized MEL was also significantly higher than in the other two cases (Table 21).

The PS was a determining factor as regards the amount of diffused MEL. In the spray containing nanonized MEL, the faster dissolution of the particles resulted in higher permeability.

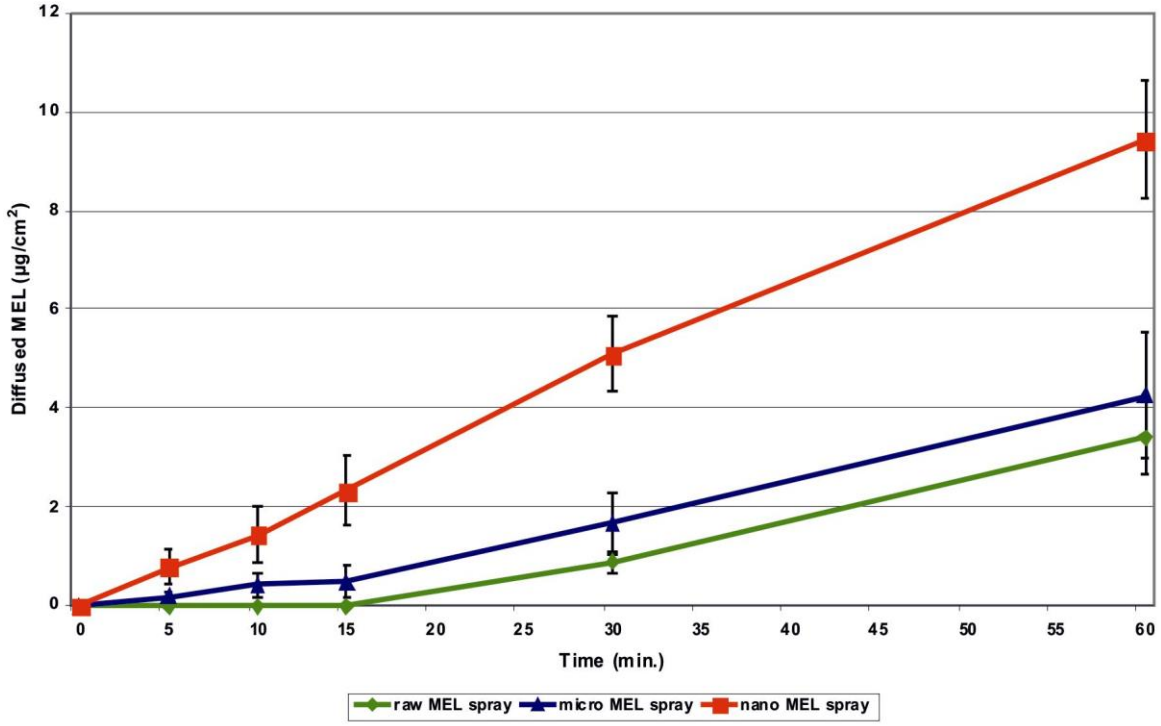

Figure 22 *In vitro* permeability of MEL-containing sprays with different PSs through a synthetic membrane

Table 21 Flux and permeability coefficient values of nasal sprays containing MEL with different PS

	J **(µg/cm²/h)**	***K_p*** **(cm/h)**
raw MEL spray	3.41	0.00341
micro MEL spray	4.25	0.00425
nano MEL spray	9.43	0.00943

It emerged that the nasal mucosa retained the MEL and its PS did not influence the permeability. Figure 23 demonstrates significant differences between the MEL contents remaining in the donor phase: 71.38 ± 6.33% (raw MEL spray), 19.52 ± 4.18% (micro MEL spray) and 8.85 ± 0.94% (nano MEL spray). The residual MEL content in the donor phase correlated with the decreasing MEL PS of the spray samples.

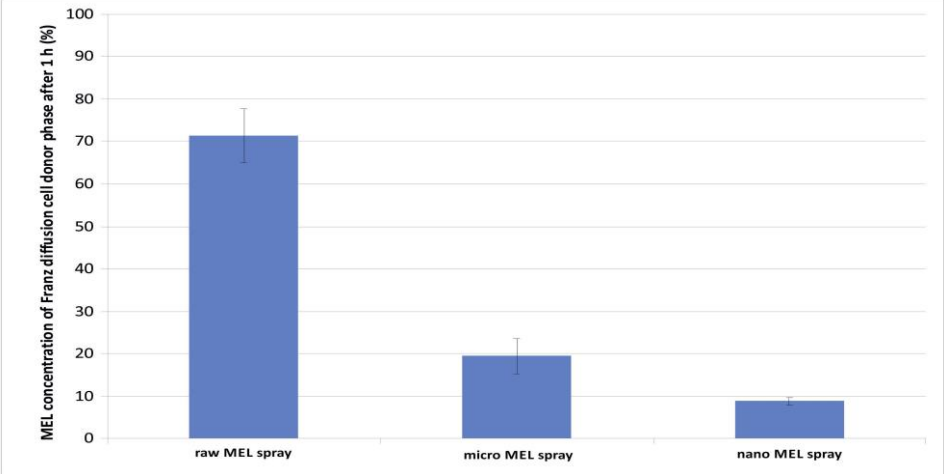

Figure 23 Residual MEL content in the donor phase

5.4.2.3. In vivo study of MEL

The drug concentrations in the blood plasma as a function of time after nasal administration of the sprays are shown in Figure 24. In the case of the spray containing MEL nanoparticles, a 3 times higher plasma level of MEL was observed after 5 min as compared with the formulations containing raw or micronized MEL. This result is in accordance with the reduction of the PS of MEL, and especially with the faster dissolution of nanonized MEL as compared with that of the microsized agent. The plasma concentrations tended to increase slowly during the initial ~ 30 min, but the 3-fold difference between the sprays containing nanonized or micronized MEL remained during 60 min after treatment. The controlled release of MEL in the case of the nano MEL spray could be explained in terms of the better adhesion and distribution of the nanoparticles and the formation of a well-structured system. This controlled release was enhanced by the HA–PVA system (Battistini et al., 2013). The PVA-coated particles played a role in the release of the drug, because the synthetic polymers reduced the rate of degradation of the natural polymers and prevented their rapid dissolution in the biological fluids (Ding et al., 2012).

The AUC is proportional to the amount of drug absorbed during the investigated time interval. The calculated AUC values gradually increased with decreasing PS (the highest AUC was observed for the nano MEL spray; Figure 25). The occurrence of micronization did not significantly increase the AUC as compared with the raw MEL ($AUC_{raw\ MEL\ spray}$: 13.97 ± 3.223 min µg/ml, $AUC_{micro\ MEL\ spray}$: 21.95 ± 5.527 min µg/ml, $p = 0.1552$), whereas nanonization led to a significant increase in the amount of MEL absorbed ($AUC_{nano\ MEL\ spray}$: 49.86 ± 5.632 min µg/ml; nano MEL spray vs raw MEL spray: $p = 0.0021$; nano vs micro MEL

spray: p = 0.0061). Our results demonstrated a strict correlation between the AUC and the MEL PS (R^2 = 0.9848) (Figure 26).

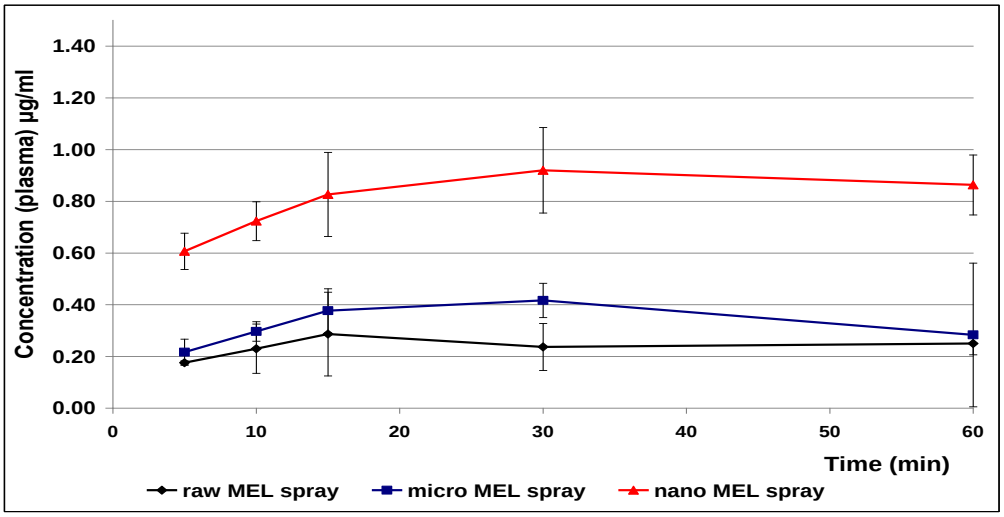

Figure 24 Plasma drug concentration vs. time profiles in rats after intranasal administration of sprays containing MEL with different PSs

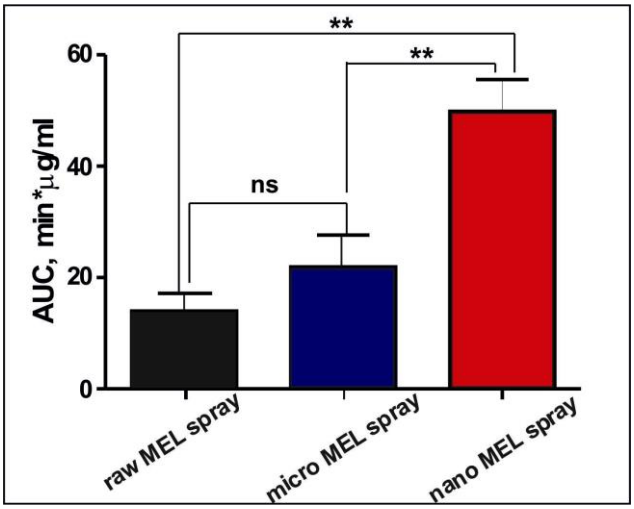

Figure 25 AUC values of the MEL-containing sprays with different PSs

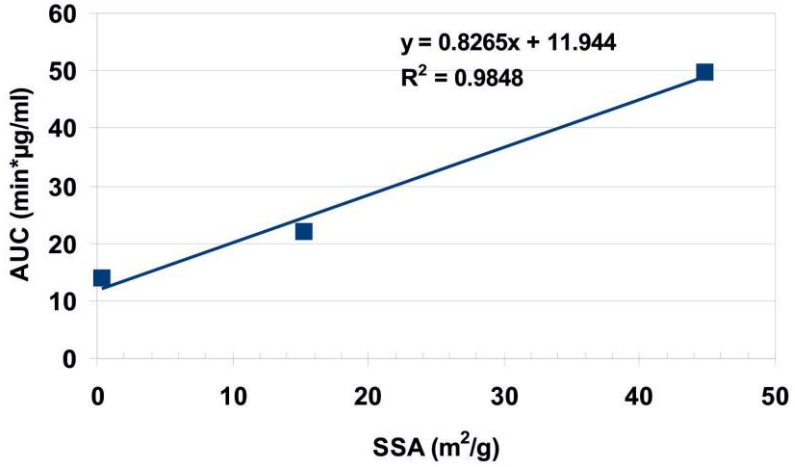

Figure 26 Correlation between the AUC values and different MEL SSAs

It can be concluded that the reduction of the PS of MEL into the nano range resulted in special features of nanocrystals (Müller et al, 2011) such as increased saturation and dissolution velocities, and increased adhesiveness to surfaces relative to micro-sized MEL particles. In the case of nano MEL spray, the high SSA and the increased saturation solubility resulted in rapid dissolution and better diffusion of the drug and a high AUC value. The linear correlation between the SSA of MEL and the AUC values (R^2 = 0.9848) confirmed that the dissolution of particles with different sizes is the key factor determining the amount of absorbed drug. Different mucoadhesivities were measured for the nanonized MEL–HA–mucin system and in case of the micro-sized MEL-containing sprays. The *in vivo* studies revealed that the prolonged residence time and the uniform distribution of the nano MEL spray throughout the nasal mucosa resulted in higher AUC values.

6. CONCLUSIONS

In this work, effects of different wet milling techniques in reducing the PS were investigated. The results showed that these techniques are suitable for PS reduction and for the preparation of pre-dispersions as intermediates that which are directly applicable for the development of innovative liquid pharmaceutical formulations. The applicability of nanosuspensions in nasal formulations is a new approach in pharmaceutical technology. Drug delivery to the systemic circulation via the nose is considered to be a promising route.

i. The effect of acoustic cavitation in reducing the PS, based on the collapse of the bubbles created by ultrasound waves, was investigated. During the preliminary study, static sonication was investigated in the cases of IBU and MEL, and the optimum process parameters (temperature, amplitude, sonication period and stabilizers) were determined. The PSDs of these drugs were measured after sonication and compared with those of the raw drugs (IBU: *D50* = 153 μm and MEL: *D50* = 85 μm), as the response factor after sonication. Due to acoustic cavitation, the PS decreased (IBU: *D50* = 25 μm and MEL: *D50* = 14 μm), but the use of a stabilizer was needed for a further decrease (IBU–Poloxamer: *D50* = 11 μm; MEL–PVP: *D50* = 4 μm). It was established that static sonication can be applied to decrease the PS to the micrometre range in the presence of additives.

ii. After the investigation of static sonication, the effects of static and dynamic sonication on PS reduction were compared. In dynamic sonication, the samples were circulated continuously during the sonication. The most effective process parameters were determined by a factorial design plan for the PSD of MEL. A long sonication (30 min), high amplitude (70%), a high temperature (36 ºC) and a low concentration of MEL (2 mg/ml) proved to play important roles in the sonication procedures. Samples sonicated with appropriate parameters were dried and investigated. The SEM images showed that the sonication resulted in rounded, micro-sized particles. XRPD and DSC examinations revealed the crystalline structure of the MEL produced by both sonication methods. FT-IR demonstrated that no chemical degradation occurred.
These two methods are also appropriate for reduction of the PSs of materials, with application of a short-term E input. Static sonication is not suitable for scaling-up; this method is recommended primarily for PS reduction in preclinical samples, where the amount of the drug candidate is very small, while dynamic sonication may be suitable for the wet milling of different active substances to prepare pre-dispersions because larger volumes of sample can be used in this method. Scaling-up and standardization are possible, which is important for industry.

iii. A combination of planetary ball and pearl milling was investigated in the case of MEL. In the presence of a stabilizer, at constant rotation rate, the effects of the milling time, the applied pearl weight and the additive concentration on the reduction of the PS were determined. Depending on the milling time, the PS of the drug could be reduced to the micro-(10 min) or nanometre (50 min) range. Increase of the pearl weight above 20 g did not result in the higher

effectiveness of milling. The use of a higher concentration of PVA was required to prevent the aggregation of the MEL particles. SEM images revealed the aggregation of nano-sized particles, resulting in micronized MEL particles (D50 = 1.625 µm). The nanonized MEL crystals (D50 = 126 nm) exhibited a regular shape and a smooth surface. XRPD and DSC examinations revealed the change in the crystallinity of MEL. This combined technique is applicable for the production of intermediate (in pre-dispersion form) and (after drying) dried products for additional pharmaceutical formulations.

iv. Of the investigated techniques, the combined milling technique was suitable for the micro- and nanonization of MEL. At pH 5.6, pre-dispersions with different MEL PSs were prepared as intermediates for the design of intranasal liquid formulations with the addition of HA as mucoadhesive agent. Reduction of the MEL PS into the nano range led to increased saturation solubility and dissolution velocities, and increased adhesiveness to surfaces as compared with microsized MEL particles. A linear correlation was demonstrated between the specific surface area of MEL and the AUC. The *in vitro* and *in vivo* studies indicated that a longer residence time and uniform distribution of the nano MEL spray throughout an artificial membrane and the nasal mucosa resulted in better diffusion and a higher AUC. Nanosized MEL may be suggested for the development of an innovative dosage form with a different dose of the drug, as a possible administration route for pain management.

v. It can be concluded that wet milling is applicable for the preparation of pre-dispersions, whereby dosage forms can be prepared in one step. Sonication is suitable for reduction of the PS of drugs to the micro range, but it requires a large amount of dispersion medium, and it is therefore not applicable to obtain intermediate products for the preparation of dosage forms. Metal contamination through degradation of the sonotrode should be borne in mind.

In contrast, because of low need for dispersant medium, the combined method can be used for more efficient milling in comparison with sonication, and it is also suggested for the preparation of pre-dispersions with micro- and nanosized particles, and recommended for the development of PS-controlled intranasal therapeutic systems.

The applicability of a nanosuspension in a nasal formulation is a new approach in pharmaceutical technology, and consequently few data on such systems are available (the intranasal usage of other analgesic NSAID agents (e.g. a ketorolac tromethamine-containing

solution) (Li et al., 2015)). A patent has been granted which describes the nasal application of MEL in solution form (Castile et al., 2005), but there have been no publications on the development of MEL-containing nanosuspensions for nasal application.

REFERENCES

Afolabi A, Akinlabi O, Bilgili E. Impact of process parameters on the breakage kinetics of poorly water-soluble drugs during wet stirred media milling: A microhydrodynamic view. *Eur. J. Pharm. Sci.* 51 (2014) 75-86.

Ambrus R, Amirzadi NN, Aigner Z, Szabó-Révész P. Formulation of poorly water-soluble Gemfibrozil applying power ultrasound. *Ultrason. Sonochem.* 19 (2012) 286-291.

Ambrus R, Kocbek P, Kristl J, Šibanc R, Rajkó R, Szabó-Révész P. Investigation of preparation parameters to improve the dissolution of poorly water-soluble meloxicam. *Int. J. Pharm.* 381 (2009) 153–159.

Anand U, Feridooni T, Agu RU. Novel Mucoadhesive Polymers for Nasal Drug Delivery, Sezer, A. D., (Ed.), *Pharmacology, Toxicology and Pharmaceutical Science,* Halifax, 2012.

Anarjan N, Jafarizadeh-Malmiri H, Nehdi IA, Sbihi HM, Al-Resayes SI, Tan CP. Effects of homogenization process parameters on physicochemical properties of astaxanthin nanodispersions prepared using a solvent diffusion technique. *Int. J. Nanomed.* 10 (2015) 1109-1118.

Bajpai AK, Shukla SK, Bhanu S, Kankane S. Responsive polymers in controlled drug delivery. *Prog. Polym. Sci.* 33 (2008) 1088-1118.

Bakar MRA, Nagy ZK., Saleemi AN, Rielly CD. The impact of direct nucleation control on crystal size distribution in pharmaceutical crystallization processes. *Cryst. Growth and Des*. 9 (2009) 1378-1384.

Bartos Cs, Ambrus R, Sipos P, Budai-Szűcs M, Csányi E, Gáspár R, Márki Á, Seres AB, Sztojkov-Ivanov A, Horváth T, Szabó-Révész P. Study of sodium hyaluronate-based intranasal formulations containing micro- or nanosized meloxicam particles. *Int. J. Pharm.* 491 (2015) 198-207. (B)

Bartos Cs, Kukovecz Á, Ambrus R, Farkas G, Radacsi N, Szabó-Révész P. Comparison of static and dynamic sonication as process intensification for particle size reduction using a factorial design. *Chem. Eng. Process.* 87 (2015) 26-34. (A)

Bartos Cs, Szabó-Révész P, Ambrus R. Optimization of technological parameters by acoustic cavitation to achieve particle size reduction. *Farmacia* 62 (2014) 34-46.

Battistini FD, Olivera ME, Manzo RH. Equilibrium and release properties of hyaluronic acid-drug complexes. *Eur. J. Pharm. Sci.* 49 (2013) 588-594.

Baumann D, Bacher C, Högger P. Development of a novel model for comparative evaluation of intranasal pharmacokinetics and effects of anti-allergic nasal sprays. *Eur. J. Pharm. Biopharm.* 80 (2012) 156-163.

Baumann D, Bacher C, Högger P. Development of a novel model for comparative evaluation of intranasal pharmacokinetics and effects of anti-allergic nasal sprays. *Eur. J. Pharm. Biopharm.* 80 (2012) 156-163.

Behrend O, Ax K, Schubert H. Influence of continuous phase viscosity on emulsification by ultrasound. *Ultrason. Sonochem.* 7 (2000) 77-85.

Beig A, Miller JM, Dahan A. Accounting for the solubility-permeability interplay in oral formulation development for poor water solubility drugs: The effect of PEG-400 on carbamazepine absorption. *Eur. J. Pharm. Biopharm.* 81 (2012) 386-391.

Benes E, Grösschl M, Handl B, Trampler F, Nowotny H. Das europaische TMR- Netzwerk Ultrasonic Separation of Suspended Particles. *Proc. Joint Symposium AAA and ÖPG TC Acoustics*, Graz, Austria 2 (1998) 14-15.

Berkó Sz, Maroda M, Bodnár M, Erős G, Hartmann P, Szentner K, Szabó-Révész P, Kemény L, Borbély J, Csányi E. Advantages of cross-linked versus linear hyaluronic acid for semisolid skin delivery systems. *Eur. Polym. J.* 49 (2013) 2511-2517.

Bilgili E, Afolabi A. A combined microhydrodynamics-polymer adsorption analysis for elucidation of the roles of stabilizers in wet stirred media milling. *Int. J. Pharm.* 439 (2012) 193-206.

Blagden N, Matas M, Gavan PT, York P. Crystal engineering of active pharmaceutical ingredients to improve solubility and dissolution rates. *Adv. Drug Deliver. Rev*. 59 (2007) 617-630.

Boudriche L, Chamayou A, Calvet R, Hamdi B, Balard H. Influence of different dry milling processes on the properties of an attapulgite clay, contribution of inverse gas chromatography. *Powder Technol.* 254 (2014) 352-363.

Bujňáková Z, Dutková E, Baláž M, Turianicová E, Baláž P. Stability studies of As4S4 nanosuspension prepared by wet milling in Poloxamer 407. *Int. J. Pharm.* 478 (2015) 187-192.

Bund RK, Pandit AB. Sonocrystallization: Effect on lactose recovery and crystal habit. *Ultrason. Sonochem*. 14 (2007) 143-152.

Castile JD, Lin W, Smith A, Watts PJ. inventors. Intranasal formulation of meloxicam. World Intellectual Property Organization patent WO 2005021041 A1. 2005 March 10. Accessed: 03/11/2014

Chen D, Li D, Zhang Y, Kang Z. Preparation of magnesium ferrite nanoparticles by ultrasonic wave-assisted aqueous solution ball milling. *Ultrason. Sonochem.* 20 (2013) 1337-1340.

Chen H, Khemtong C, Yang X, Chang X, Gao J. Nanonization strategies for poorly water-soluble drugs, *Drug Discovery Today*, Vol. 16, 2011.

Chunga TW, Liu DZ, Yang JS. Effects of interpenetration of thermo-sensitive gels by crosslinking of chitosan on nasal delivery of insulin: *In vitro* characterization and *in vivo* study. *Carbohyd. Polym*. 82 (2010) 316-322.

Ding J, He R, Zhou G, Tang C, Yin C. Multilayered mucoadhesive hydrogel films based on thiolated hyaluronic acid and polyvinylalcohol for insulin delivery. *Acta Biomater*. 8 (2012) 3643-3651.

disintegrant agglomerates for direct compression by a crystallo-co- agglomeration technique. *Int. J. Pharm.* 351 (2008) 45-54.

Fan G, Gu Z, Yang L, Li F. Nanocrystalline zinc ferrite photocatalysts formed using the colloid mill and hydrothermal technique. *Chem. Eng. J.* 155 (2009) 534-541.

Fortuna A, Alves G, Serralheiro A, Sousa J, Falcão A. Intranasal delivery of systemic-acting drugs: Small-molecules and biomacromolecules. *Eur. J. Pharm. Biopharm.* 88 (2014) 8-27.

Friedrich H, Fussnegger B, Kolter K, Bodmeier R. Dissolution rate improvement of poorly water-soluble drugs obtained by adsorbing solutions of drugs in hydrophilic solvents onto high surface area carriers. *Eur. J. Pharm. Biopharm*. 6 (2006) 171-177.

Furubayashi T, Inoue D, Kamaguchi A, Higashi Y, Sakane T. Influence of Formulation Viscosity on Drug Absorption Following Nasal Application in Rats. Drug *Metab. Pharmacokinet.* 22 (2007) 206-211.

Ghosh I, Bose S, Vippagunta R, Harmon F. Nanosuspension for improving the bioavailability of a poorly soluble drug and screening of stabilizing agents to inhibit crystal growth. *Int. J. Pharm*. 409 (2011) 260-268.

Ghosh I, Schenck D, Bose S, Ruegger C. Optimization of formulation and process parameters for the production of nanosuspension by wet media milling technique: Effect of Vitamin E TPGS and nanocrystal particle size on oral absorption. *Eur. J. Pharm. Sci*. 47 (2012) 718-728.

Hasçiçek C, Gönül N, Erk N. Mucoadhesive microspheres containing gentamicin sulfate for nasal administration: preparation and *in vitro* characterization. *II Farmaco* 58 (2003) 11-16.

Hatkar UN, Gogate PR. Process intensification of anti-solvent crystallization of salicylic acid using ultrasonic irradiation. *Chem. Eng. Process.* 57-58 (2012) 16-24.

Horvát S, Fehér A, Wolburg H, Sipos P, Veszelka Sz, Tóth A, Kis L, Kurunczi A, Balogh G, Kürti L, Erős I, Szabó-Révész P, Deli MA. Sodium hyaluronate as a mucoadhesive component in nasal formulation enhances delivery of molecules to brain tissue. *Eur. J. Pharm. Biopharm*. 72 (2009) 252-259.

Hou T-H, Su C-H, Liu W-L. Parameters optimization of a nano-particle wet milling process using the Taguchi method, response surface method and genetic algorithm. *Powder Technol.* 173 (2007) 153-162.

Jug M, Bećirević-Laćan M. Screening of Mucoadhesive Microparticles Containing Hydroxypropyl-Beta-Cyclodextrin for the Nasal Delivery of Risperidone. *Comb. Chem. High T. Scr. 10* (2007) 358-367.

Juhnke M, Märtin D, John E. Generation of wear during the production of drug nanosuspensions by wet media milling. *Eur. J. Pharm. Biopharm.* 81 (2012) 214-222.

Junyaprasert VB, Morakul B. Nanocrystals for enhancement of oral bioavailability of poorly water-soluble drugs. *Asian J. Pharm. Sci.* 10 (2015) 13-23.

Kaye RS, Purewal TS, Alpar OH. Development and testing of particulate formulations for the nasal delivery of antibodies. *J. Control. Release* 135 (2009) 127-135.

Kürti L, Gáspár R, Márki Á, Kápolna E, Bocsik A, Veszelka Sz, Bartos Cs, Ambrus R, Vastag M, Deli MA, Szabó-Révész P. In vitro and in vivo characterization of meloxicam nanoparticles designed for nasal administration. *Eur. J. Pharm. Sci.* 50 (2013) 86-92.

Kürti L, Kukovecz Á, Kozma G, Ambrus R, Deli MA, Szabó-Révész P. Study of the parameters influencing the co-grinding process for the production of meloxicam nanoparticles. *Powder Technol.* 212 (2011) 210-217.

Li X, Du L, Chen X, Ge P, Wang Y, Fu Y, Sun H, Jiang Q, Jin Y. Nasal delivery of analgesic ketorolac tromethamine thermo- and ion-sensitive *in situ* hydrogels. *Int. J. Pharm.* 489 (2015) 252-260.

Liao YH, Jones SA, Forbes B, Martin GP, Brown MB. Hyaluronan: pharmaceutical characterization and drug delivery. *Drug. Deliv.* 12 (2005) 327-342.

Lim ST, Martin GP, Berry DJ, Brown MB. Preparation and evaluation of the *in vitro* drug release properties and mucoadhesion of novel microspheres of hyaluronic acid and chitosan. *J. Control. Release* 66 (2000) 281-292.

Liu X, Wang S, Chai L, Zhang D, Suna Y, Xuc L, Sun J. A two-step strategy to design high bioavailable controlled-release nimodipine tablets: The push–pull osmotic pump in combination with the micronization/solid dispersion techniques. *Int. J. Pharm.* 461 (2014) 529-539.

Loh ZH, Samanta AK, Heng PWS. Overview of milling techniques for improving the solubility of poorly water-soluble drugs *Asian J. Pharm. Sci.* 10 (2015) 255-274.

Maggi L, Bruni G, Maietta M, Canobbio A, Cardini A, Conte U. II. Technological approaches to improve the dissolution behavior of nateglinide, a lipophilic insoluble drug: Co-milling. *Int. J. Pharm.* 454 (2013) 568-572.

Maghsoodi M, Taghizadeh O, Martin GP, Nokhodchi A. Particle design of naproxen-mannitol systems containing crystalline microcomposites. *J. Pharm. Biomed. Anal.* 56 (2011) 183-190.

Marttin E, Romeijn SG, Verhoef JC, Merkus FWHM. Nasal Absorption of Dihydroergotamine from Liquid and Powder Formulations in Rabbits. *J. Pharm. Sci.* 86 (2000) 802-807.

Meng D, Lu H, Huang S, Wei M, Ding P, Xiao X, Xu Y, Wu C. Comparative pharmacokinetics of tetramethylpyrazine phosphate in rat plasma and extracellular fluid of brain after intranasal, intragastric and intravenous administration. *Acta Pharm. Sin.* 4 (2014) 74-78.

Möschwitzer JP. Drug nanocrystals in the commercial pharmaceutical development process. *Int. J. Pharm.* 453 (2013) 142-156.

Müller RH, Gohla S, Keck CM. State of the art of nanocrystals - Special features, production, nanotoxicology aspects and intracellular delivery. *Eur. J. Pharm. Biopharm.* 78 (2011) 1-9.

Niwa T, Miura S, Danjo K. Universal wet-milling technique to prepare oral nanosuspension focused on discovery and preclinical animal studies - Development of particle design method. *Int. J. Pharm.* 405 (2011) 218-227.

Noyes AA, Whitney WR, The rate of solution of solid substances in their own solutions. *J. Am. Chem. Soc.* 19 (1897) 930-934.

Osth K, Paulsson M, Bjork E, Edsman K. Evaluation of drug release from gels on pig nasal mucosa in a horizontal Ussing chamber. *J. Control. Release* 83 (2002) 377-388.

Paltonen L, Hirvonen J. Pharmaceutical nanocrystals by nanomilling: critical process parameters, particle fracturing and stabilization methods. *J. Pharm. Pharmacol.* 62 (2010) 1569-1579.

Pathak K. Mucoadhesion; A prerequisite or a constraint in nasal drug delivery? *Int. J. Pharm. Investig.* 1 (2011) 62-63.

Patil MN, Pandit AB. Cavitation - a novel technique for making stable nano-suspensions. *Ultrason. Sonochem.* 14 (2007) 519-530.

Patil R, Bhoir P, Deshpande P, Wattamwar T, Shirude M, Chaskar P. Relevance of sonochemistry or ultrasound (US) as a proficient means for the synthesis of fused heterocycles. *Ultrason. Sonochem.* 20 (2013) 1327-1336.

Patravale VB, Date AA, Kulkarni RM. Nanosuspensions: a promising drug delivery strategy. *J. P. P.* 56 (2004) 827-840.

Pawar VK, Singh Y, Meher JG, Gupta S, Chourasia MK. Engineered nanocrystal technology: *In-vivo* fate, targeting and applications in drug delivery. *J. Control. Release* 183 (2014) 51-66.

Pomázi A, Ambrus R, Sipos P, Szabó-Révész P. Analysis of co-spray-dried meloxicam-

Pomázi A, Buttini F, Ambrus R, Colombo P, Szabó-Révész P. Effect of polymers for aerolization properties of mannitol-based microcomposites containing meloxicam. *Eur. Polym. J.* 49 (2013) 2518-2527.

Prommer E, Thompson L. Intranasal fentanyl for pain control: current status with a focus on patient considerations. *Patient. Pref. Adher.* 5 (2011) 157-164.

Raman V, Abbas A. Experimental investigations on ultrasound mediated particle breakage. *Ultrason. Sonochem.* 15 (2008) 55-64.

Salazar J, Ghanem A, Müller RH, Möschwitzer JP. Nanocrystals: Comparison of the size reduction effectiveness of a novel combinative method with conventional top-down approaches. *Eur. J. Pharm. Biopharm.* 81 (2012) 82-90.

Sandilya DK, Kannan A. Effect of ultrasound on the solubility limit of sparingly soluble solid. *Ultrason. Sonochem.* 17 (2010) 427-434.

Sinha B, Müller RH, Möschwitzer JP. Bottom-up approaches for preparing drug nanocrystals: Formulations and factors affecting particle size. *Int. J. Pharm.* 453 (2013) 126-141.

Sosnik A, Neves J, Sarmento B. Mucoadhesive polymers in the design of nano-drug delivery systems for administration by non-parenteral routes: A review. *Prog. Polym. Sci.* 39 (2014) 2030-2075.

Sushant S, Archana K. Methods of size reduction and factors affecting size reduction in pharmaceutics, *Int. Res. J. Pharm.* 4 (2013) 57-64.

Suslick KS. Sonochemistry, *Kirk-Othmer Encyclopedia of Chemical Technology* (4th ed.) J. Wiley and Sons, New York, 1998.

Swarbrick J. *Encyclopedia of Pharmaceutical Technology* (3rd ed.), Vol. 6, PharmaceuTech, Inc. USA, 2013.

Temmerman M, Jensen PD, He´bert J. Von Rittinger theory adapted to wood chip and pellet milling, in a laboratory scale hammermill. *Biomass Bioenerg.* 56 (2013) 70-81.

Wang Y, Zheng Y, Zhang L, Wang Q, Zhang D. Stability of nanosuspensions in drug delivery. *J. Control. Release* 172 (2013) 1126-1141.

Web reference 1 Manfredini & Schianchi: http://www.manfredinieschianchi.com/406-2EN-advantages-of-dry-grindiing.htm

Web reference 2 RP. King, Technical notes 8, Grinding: http://www.mineraltech.com/MODSIM/ModsimTraining/Module6/Module6.html

Web reference 3 W. Cao, Synthesis of Nanomaterials by High Energy Ball Milling: http://www.understandingnano.com/nanomaterial-synthesis-ball-milling.html

Web reference 4 Electrowave Ultrasonics Corporation: http://www.electrowave.org/Cavitation.html

Web reference 5 T. Hielscher, Ultrasonic production of nano-size dispersions and emulsions: http://www.hielscher.com

Web reference 6 Retsch®: http://pdf.directindustry.com/pdf/retsch/the-sample-high-energy-ball-mills/19308-518973.html

Zelkó R, Süvegh K. Correlation between the release characteristics of theophylline and the free volume of polyvinylpyrrolidone. *Eur. J. Pharm. Sci.* 24 (2005) 351-354.

Zhang Y, Huo M, Zhou J, Xie S. PKSolver: An add-in program for pharmacokinetic and pharmacodynamic data analysis in Microsoft Excel. *Comput. Meth. Prog. Bio.* 99 (2010) 306-314.

ACKNOWLEDGEMENTS

I am grateful to my supervisors Prof. Dr. Piroska Szabó-Révész and Dr. Rita Ambrus for their scientific guidance, encouragement and support throughout my PhD studies.

I am thankful to Dr. Mária Budai-Szűcs, Dr. Erzsébet Csányi, Gabriella Farkas and Dr. Péter Sipos for their inspiring help in my studies.

I am grateful to co-authors for cooperation and their great help.

I would like to thank Erika Boda, Zoltánné Lakatos, Klára Kovács for excellent technical assistance.

Finally, I am especially thankful to my family for their love and untiting support during my studies.

Financial support

This research was supported by Gedeon Richter Plc., and by the projects TÁMOP-4.2.2.A-11/1/KONV-2012-0047 and TÁMOP-4.2.2.A-11/1/KONV-2012-0060.

ANNEX

PUBLICATION I.

International Journal of Pharmaceutics 491 (2015) 198–207

Contents lists available at ScienceDirect

International Journal of Pharmaceutics

journal homepage: www.elsevier.com/locate/ijpharm

Study of sodium hyaluronate-based intranasal formulations containing micro- or nanosized meloxicam particles

Csilla Bartos[a,b], Rita Ambrus[a], Péter Sipos[a], Mária Budai-Szűcs[a], Erzsébet Csányi[a], Róbert Gáspár[c], Árpád Márki[c], Adrienn B. Seres[c], Anita Sztojkov-Ivanov[c], Tamás Horváth[a], Piroska Szabó-Révész[a,*]

[a] Department of Pharmaceutical Technology, University of Szeged, Szeged, Hungary
[b] Richter Gedeon Nyrt., Budapest, Hungary
[c] Department of Pharmacodynamics and Biopharmacy, University of Szeged, Szeged, Hungary

ARTICLE INFO

Article history:
Received 4 May 2015
Received in revised form 23 June 2015
Accepted 24 June 2015
Available online 30 June 2015

Keywords:
Meloxicam
Combined wet milling
Intranasal formulation
Mucoadhesivity
Permeability
AUC

ABSTRACT

This article reports on the micro- and nanonization of meloxicam (MEL) with the aim of developing pre-dispersions as intermediates for the design of intranasal formulations. As a new approach, combined wet milling technology was developed in order to reduce the particle size of the MEL. Different milling times resulted in micro- or nanosized MEL in the pre-dispersions with polyvinyl alcohol as stabilizer agent, which were directly used for preparing intranasal liquid formulations with the addition of sodium hyaluronate as mucoadhesive agent. Reduction of the MEL particle size into the nano range led to increased saturation solubility and dissolution velocities, and increased adhesiveness to surfaces as compared with microsized MEL particles. A linear correlation was demonstrated between the specific surface area of MEL and the AUC. The *in vitro* and *in vivo* studies indicated that the longer residence time and the uniform distribution of nano MEL spray throughout an artificial membrane and the nasal mucosa resulted in better diffusion and a higher AUC. Nanosized MEL may be suggested for the development of an innovative dosage form with a different dose of the drug, as a possible administration route for pain management.

1. Introduction

Intranasal administration is an alternative route for the delivery of drugs to reach the systemic circulation (Prommer and Thompson, 2011), offering certain advantages, including rapid absorption, avoidance of the hepatic first-pass metabolism and gastrointestinal side-effects and painless application, with sterility not a requirement (Meng et al., 2014). Pharmaceutical formulations delivered intranasally may be liquid (spray) (Baumann et al., 2012), gel (Osth et al., 2002) or powder forms.

In order to achieve a systemic effect, intranasal compounds can be mixed with different additives to ensure a longer residence time, better mucoadhesion (Horvát et al., 2009) and increased permeability (Chunga et al., 2010). Because of the rapid mucociliary clearance in the nasal cavity, mucoadhesive formulations are needed in order to prolong the contact time with the nasal mucosa, thereby enhancing the delivery of the drugs (Hasçiçek et al., 2003). Different agents are used to increase the mucoadhesive strength in the intranasal formulation (carbomers, chitosans, lectins, thiomers, alginate poly-ethylene glycol acrylate or poloxamer) (Pathak, 2011 and Anand et al., 2012). One of the most important biocompatible, mucoadhesive agent is sodium hyaluronate (HA). This natural anionic polysaccharide has an excellent mucoadhesive capacity (Liao et al., 2005), high biocompatibility and low immunogenicity (Ding et al., 2012). Besides its mucoadhesive properties, it may enhance the absorption of drugs and proteins via the mucosal tissues (Lim et al., 2000).

The solubility, the rate of dissolution and the permeability of drugs are of great importance (Zelkó and Süvegh, 2005), and reduction of the particle size to the micro- or nano range is therefore the strategy of first choise with the aim of increasing the bioavailability of poorly-soluble drugs (Sinha et al., 2013 and Anarjan et al., 2015). Nanoparticles are controlled by surface forces and, if the particles are not stabilized, they may coagulate because of the high particle mobility. Different additives are used to stabilize these particles: polysorbate, hydroxypropyl methylcellulose, poloxamer, polyvinylpyrrolidone, etc (Paltonen and Hirvonen,

* Corresponding author at: Department of Pharmaceutical Technology, University of Szeged H-6720 Szeged, Eötvös u. 6, Hungary. Fax: +36 62 545571.
E-mail address: revesz@pharm.u-szeged.hu (P. Szabó-Révész).

http://dx.doi.org/10.1016/j.ijpharm.2015.06.046
0378-5173/

2010). Polyvinyl alcohol (PVA) is frequently used as a stabilizer, coating the particles and promoting their separation from each other.

For particle size reduction, dry (Branham et al., 2012) and wet milling (Afolabi et al., 2014) processes are commonly used. Wet milling requires less energy and time than dry milling. Thanks to the closed system, dust is not produced and the material is less heated up (Merisko-Liversidge and Liversidge, 2011). Dry milling is used for micronization (Zhang et al., 2009), while wet milling is required for nanonization (Juhnke et al., 2012). The pre-dispersion prepared by wet milling can be utilized directly to develop liquid or semisolid formulations.

Nanosuspension drug delivery via the nose into the systemic circulation and the brain is considered a promising route. The applicability of a nanosuspension in a nasal formulation is a new approach in pharmaceutical technology, and consequently few data are available on this system. Saindane et al. (2012) incorporated a carvedilol-containing nanosuspension into an *in situ* gelling nasal spray, in order to improve the therapeutic efficacy and patient compliance. Bhavna et al. (2014) developed a donepezil-loaded nanosuspension for direct olfactory administration.

MEL, a non-steroidal anti-inflammatory drug (NSAID) was chosen in our work as a model crystalline drug because it can be administered intranasally in order to attain an analgesic effect. WHO (World Health Organization) developed the model to guide the management of different pain. NSAIDs are suggested for acute pain therapy or are co-administered as adjuvants to enhance analgesia (WHO, web reference[1]). Other analgesic NSAID agents (*e.g.* a ketorolac tromethamine-containing solution) have been administered intranasally (Li et al., 2015). A dissolved MEL-containing nasal formulation was patented by Castile et al. (2005), but a MEL-containing nanosuspension has not been described to date. MEL proved not to be toxic in a cell culture model of the nasal epithelium and did not influence the paracellular pathway (Kürti et al., 2013). MEL has poor aqueous solubility (4.4 μg/ml) (Ambrus et al., 2009) and high melting point (270 °C) (Hughey et al., 2011). We earlier investigated "top-down" methods with the aim of reducing the particle size of MEL and hence improving its bioavailability, such as dry ball-milling (Kürti et al., 2011) and high-pressure homogenization (Pomázi et al., 2013).

In order to enhance the bioavailability of MEL-containing intranasal formulations, (i) its solubility should be improved through the use of solubility-enhancing agents, *e.g.* co-solvents such as benzyl alcohol, complexing agents such as cyclodextrins, etc (for intranasal solutions) (Castile et al., 2005), (ii) its dissolution rate should be increased, *e.g.* by particle size reduction (for a liquid or gel form containing the suspended active agent), and (iii) the residence time of the formulation in the nasal cavity should be lengthened through the use of mucoadhesive agents.

We set out to utilize particle size reduction to increase the dissolution rate so as to reach a higher saturated concentration of MEL and better absorption. Pre-dispersions of micronized and nanonized MEL were produced through wet milling, applying a combination of planetary ball and pearl milling. PVA was used as an aggregation inhibiting polymer. To prepare the intranasal formulations directly from the pre-dispersions containing micro- or nanonized MEL, a low concentration of HA was used. Pre-dispersions were tested from the aspects of the particle size distribution (PSD), the habit of the MEL and the holding time. The viscoelastic character and the mucoadhesivity of the intranasal formulation was determined rheologically. We additionally investigated the influence of the MEL particle size reduction of the intranasal formulations on the *in vitro* and *in vivo* permeabilities.

[1] WHO; Pain guidelines: http://www.who.int/medicines/areas/quality_safety/delphi_study_pain_guidelines.pdf, Accessed: 02/04/2015.

2. Materials

Meloxicam (MEL) (4-hydroxy-2-methyl-N-(5-methyl-2-thiazolyl)-2H-benzothiazine-3-carboxamide-1,1-dioxide) was obtained from EGIS Ltd. (Budapest, Hungary). Piroxicam, the internal standard for the HPLC method, was purchased from Alfa Aeasar Co. (Alfa Aeasar GmbH & Co. KG, Karlsruhe, Germany). The grinding additive, PVA 4-98 ($M_w \sim 27000$), was procured from Sigma Aldrich (Sigma–Aldrich Co. LLC, St. Louis MO, US). HA ($M_w = 1400$ kDa) was obtained a gift from Gedeon Richter Plc. (Budapest, Hungary). Mucin (porcine gastric mucin type II) was from Sigma Aldrich (Sigma Aldrich Co. LLC, St. Louis MO, US).

3. Methods

The intranasal viscous liquid formulations containing suspended MEL (referred to below as nasal sprays) were prepared and characterized according to an investigational protocol (Fig. 1). The PSD, the morphology (scanning electron microscopy-SEM), the solubility of the MEL and the holding time of the pre-dispersions were determined. Nasal sprays prepared directly from the pre-dispersions were characterized in terms of the solubility of MEL and the pH and mucoadhesivity of the sprays. These intranasal formulations were subjected to both *in vitro* and *in vivo* studies.

3.1. Preparation of pre-dispersions containing micronized or nanonized MEL and preparation of intranasal formulations

On the basis of preliminary experiments, a modified wet milling technique (a combination of planetary ball and pearl milling) was employed to prepare the pre- dispersions. Intranasally administered formulations usually contain particles with a particle size from 5 to 40 μm (Billotte et al., 2003). In the optimization of the milling parameters, the particle size was set to the micro- or nanometer range in order to investigate the influence of the particle size on the dissolution rate and absorption through the nasal mucosa. 0.5 g PVA was dissolved in 17.5 ml phosphate buffer (at pH 5.6, the pH of the nasal mucosa); the solution was used as a dispersant medium in which 2.0 g of MEL was suspended. The suspension (10% drug content) was wet-milled for 10 or 50 min in the milling chamber (50 ml) of the planetary mill (Retsch PM 100) (Retsch GmbH, Haan, Germany), which resulted micronized or nanonized MEL (Table 1). The milling medium for this study was zirconium dioxide beads. The milled suspensions were separated from the beads through sieving.

The intranasal formulations were prepared directly from the pre-dispersions. 3.0 ml of the pre-dispersions were diluted with phosphate buffer (pH 5.6) in order to reach 1 mg/ml concentration of MEL and 0.15 g HA was added, therefore the final formulation contained 5 mg/ml HA. The formulations were stored in a fridge for 24 h. (in the text: raw MEL spray, micro MEL spray and nano MEL spray).

3.2. Determination of PSD

The volume-based PSD of MEL in the pre-dispersions was measured by laser diffraction (Mastersizer 2000) (Malvern Instruments Ltd, Worcestershire, UK) with the following parameters: 300RF lens; small volume dispersion unit (2500 rpm); refractive index for dispersed particles 1.720; refractive index for dispersion medium 1.330. A dynamic laser light scattering method was used to determine the PSD. Water was applied as dispersant and the

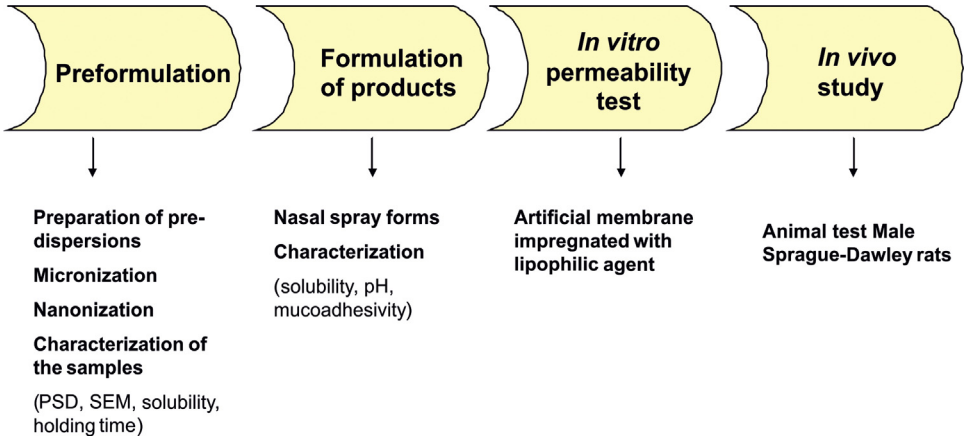

Fig. 1. Protocol of the development and characterization of nasal sprays containing MEL.

obscuration was in the range 11–16% for all measurements. In all cases, the volume-weighted PSDs, D10, D50 and D90 (where, for example, D50 is the maximum particle diameter below which 50% of the sample volume exists—also known as the median particle size by volume) were determined and evaluated. The size analysis was repeated three times. The specific surface area (SSA) was derived from the PSD data. The assumption was made that all the particles measured were spherical.

3.3. Image analysis (SEM)

Pre-dispersions were dried in a vacuum dryer (Binder GmbH, Tuttlingen, Germany) at 40 °C in order to obtain solid products for physical–chemical investigations. After drying, the shape and surface characteristics of the samples were visualized by using SEM (Hitachi S4700, Hitachi Scientific Ltd., Tokyo, Japan). The samples were sputter-coated with gold–palladium under an argon atmosphere, using a gold sputter module in a high-vacuum evaporator, and the samples were examined at 15 kV and 10 μA. The air pressure was 1.3–13 MPa.

3.4. Solubility testing of MEL

The solubility of MEL in the different pre-dispersions was determined. The pre-dispersions were stirred with a magnetic stirrer at 25 °C for 24 h and then filtered (0.1 μm, FilterBio PES Syringe Filter) (Labex Ltd., Budapest, Hungary), and the content of dissolved drug was analysed spectrophotometrically (Unicam UV/VIS) (Thermo Fisher Scientific Inc., Waltham, MA, USA). Each sample was analysed in triplicate. The pH of each nasal spray was determined (Orion 3 star pH-meter), (Thermo Fisher Scientific Inc., Waltham, MA, USA).

3.5. Holding time determination

For intermediate products such as pre-dispersions, the holding time was determined through the PSD. Pre-dispersions were stored in sealed glass bottles at room temperature (25 ± 1 °C) for 3 days. The PSD of the MEL in a prepared sample was analysed on the day of production (day 0) and after 1, 2 or 3 days of storage.

3.6. Rheology and mucoadhesion

Rheological measurements were carried out at 37 °C with a Physica MCR101 rheometer (Anton Paar GmbH, Graz, Austria). A concentric cylindrical measuring device with a diameter of 10.835 mm was used. Frequency sweep curves were plotted to determine the viscoelastic character of the samples. Storage modulus (G') and loss modulus (G") measurements were made over the frequency range from 0.01 to 100 Hz. The flow curves of the samples were also determined. The shear rate was increased from 0.1 to 100 1/s in controlled rate mode. The shearing time was 150 s.

In order to clarify the role of MEL particle size in mucoadhesion, samples with and without mucin were also prepared (Table 2); the samples containing mucin were stirred for 3 h before the

Table 1
Pre-dispersions: MEL suspended in a dispersant medium consisting of PVA and phosphate buffer.

Abbreviation in the text (pre = pre-dispersion)	rpm	Volume of the milling chamber (ml)	Milling time (min)
Raw MEL pre	–	–	0
Micro MEL pre	400	50	10
Nano MEL pre	400	50	50

Table 2
Samples for mucoadhesive measurements.

Sample name	HA (mg/ml)	PVA (mg/ml)	MEL (mg/ml)	MEL size; D50 (μm)
HA solution	5	–	–	–
PVA solution	–	0.225	–	–
Blank	5	0.225	–	–
Raw MEL spray	5	0.225	1	34.26
Micro MEL spray	5	0.225	1	1.887
Nano MEL spray	5	0.225	1	0.135

measurements (the final mucin concentration was 5% w/w). The mucoadhesivity was determined on the basis of rheological synergism between the polymer and the mucin. The synergism parameter (bioadhesive viscosity component, η_b) can be calculated from the following equation:

$$\eta_b = \eta_t - \eta_m - \eta_p,$$

where η_t is the viscosity of the mucin and polymer-containing samples, and η_m and η_p are the viscosities of the mucin and nasal spray, respectively (Hassan and Gallo, 1990). Three parallel measurements were used to determine the viscosity values (η_t, η_m and η_p) and the standard deviations.

3.7. In vitro *permeability of MEL*

In vitro permeability studies were performed on a vertical Franz diffusion cell system (Hanson Microette Topical and Transdermal Diffusion Cell System) (Hanson Research, Chatsworth CA, USA). 5 parallel measurements were carried out. The donor phase contained 300 mg of nasal formulation, which was placed on the polyvinylidene fluoride synthetic membrane (Durapore® Membrane Filter) (EMD Millipore, Billerica, MA, USA) impregnated with isopropyl myristate. The effective diffusion surface was 1.33 cm^2. Phosphate buffer (PBS, pH 7.4, 37 °C) was used as an acceptor phase (7 ml). The rotation of the stir-bar was set to 450 rpm. Sampling was carried out at 5, 10, 15, 30 and 60 min of diffusion. 0.8 ml samples were taken from the acceptor phase by autosampler (Hanson Microette Autosampling System) (Hanson Research, Chatsworth CA, USA) and were replaced with fresh receiving medium. The amount of MEL diffused was determined spectrophotometrically (Unicam UV/VIS). The flux (J) of the drug was calculated from the quantity of MEL which permeated through the membrane, divided by the surface of the membrane insert and the duration [$\mu g/cm^2/h$]. The permeability coefficient (K_p) was determined from J and the drug concentration in the donor phase (C_d [$\mu g/cm^3$]):

$$K_p\left[\frac{cm}{h}\right] = \frac{J}{Cd}.$$

For determination of the residual MEL content in the donor phase, the vertical Franz diffusion cell system was used to model the nasal cavity. The donor phase contained 300 mg of nasal formulation, which was placed on the polyvinylidene fluoride synthetic membrane (Durapore® Membrane Filter) (EMD Millipore, Billerica, MA, USA). To model the nasal environment, the membrane was impregnated with simulated nasal fluid (8.77 g NaCl, 2.98 g KCl and 0.59 g $CaCl_2$, containing 1% of mucin) (Jug and Bećirević-Laćan, 2007). The effective diffusion surface was 1.33 cm^2. Phosphate buffer (PBS, pH 7.4, 37 °C) was the acceptor phase (7 ml). The rotation of the stir-bar was set to 450 rpm. The content of the donor phase was removed after 60 min of diffusion and the amount of MEL remaining was determined with an Agilent 1260 RP-HLPC system (QP, DAD, ALS).

3.8. In vivo study of MEL

3.8.1. Intranasal administration and blood sample collection

The intranasal formulations prepared directly from the predispersions contained 1 mg/ml MEL and 5 mg/ml HA. A dose of 60 μg MEL per animal was administered into the right nostril of 160–180 g male Sprague-Dawley rats ($n = 5$) via a pipette. Directly before the drug administration, the animals were narcotized with isoflurane. Blood samples were withdrawn from the tail vein before and at 5, 15, 30 and 60 min post-dosing. The experiments performed conformed to the European Communities "Council directive for the care and use of laboratory animals" and were approved by the Hungarian Ethical Committee for Animal Research (permission number: IV/198/2013).

3.8.2. Determination of MEL from the blood samples

The MEL contents of blood samples were quantitated with an Agilent 1260HLPC system (QP, DAD, ALS). MEL and piroxicam as internal standard were separated on a 250 mm × 4.6 mm column packed with 5-μm Kromasil C_{18}, 100 Å (Phenomenex Inc., Torrance CA, USA).

Isocratic elution was performed with 45:55 (*v/v*) acetonitrile-potassium phosphate buffer solution (0.05 M) (pH adjusted to 2.7 with orthophosphoric acid) at a flow rate of 1.1 ml/min. Before use, the eluent was degassed and all the samples were filtered through a 0.20 μm PES syringe membrane filter (Phenomenex Inc., Torrance CA, USA). The total run-time was 12 min. Detection was achieved through the UV absorbance at 254 ± 4 nm. The sample injection volume was 10 μl, and the elution was performed at a column temperature of 30 °C. Qualitative determination was carried out by comparison of the spectra of standards. Primary stock solutions of MEL and piroxicam (both 0.1 mg/ml) were prepared in methanol and stored at −8 °C. Working standards of MEL and piroxicam (0.25, 0.5, 1, 2, 5, 7.5 and 10 μg/ml) were freshly prepared by diluting the stock solution with mobile phase prior to the HPLC analysis. Calibration plots of MEL and piroxicam were freshly prepared and were linear ($R^2 > 0.9996$ and 0.999, respectively) in the concentration range 0.25–10.0 μg/ml ($n = 3$). The retention times of MEL and piroxicam were 10.12 ± 0.01 and 7.36 ± 0.003 min, respectively.

Blank (drug-free) rat plasma was pooled, stored at −8 °C and used for the QC samples. The QC samples were spiked with the appropriate amount of working standard MEL and piroxicam solutions (0.5, 1, 1.5, 2 and 2.5 μg/ml ($n = 3$). Potassium phosphate buffer solution (0.03 M) (pH adjusted to 2.7 with orthophosphoric acid) was prepared as an additional extraction liquid. The limit of quantification (LOQ) was determined via the formula LOQ = SD × 3/S in which SD is the standard deviation and S is the mean slope of the calibration curve. Based on these data, the LOQ of MEL and piroxicam was calculated to be 0.171 and 0.275 μg/ml ($n = 3$), respectively.

The animal blood samples (200 μl) were diluted with 500 μl of extraction liquid and spiked with 10 μl of the working IS solution at a final plasma concentration of 1.3 μg/ml. The SPE cartridges used (Strata-X-C 33 μm Polymeric Strong Cation tubes, Phenomenex Inc., Torrance CA, USA) were conditioned with 0.5 ml of methanol, followed by 0.5 ml of extraction liquid. The prepared blood samples were allowed to run through the SPE cartridge at a flow rate of 1.0 ml/min. Cartridges were rinsed with 0.5 ml of extraction liquid and 0.5 ml methanol and dried in vacuum for 5 min. The analytes were then eluted with 0.5 ml of 5:95 (*v/v*) ammonium hydroxide-methanol elution solution. The eluent liquids were dried in a vacuum oven (Binder, Germany) at 20–30 mbar and 45 °C for 2–3 h. The dried residue was reconstituted in 300 μl of mobile phase and then vortexed (30 s), sonicated (2 min) and centrifuged at 12,000 × *g* for 5 min. 20 μl of supernatant was injected onto the C_{18} column.

Calculations of the area under the time-concentration curve (AUC) and statistical analysis

Pharmacokinetic parameters were analysed by means of PK Solver 2.0 software (Zhang et al., 2010) through non-compartmental analysis of plasma data using the extravascular input model. The area under the curve (AUC) of the time (min)–concentration (μg/ml) curves of each animal were fitted with a linear trapezoidal method. The statistical analysis was performed with Prism 5.0 software (Graphpad Software Inc., La Jolla, CA, USA). All reported data are means ± SD. Student's unpaired *t*-test was

Table 3
PSD of MEL in the pre-dispersions.

	D10 (μm)	D50 (μm)	D90 (μm)	SSA (m^2/g)
Raw MEL pre	11.40 ± 1.62	34.26 ± 4.86	73.59 ± 27.11	0.332
Micro MEL pre	0.120 ± 0.005	1.887 ± 0.112	6.429 ± 0.318	15.3
Nano MEL pre	0.077 ± 0.005	0.135 ± 0.002	0.253 ± 0.010	44.8

used to determine statistical significance. Changes were considered statistically significant at $p < 0.05$.

4. Results and discussion

4.1. Characterization of the pre-dispersions

4.1.1. PSD and morphology of MEL

The MEL particle size measured by laser diffraction decreased from approximately 35 μm to 1.887 μm during the 10 min, and to 0.135 μm during the 50 min milling time (Table 3). The SSA of MEL rose 46-fold and 135-fold as a result of the micronization and the nanonization, respectively, relative to the raw MEL in the pre-dispersion. The coating effect of PVA prevented aggregation, and the stability of the system was therefore improved.

The SEM images (Fig. 2) provided an indication of the morphology of the modified particles. We checked how the surface and shape were changed after the milling and drying as compared with the raw MEL. After milling, the pre-dispersions were dried and characterized. The raw MEL consisted mainly of angular, prismatic crystals with a broad size distribution. The micronized MEL particles (1.887 μm) consisted of aggregations of nano-sized particles. The nanonized MEL crystals (135 nm) exhibited a regular shape and a smooth surface. The treatment accounted for the smooth surfaces of the particles.

4.1.2. Solubility of MEL in the pre-dispersions

In order to check on the effects of particle size reduction on the solubility of MEL in the pre-dispersions, solubility tests were performed at 25 °C, pH 5.6 (Table 4). Micronization did not result in a change in the solubility of MEL. Following nanonization, a slight increase in solubility was observed, but the difference did not attain an order of magnitude.

4.1.3. Holding time determination

Aggregation did not occur in the pre-dispersions during the first 24 h of storage (micro MEL pre: D90 = 6.462 μm; nano MEL pre: D90 = 0.270 μm). During the second day, however, aggregates were formed in both cases (micro MEL pre: D90 = 1035.340 μm; nano MEL pre: D90 = 695.767 μm), and the number and size of the aggregates increased still further during the third day. To avoid aggregation, the pre-dispersions should be utilized to prepare the formulations within 24 h.

4.2. Characterization of the nasal sprays

Nasal sprays (raw MEL, micro MEL and nano MEL sprays) were prepared directly from the pre-dispersions with MEL of different particle sizes, using HA as a mucoadhesive polymer. The pH of the formulations did not change significantly after the addition of HA to the systems (pH 5.5) relative to the pH of the pre-dispersions (pH 5.6).

The solubility of MEL in the nasal sprays was investigated in the freshly prepared formulations after stirring for 24 h. The solubility of the drug in the sprays was increased approximately 3–5-fold (raw MEL spray: 13.9 μg/ml; micro MEL spray: 32.1 μg/ml; nano MEL spray: 42.8 μg/ml). This can be explained by the interaction between the HA and MEL which resulted in complex between the carboxylic groups in HA and the protonable groups in MEL (Battistini et al., 2013).

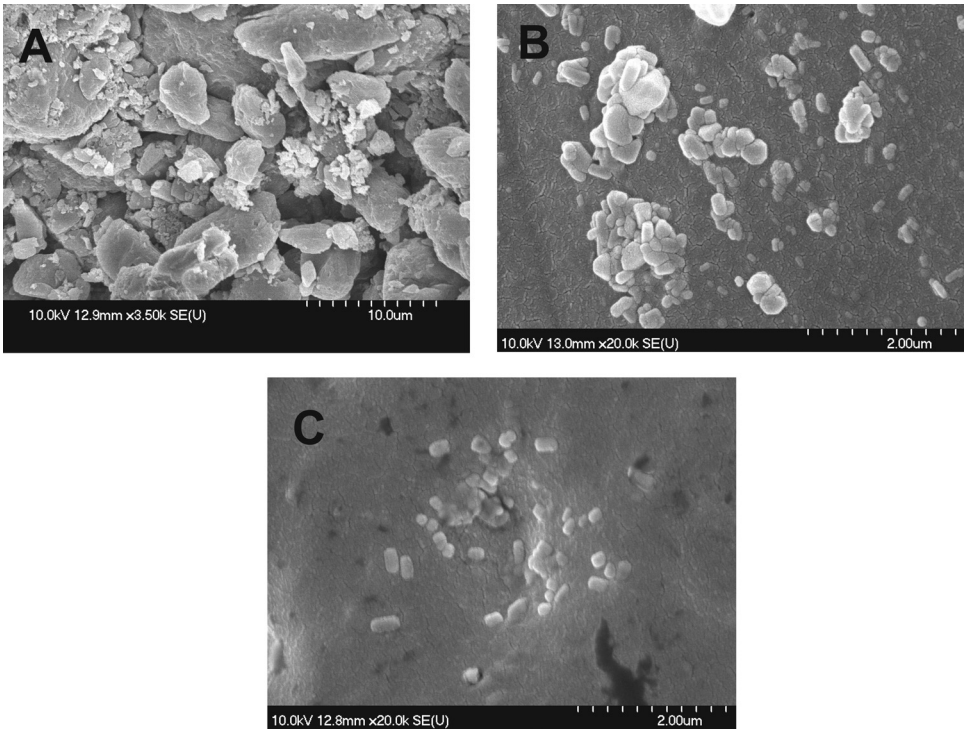

Fig. 2. SEM images of meloxicam from raw (**A**), micro (**B**) and nano (**C**) pre-dispersions.

Table 4
Solubility of MEL in the pre-dispersions.

	c (μg/ml)
Raw MEL pre	6.4 ± 0.2
Micro MEL pre	6.6 ± 0.3
Nano MEL pre	9.3 ± 0.5

4.2.1. Rheology and mucoadhesion

The viscoelastic characters of the sprays were determined by frequency sweep measurements in the range from 0.01 Hz to 100 Hz. G' corresponds to the elastic (storage) and G" to the viscous (loss) modulus. Fig. 3 presents frequency sweep curves of samples with different particle sizes (blank, MEL-free) spray, raw MEL spray, micro MEL spray, nano MEL spray). The cross-over points of these curves, which is typical for gel-containing hyaluronans, could not be seen (Berkó et al., 2013). The ratio of G' and G" indicates the sol state of the samples. The findings can be explained by the pH of the formulations (pH 5.6) and the low concentration of HA.

The intranasal formulations containing MEL displayed shear-thinning behaviour, *i.e.* the shear viscosity depended on the degree of shear load and the flow curve displayed a decreasing slope, which is typical for polymer solutions. The different formulations did not indicate changes in the flow characters (Fig. 4). The presence of MEL and variation of its particle size did not affect the viscosity of the samples, and this HA-containing drug carrier system is therefore suitable for the formulation of drugs with different particle sizes without alteration of the flow behaviour.

For the rheological determination of mucoadhesivity, the samples were mixed with mucin (final mucin concentration 5%) and the synergism parameter (bioadhesive viscosity component, η_b) was calculated. The mucoadhesivity of the HA solution in phosphate buffer (at pH 5.6), without PVA, of the PVA solution without HA, of the blank and of the three sprays with different MEL particle size were investigated.

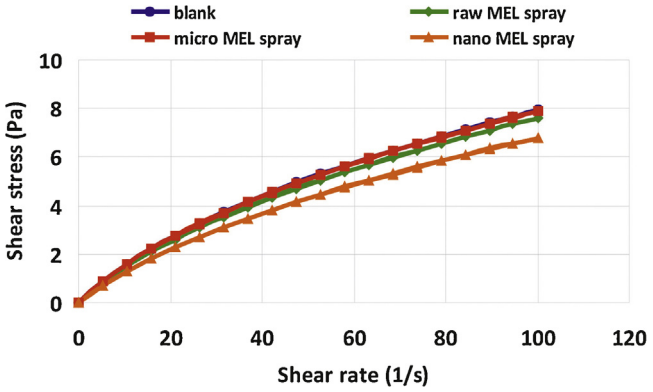

Fig. 4. Flow curves of the sprays with different MEL particle sizes.

The synergism parameter indicated the mucoadhesivity of the samples, with an interaction between the HA and the mucin (Fig. 5). PVA did not reveal mucoadhesive features, even destroy the mucin-HA interactions, accordingly the mucoadhesivity of blank decreased compared to the HA solution without PVA. Addition of MEL to the blank increased the mucoadhesivity of the formulations compared to the HA solution without PVA. This can be explained by interactions between the mucin and dispersed particles, and significant differences were observed between the calculated synergism data for the raw, micro and nano MEL samples ($p < 0.05$). The highest synergism was observed between the nasal spray containing nanonized MEL and the mucin, the mucoadhesivity increased 2-fold compared to the MEL-free blank, and hence the longest residence time could be reached. This could be explained in the one hand by the particle size of MEL; the nanosized particles have increased adhesiveness to surfaces (Müller et al., 2011). On the other hand nano sized MEL is in size of polymeric molecules, such as HA, PVA and mucin chains, which can result a well-structured complex, and better interaction among the components and thus it shows more remarkable mucoadhesivity.

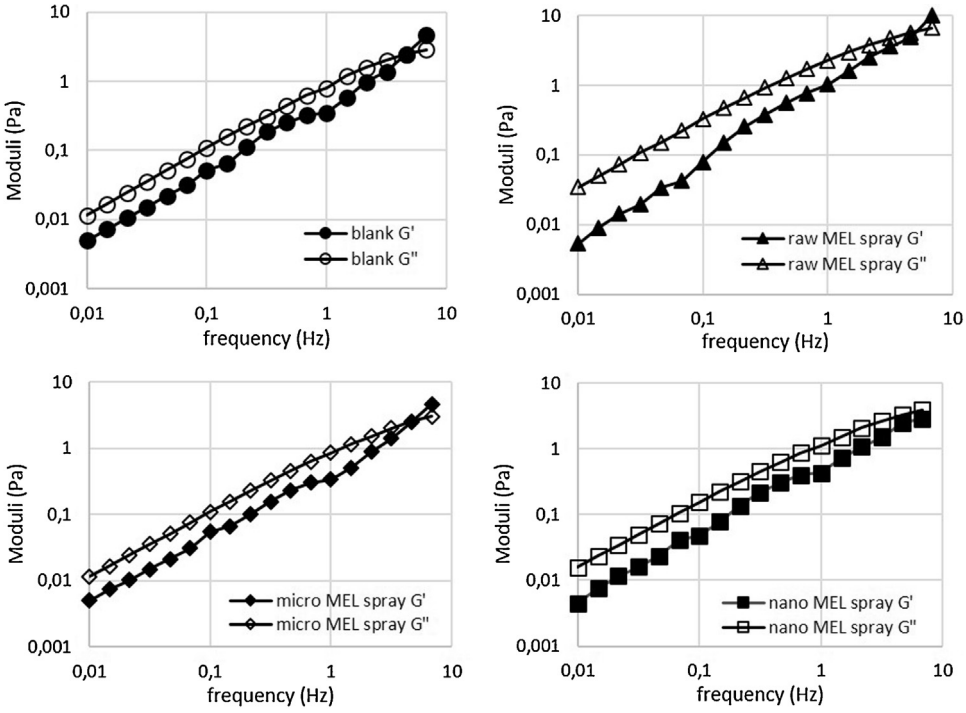

Fig. 3. Frequency sweep curves of the sprays with different MEL particle sizes.

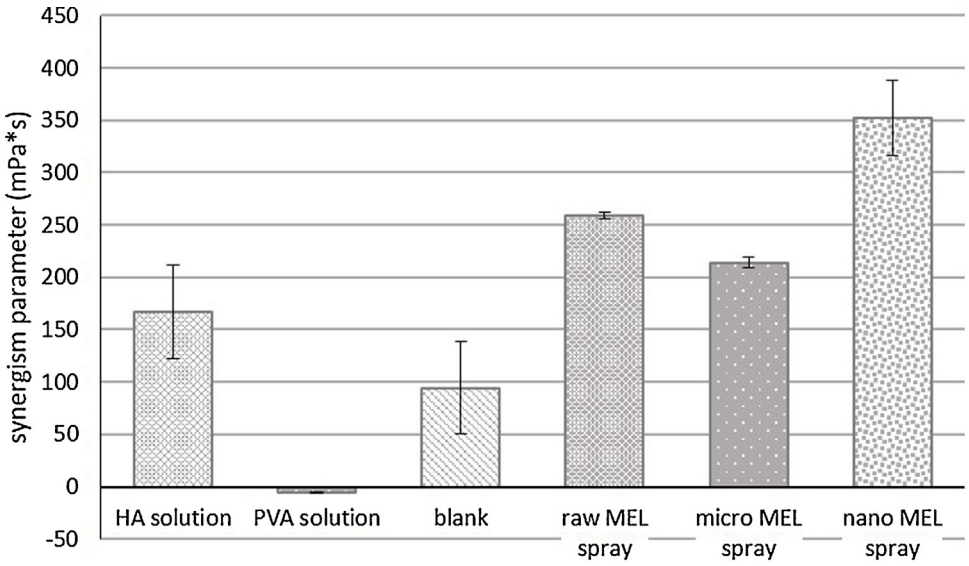

Fig. 5. Calculated synergism parameters at a shear rate of 100 1/s of samples.

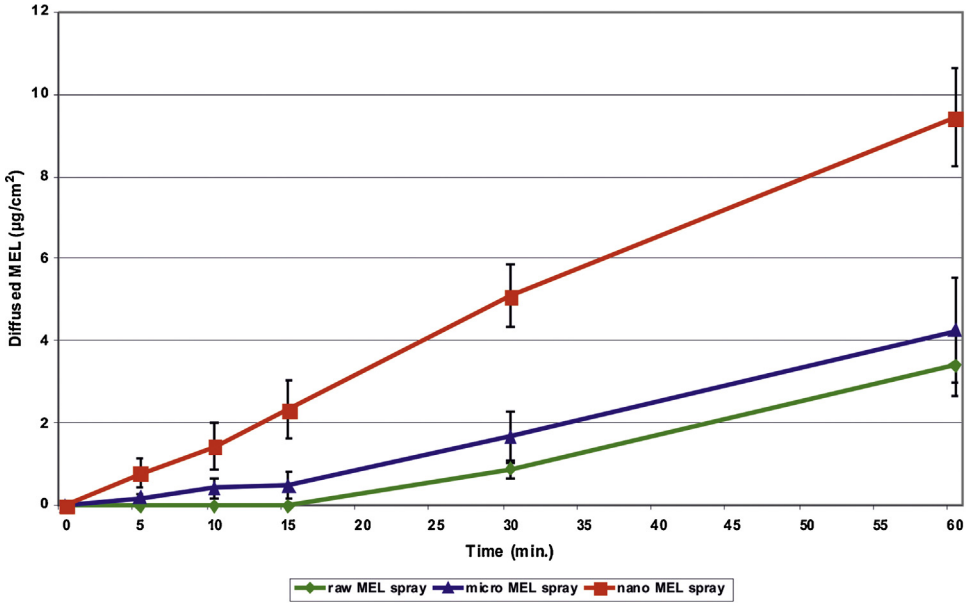

Fig. 6. *In vitro* permeability of the sprays through a synthetic membrane containing MEL with different particle sizes.

4.2.2. In vitro permeability of MEL

The cumulative amount of MEL that diffused through a synthetic membrane from a nasal spray was measured against time on a Franz diffusion cell system. The diffusion from the formulation containing MEL nanoparticles was the quickest, due to the rapid dissolution of the drug. The diffusion started in the first 5 min from the nanonized MEL-containing spray (Fig. 6). As concerns the fastest diffusion, the question arose as to whether it was influenced by the particle size or some other factor. It should be excluded that the nanosized MEL particles (D50 = 0.135 μm) passed through the membrane without dissolving (they dissolved in the acceptor phase). Since the particle size was larger than the membrane pore size (100 nm) and the membrane was impregnated with isopropyl myristate, this phenomenon was not observed. In this case, therefore, the particle size and the resulting surface area had significant effects on the rate of passive diffusion.

The flux (J), which shows the amount of MEL that permeates through 1 cm^2 of the membrane within 1 h, was significantly increased in the case of the nasal formulation which contained nanoparticles as compared with the sprays containing micronized or raw MEL. The permeability coefficient (K_p) calculated from the flux data for the nanonized MEL was also significantly higher than in the other two cases (Table 5).

Table 5
Flux (J) and permeability coefficient (K_p) values of nasal sprays containing MEL with different particle sizes.

	J [μg/cm^2/h]	K_p [cm/h]
Raw MEL spray	3.41	0.00341
Micro MEL spray	4.25	0.00425
Nano MEL spray	9.43	0.00943

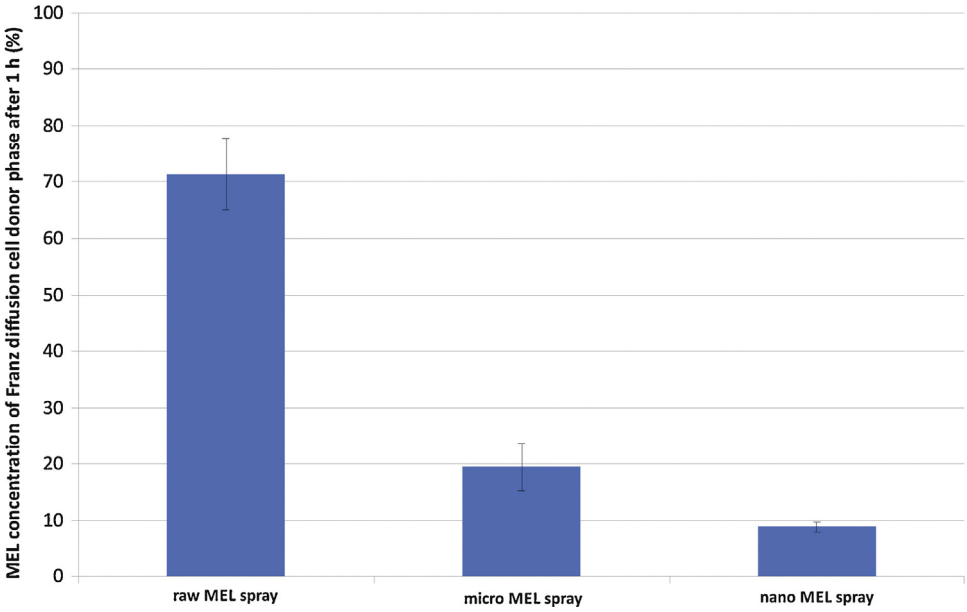

Fig. 7. Remained MEL content in the donor phase.

The particle size was a determining factor as regards the amount of diffused MEL. In the spray containing nanonized MEL, the faster dissolution of the particles resulted in higher permeability.

It was revealed that the nasal mucosa retained the MEL and its particle size did not influence the permeability. Fig. 7 demonstrates significant differences between the MEL content remaining in the donor phase: 71.38 ± 6.33% (raw MEL spray), 19.52 ± 4.18% (micro MEL spray) and 8.85 ± 0.94% (nano MEL spray). The residual MEL content in the donor phase correlated well with the decreasing MEL particle size of the spray samples.

4.2.3. In vivo studies of MEL

The drug concentration in the blood plasma as a function of time after nasal administration of the sprays is shown in Fig. 8. In the case of the spray containing MEL nanoparticles, a 3 times higher plasma level of MEL was observed after 5 min as compared with the formulations containing raw or micronized MEL. This result is in accordance with the particle size reduction of MEL, and especially with the faster dissolution of nanonized MEL as compared with that of the microsized agent. The plasma concentrations tended to increase slowly during the first approximately 30 min, but the 3-fold difference between the sprays containing nanonized or micronized MEL remained during 60 min after treatment.

The AUC is proportional to the amount of drug absorbed during the investigated time interval. The calculated AUC values gradually increased with decreasing particle size (the highest AUC was observed for the nano MEL spray; Fig. 9). Micronization did not significantly increase the AUC as compared with raw MEL ($AUC_{rawMELspray}$: 13.97 ± 3.223 min μg/ml, $AUC_{microMELspray}$: 21.95 ± 5.527 min μg/ml, $p = 0.1552$), whereas nanonization led to a significant increase of the amount of MEL absorbed ($AUC_{nanoMELspray}$: 49.86 ± 5.632 min μg/ml; nano MEL spray *vs*

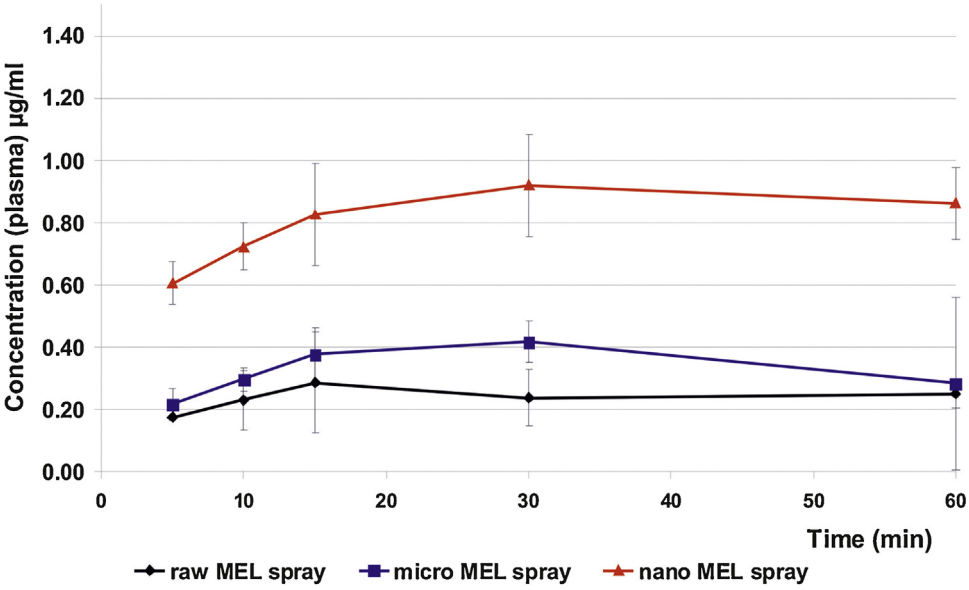

Fig. 8. Plasma drug concentration *vs.* time profiles in rats after intranasal administration of the sprays containing MEL with different particle sizes.

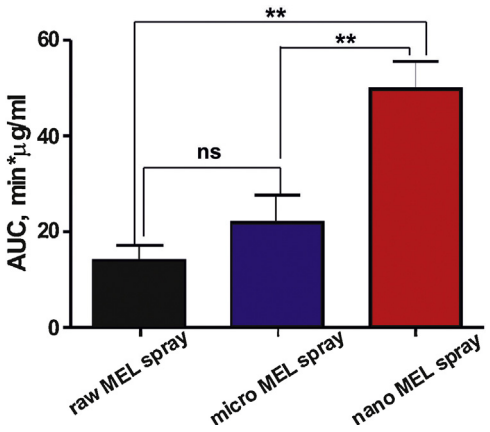

Fig. 9. AUC of the sprays containing MEL with different particle sizes.

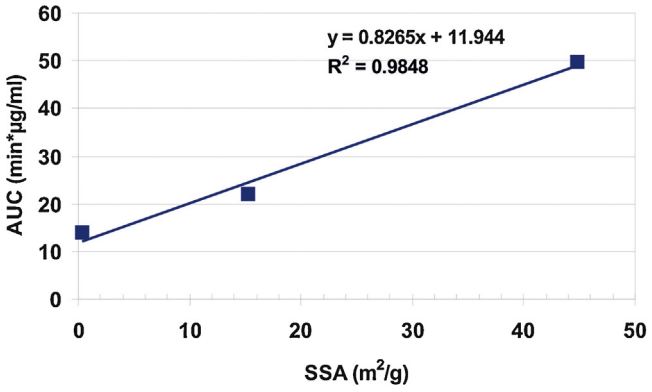

Fig. 10. Correlation between the AUC and different MEL particle sizes.

raw MEL spray: $p = 0.0021$; nano *vs* micro MEL spray: $p = 0.0061$). Our results demonstrated a strict correlation between the AUC and the MEL particle size ($R^2 = 0.9848$) (Fig. 10).

5. Conclusions

A combination of planetary ball and pearl milling can be applied as a wet milling procedure to decrease the particle size of MEL. Depending on the milling time, micro- and nanosized particles can be produced. This wet milling technology was suitable for the preparation of pre-dispersions in the presence of PVA as additive, which were then directly applicable for the development of innovative liquid nasal pharmaceutical formulations.

Intranasal viscous sprays were prepared from micronized and nanonized MEL-containing pre-dispersions with HA as mucoadhesive agent, which is important from the aspect of a longer residence time. The pre-dispersions as intermediate products were suitable for preparing intranasal formulations for use within 24 h.

Nasal absorption can be improved not only by increasing the transcellular and paracellular uptake of a drug through the nasal mucosa; increase of its saturation solubility in the nasal fluid results in passive diffusion and a higher plasma concentration. Reduction of the MEL particle size into the nano range resulted in special features of the nanocrystals (Müller et al., 2011), such as increased saturation solubility and dissolution velocities, and increased adhesiveness to surfaces as compared with microsized MEL particles. The higher SSA and the enhanced saturation solubility of the nano MEL spray resulted in rapid dissolution of the drug and a higher AUC. The linear correlation between the SSA of MEL and the AUC ($R^2 = 0.9848$) confirmed that the dissolution of particles with different sizes is the key factor determining the amount of drug absorbed.

The adhesiveness of nanonized MEL to the nasal mucosa is another important advantage of this system because of the longer contact time in the nasal cavity. Different mucoadhesivities were measured for the nanonized MEL-HA-mucin system and microsized MEL-containing sprays. The *in vitro* and *in vivo* studies indicated that the longer residence time and the uniform distribution of the nano MEL spray throughout an artificial membrane and the nasal mucosa resulted in better diffusion and a higher AUC. Thanks to the better adhesion and distribution of the nanoparticles and the formation of a well-structured system, the release of MEL was controlled. This controlled release was enhanced by the HA-PVA system (Battistini et al., 2013). The PVA-coated particles played a role in the release of the drug, because the synthetic polymers reduced the rate of degradation of the natural polymers and prevented their rapid dissolution in the biological fluids (Ding et al., 2012).

Our results indicate that nanosized MEL may be suggested for the development of an innovative intranasal liquid dosage form to decrease the acute pain or it may be added as an adjuvant to enhance analgesia.

References

Afolabi, A., Akinlabi, O., Bilgili, E., 2014. Impact of process parameters on the breakage kinetics of poorly water-soluble drugs during wet stirred media milling: a microhydrodynamic view. Eur. J. Pharm. Sci. 51, 75–86.
Ambrus, R., Kocbek, P., Kristl, J., Šibanc, R., Rajkó, R., Szabó-Révész, P., 2009. Investigation of preparation parameters to improve the dissolution of poorly water-soluble meloxicam. Int. J. Pharm. 381, 153–159.
Anand, U., Feridooni, T., Agu, R.U., 2012. Novel Mucoadhesive Polymers for Nasal Drug Delivery, in: Sezer, A.D., (Ed.), Pharmacology, Toxicology and Pharmaceutical Science, Halifax, pp. 315–330.
Anarjan, N., Jafarizadeh-Malmiri, H., Nehdi, I.A., Sbihi, H.M., Al-Resayes, S.I., Tan, C.P., 2015. Effects of homogenization process parameters on physicochemical properties of astaxanthin nanodispersions prepared using a solvent diffusion technique. Int. J. Nanomed. 10, 1109–1118.
Battistini, F.D., Olivera, M.E., Manzo, R.H., 2013. Equilibrium and release properties of hyaluronic acid–drug complexes. Eur. J. Pharm. Sci. 49, 588–594.
Baumann, D., Bacher, C., Högger, P., 2012. Development of a novel model for comparative evaluation of intranasal pharmacokinetics and effects of anti-allergic nasal sprays. Eur. J. Pharm. Biopharm. 80, 156–163.
Berkó, Sz., Maroda, M., Bodnár, M., Erős, G., Hartmann, P., Szentner, K., Szabó-Révész, P., Kemény, L., Borbély, J., Csányi, E., 2013. Advantages of cross-linked versus linear hyaluronic acid for semisolid skin delivery systems. Eur. Polym. J. 49, 2511–2517.
Bhavna, Md, S., Ali, M., Ali, R., Bhatnagar, A., Baboota, S., Ali, J., 2014. Donepezil nanosuspension intended for nose to brain targeting: *in vitro* and *in vivo* safety evaluation. Int. J. Biol. Macromol. 67, 418–425.
Billotte, A., Dunn, P.J., Henry, B.T., Marshall, P.V., Woods, J.J., inventors; Pfizer Research And Development Company N.V./S.A., Billotte A., Dunn P.J. et al., assignees. Intranasal formulations for treating sexual disorders. Canadian Intellectual Property Office CA 2275554C. 2003 Jun 3. accessed: 05/01/2015.
Branham, M.L., Moyo, T., Govender, T., 2012. Preparation and solid-state characterization of ball milled saquinavir mesylate for solubility enhancement. Eur. J. Pharm. Biopharm. 80, 194–202.
Castile, J.D., Lin, W., Smith, A., Watts, P.J., inventors. Intranasal formulation of meloxicam. World Intellectual Property Organization patent WO 2005021041 A1. 2005 March 10. accessed: 03/11/2014.
Chunga, T.W., Liu, D.Z., Yang, J.S., 2010. Effects of interpenetration of thermo-sensitive gels by crosslinking of chitosan on nasal delivery of insulin: *in vitro* characterization and *in vivo* study. Carbohyd. Polym. 82, 316–322.
Ding, J., He, R., Zhou, G., Tang, C., Yin, C., 2012. Multilayered mucoadhesive hydrogel films based on thiolated hyaluronic acid and polyvinylalcohol for insulin delivery. Acta Biomater 8, 3643–3651.
Hasçiçek, C., Gönül, N., Erk, N., 2003. Mucoadhesive microspheres containing gentamicin sulfate for nasal administration: preparation and *in vitro* characterization. II Farmaco 58, 11–16.
Hassan, E.E., Gallo, J.M., 1990. A simple rheological method for the *in vitro* assessment of mucin-polymer bioadhesive bond strength. Pharm. Res. 7, 491–495.
Horvát, S., Fehér, A., Wolburg, H., Sipos, P., Veszelka, S.z., Tóth, A., Kis, L., Kurunczi, A., Balogh, G., Kürti, L., Erős, I., Szabó-Révész, P., Deli, M.A., 2009. Sodium hyaluronate as a mucoadhesive component in nasal formulation enhances delivery of molecules to brain tissue. Eur. J. Pharm. Biopharm. 72, 252–259.

Hughey, J.R., Keen, J.M., Brough, C., Saeger, S., McGinity, J.W., 2011. Thermal processing of a poorly water-soluble drug substance exhibiting a high melting point: the utility of KinetiSol® Dispersing. Int. J. Pharm. 419, 222–230.
Jug, M., Bećirević-Laćan, M., 2007. Screening of mucoadhesive microparticles containing hydroxypropyl-beta-cyclodextrin for the nasal delivery of risperidone. Comb. Chem. High T. Scr. 10, 358–367.
Juhnke, M., Märtin, D., John, E., 2012. Generation of wear during the production of drug nanosuspensions by wet media milling. Eur. J. Pharm. Biopharm. 81, 214–222.
Kürti, L., Gáspár, R., Márki, Á., Kápolna, E., Bocsik, Á., Veszelka, S.z., Bartos, C.s., Ambrus, R., Vastag, M., Deli, M.Á., Szabó-Révész, P., 2013. *In vitro* and *in vivo* characterization of meloxicam nanoparticles designed for nasal administration. Eur. J. Pharm. Sci. 50, 86–92.
Kürti, L., Kukovecz Á, Kozma, G., Ambrus, R., Deli, M.A., Szabó-Révész, P., 2011. Study of the parameters influencing the co-grinding process for the production of meloxicam nanoparticles. Powder Technol. 212, 210–217.
Li, X., Du, L., Chen, X., Ge, P., Wang, Y., Fu, Y., Sun, H., Jiang, Q., Jin, Y., 2015. Nasal delivery of analgesic ketorolac tromethamine thermo- and ion-sensitive in situ hydrogels. Int. J. Pharm. 489, 252–260.
Liao, Y.H., Jones, S.A., Forbes, B., Martin, G.P., Brown, M.B., 2005. Hyaluronan: pharmaceutical characterization and drug delivery. Drug Deliv. 12, 327–342.
Lim, S.T., Martin, G.P., Berry, D.J., Brown, M.B., 2000. Preparation and evaluation of the *in vitro* drug release properties and mucoadhesion of novel microspheres of hyaluronic acid and chitosan. J. Control. Release 66, 281–292.
Meng, D., Lu, H., Huang, S., Wei, M., Ding, P., Xiao, X., Xu, Y., Wu, C., 2014. Comparative pharmacokinetics of tetramethylpyrazine phosphate in rat plasma and extracellular fluid of brain after intranasal, intragastric and intravenous administration. Acta Pharm. Sin. B 4, 74–78.
Merisko-Liversidge, E., Liversidge, G.G., 2011. Nanosizing for oral and parenteral drug delivery: a perspective on formulating poorly-water soluble compounds using wet media milling technology. Adv. Drug. Deliv. Rev. 63, 427–440.
Müller, R.H., Gohla, S., Keck, C.M., 2011. State of the art of nanocrystals—special features production. Nanotoxicol. Aspects Intracellular Deliv. Eur. J. Pharm. Biopharm. 78, 1–9.
Osth, K., Paulsson, M., Bjork, E., Edsman, K., 2002. Evaluation of drug release from gels on pig nasal mucosa in a horizontal Ussing chamber. J. Control. Release 83, 377–388.
Paltonen, L., Hirvonen, J., 2010. Pharmaceutical nanocrystals by nanomilling: critical process parameters, particle fracturing and stabilization methods. J. Pharm. Pharmacol. 62, 1569–1579.
Pathak, K., 2011. Mucoadhesion: a prerequisite or a constraint in nasal drug delivery? Int. J. Pharm. Investig. 1, 62–63.
Pomázi, A., Buttini, F., Ambrus, R., Colombo, P., Szabó-Révész, P., 2013. Effect of polymers for aerolization properties of mannitol-based microcomposites containing meloxicam. Eur. Polym. J. 49, 2518–2527.
Prommer, E., Thompson, L., 2011. Intranasal fentanyl for pain control: current status with a focus on patient considerations. Patient Pref. Adher. 5, 157–164.
Saindane, N.S., Pagar, K.P., Vavia, P.R., 2012. Nanosuspension based in situ gelling nasal spray of carvedilol: development, *in vitro* and *in vivo* characterization. Pharm. Sci. Technol. 14, 189–199.
Sinha, B., Müller, R.H., Möschwitzer, J.P., 2013. Bottom-up approaches for preparing drug nanocrystals: formulations and factors affecting particle size. Int. J. Pharm. 453, 126–141.
Zelkó, R., Süvegh, K., 2005. Correlation between the release characteristics of theophylline and the free volume of polyvinylpyrrolidone. Eur. J. Pharm. Sci. 24, 351–354.
Zhang, L., Xu, H., Li, S., 2009. Effects of micronization on properties of Chaenomeles sinensis (Thouin) Koehne fruit powder. Innov. Food Sci. Emerg. 10, 633–637.
Zhang, Y., Huo, M., Zhou, J., Xie, S., 2010. PKSolver: an add-in program for pharmacokinetic and pharmacodynamic data analysis in microsoft excel. Comput. Methods Programs Biomed. 99, 306–314.

PUBLICATION II.

Chemical Engineering and Processing 87 (2015) 26–34

Contents lists available at ScienceDirect

Chemical Engineering and Processing: Process Intensification

journal homepage: www.elsevier.com/locate/cep

Comparison of static and dynamic sonication as process intensification for particle size reduction using a factorial design

Csilla Bartos [a,b], Ákos Kukovecz [c,d], Rita Ambrus [a], Gabriella Farkas [a], Norbert Radacsi [a,*], Piroska Szabó-Révész [a]

[a] Department of Pharmaceutical Technology, University of Szeged, Eötvös u. 6, H-6725 Szeged, Hungary
[b] Richter Gedeon Nyrt., Gyömrői út 19-21, H-1103 Budapest, Hungary
[c] Department of Applied and Environmental Chemistry, University of Szeged, Rerrich Béla tér 1, H-6720 Szeged, Hungary
[d] MTA-SZTE Lendület Porous Nanocomposites Research Group, Rerrich Béla tér 1, H-6720 Szeged, Hungary

ARTICLE INFO

Article history:
Received 12 June 2014
Received in revised form 25 September 2014
Accepted 30 October 2014
Available online 1 November 2014

Keywords:
Acoustic cavitation
Static sonication
Dynamic sonication
Factorial design
Particle size reduction

ABSTRACT

This article reports on particle engineering by a top-down method involving organic solvent-free acoustic cavitation as a wet-grinding procedure. The effects of static and dynamic sonication on particle size reduction methods were compared to each other. The most effective process parameters were determined by a factorial design plan for the particle size distribution of an important active pharmaceutical ingredient, meloxicam, as response factor after sonication. Samples sonicated with appropriate process parameters were dried and investigated. Scanning electron microscopy images showed that the sonication resulted in a rounded shape and micronized size of the particles. Differential scanning calorimetry and X-ray powder diffraction examinations revealed the crystalline structure of the produced meloxicam by both sonication methods. Fourier transform infrared spectroscopy demonstrated that no chemical degradation occurred. Static sonication is recommended primarily for particle size reduction in preclinical samples, where the amount of the drug candidate is very small (e.g. nasal formulation), while dynamic sonication may be suitable for wet-grinding of different active substances to prepare pre-suspension (e.g. micronization and nanonization).

1. Introduction

Particle design techniques are widely used for the modification of the physico-chemical and biopharmaceutical properties of Active Pharmaceutical Ingredients (APIs) [1]. Particle engineering techniques, controlling the crystal size distribution and morphology can offer improvements for the solubility, dissolution rate and permeability of poorly water-soluble drugs and can open up new, alternative administration routes, e.g. intranasally route, where the particle size (over 10 μm) is a determining factor [2–4]. Process Intensification (PI) has the goal of making substantial improvements to the efficiency of chemical processes and plants by developing innovative methods and equipment [5]. Innovative methods for these improvements can be the useage of alternative energy forms, like centrifugal fields, ultrasounds, microwaves, solar energy, electric fields, or plasmas [6]. The advantages of intensified product design processes consist of intensified process control, and/or improved product quality.

There are many different types of size reduction techniques; dry and wet grinding can be distinguished. During the wet grinding, due to the closed system the formation of dust is prevented. Less energy and time is required for grinding, the heating of the materials is reduced and after grinding the suspension can be directly used for production formulations.

Acoustic cavitation is a novel wet grinding possibility for controlling the crystal size distribution and morphology of drugs, primarily with the aim of particle size reduction [7,8]. It has the ability to erode and break down particles and increase the specific surface area of crystals [9]. It has been proven that application of ultrasound technology in the frequency range of 20–100 kHz can induce particle size reduction [10]. During the sonication process, the ultrasound waves that form in the liquid media result in alternating high-pressure and low-pressure cycles, with rates depending on the frequency. In the low-pressure cycle the high-intensity ultrasonic waves evolve small gas- or vapor-filled bubbles (cavities) in the liquid. When the bubbles reach a volume at which they can no longer absorb energy, they collapse violently during a

* Corresponding author. Tel.: +36 62545571.
E-mail address: kefehu@gmail.com (N. Radacsi).

http://dx.doi.org/10.1016/j.cep.2014.10.015
0255-2701/

high-pressure cycle. This phenomenon is called ultrasonic cavitation. The implosion of vacuum bubbles breaks down particles [11]. Ultrasonic liquid processing is described by a number of parameters (amplitude, pressure, temperature and concentrations of compounds). The effect of the process may be determined as a function of the energy (E) divided by the processed volume (V):

$$\text{effect} = f\left(\frac{E}{V}\right)$$

The energy (*E*[*Ws*]) can calculate from the power output (*P*[W]) and the duration of exposure (*t*[s]):

$$E[J] = PW] \times tS]$$

The function alters with changes in the individual parameters. Additionally, the actual power output per surface area of the sonotrode of an ultrasonic unit depends on the parameters as was written by Hielscher [12].

There are two sonication routes for wet-grinding to achieve particle size reduction. One is the static method, which means that a sample at rest is sonicated. Another possibility is the dynamic method, which allows the continuous circulation of the sample by means of a pump during the sonication. These two methods are appropriate for particle size reduction of materials with different physico-chemical properties [13]. The production of intermediates (suspension form for example for preparation of nasal spray and gel) and powder products (after drying) is carried out by applying a short-term ultrasound energy input. Application of ultrasounds can be easily scaled up, e.g. sonification is successfully applied at industrial level for the preparation of metal nanoparticles [14]. Sonochemistry involves the use of an ultrasound technique to promote chemical reactions [15]. As regards pharmaceutics, power ultrasound can be applied for emulsification and to investigate the sedimentation of emulsions and suspensions [16,17]. Supercritical, solvent diffusion [18] and melt emulsification are well-known bottom-up methods techniques in the field of sonocrystallization for solving solubility problems of drugs [19]. The disintegration of drug particles (top-down approach) has not widely investigated so far for improving properties of drugs.

Meloxicam (MEL) is a NSAID (non-steroidal anti-inflammatory drug) with anti-inflammatory, analgesic and antipyretic effects, it can be used intranasally. MEL was chosen as a model crystalline drug because of its poor aqueous solubility [20] and high melting point (270 °C) [21].

This research investigates the applicability of ultrasound technology for intensified particle size reduction and the setting of the process. Since the literature data relating to the application of ultrasound for the particle size reduction of drug materials are lacking, in this study the static and dynamic sonication methods are compared to each other (as organic solvent-free wet-grinding techniques) and their effects in reducing the particle size of MEL are investigated, using the excipient, PVP K-25, as an agglomeration inhibitor. A two-level fractional factorial design was used to determine the most effective process parameters, and the effects of ultrasound on the physico-chemical properties of MEL were studied.

2. Experimental

2.1. Materials

Meloxicam (4-hydroxy-2-methyl-N-(5-methyl-2-thiazolyl)-2H-benzothiazine-3-carboxamide-1,1-dioxide) was obtained from EGIS Ltd. (Budapest, Hungary). The grinding additive, PVP K-25 (polyvinylpyrrolidone), was purchased from BASF (Ludwigshafen, Germany).

2.2. Methods

2.2.1. Preparation of sonicated formulations

In our systems water was used as a liquid for the sonication studies. Meloxicam has poor aqueous solubility (4.4 μg/mL). PVP is a dispersant, it is used in the pharmaceutical industry as a synthetic polymer vehicle for dispersing and suspending drugs. The presence of weak bonding between the carboxyl group of Meloxicam and the PVP helps the molecules to separate from each other. The aggregation is prevented, therefore stability of the system could be improved. In other case, PVP can work as a wetting agent, but does not increase the solubility and dissolution of the drug significantly. In each sample, 0.5% of PVP K-25 was dissolved in an appropriate volume of water (25 and 100 mL respectively for static and dynamic sonication) at pH 5.56. Before sonication, the suspensions were stirred with a magnetic stirrer for 5 min. A high-power ultrasound device (Hielscher UP 200 S Ultrasonic processor, Germany) operating at 200 W was applied as the energy input in the sample preparation in order to achieve a particle size reduction. The working wavelength of the ultrasound used in the treatment was 6.6 cm. T. During the sonication energy is transmitted from the probe directly into the sample with high intensity and the sample is processed quickly. In the case of static sonication, samples at rest were treated (the suspensions were not circulated). In the case of dynamic sonication, the samples were circulated continuously with a peristaltic pump (Heidolph PD 5006 Pump drive) in a double-walled flow cell (Flow Cell GD14 K) during the sonication. The temperature was set with a thermostat in both cases (Julabo, Germany).

The height of the medium was 8 cm in case of the dynamic sonication and 2 cm by 25 mL and 3.5 cm by 100 mL in the case of static sonication. The wavelength of the ultrasound used in the treatment was 6.6 cm. Applying different sonotrode positions, the immersed surface area of the ultrasonic horn could be changed (Fig. 1). The surface area of the ultrasonic horn in contact with the sample was determined by the amount of the immersed area of the cylinder and of the tip surface of the probe. It was 0.15 cm^2 in case

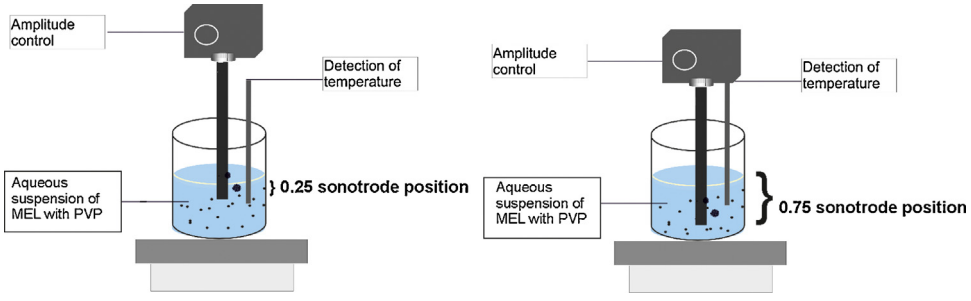

Fig. 1. Sonotrode positions in the aqueous suspension of MEL with PVP.

of the static sonication using 25 mL sample volume and at 0.25 position (means that the sonotrode was immersed to 25% of the total depth of the liquid); and 8.8 cm^2 by the position of 0.75 (the sonotrode was immersed to 75% of the total depth of the liquid). In the case of the static sonication and 100 mL sample volume, at the 0.75 position the immersed surface area was 6.77 cm^2 and at position 0.25 the immersed surface area was 1.23 cm^2. During the dynamic sonication the immersed surface area of the ultrasonic horn was constant 12 cm^2. The applied sonication parameters are given in Table 1.

Adiabatic experiments were carried out to reveal the efficiency of the transmission of the ultrasonic energy into the liquid (Fig. 2). The appropriate volume of 0.5% PVP-solution was used without the presence of meloxicam. The temperature was mesured in every 5 min, from 0 to 30 minutes under sonication processing. The temperature rise was the most notable in the case of small sample volume (25 mL). Within 5 min 90 °C could be reached using 25 mL solution. The dynamic and static methods were compared with the following parameters: 100 mL sample volume, 0.25 sonotrode position. In the case of static sonication after 10 min the temperature was higher, meaning higher energy input. In the case of the dynamic method the temperature increase was slower, due to the circulation in the vessel.

2.2.2. Preparation of solid products for physical-chemical investigations of pure MEL

Suspensions prepared with the chosen parameters were dried in order to obtain solid products for physical-chemical investigations. Samples were filtered through filter paper (MUNKTELL Filter Discs, Grade: 1290, pore size: 3–5 μm, diameter: 185 mm), the filtrate was washed with the medium of the suspension (0.5% aqueous solution of PVP K-25, pH 5.56) and the wet crystals were dried in a vacuum dryer (Binder, Germany) at 40 °C in order to obtain solid products. After drying, the percentage yield was determined and the physico-chemical properties of the products were investigated.

2.2.3. Determination of particle size distribution and specific surface area by a laser diffraction method

The volume based particle size distribution (PSD) of the raw MEL was measured by laser diffraction (Mastersizer 2000, Malvern Instruments Ltd. Worcestershire, UK) with the following parameters: 300RF lens; small volume dispersion unit (2500 rpm); refractive index for dispersed particles 1.720; refractive index for dispersion medium 1.330. Dynamic Laser Light Scattering method was used to determine the PSD. The MEL particle size was determined directly on the initial suspension in water in which PVP was dissolved. The size analysis was repeated three times. Water was used as dispersant and the obscuration was in the range 11–16% for all measurements in both cases. In all cases, the volume weighted particle size distributions, D10, D50, and D90 (where for example D50 is the maximum particle diameter below which 50% of the sample volume exists–also known as the median particle size by volume) were determined and evaluated.

Table 1
The applied sonication parameters.

	Static sonication	Dynamic sonication
Volume (mL)	25; 100	100
Position	0.25; 0.75	0.25
RPM (pump)	–	50; 100
Concentration of MEL (mg/mL)	2; 18	2; 18
Temperature (°C)	0; 36	0; 36
Amplitude (%)	30; 70	30; 70
Time (min.)	10; 30	10; 30

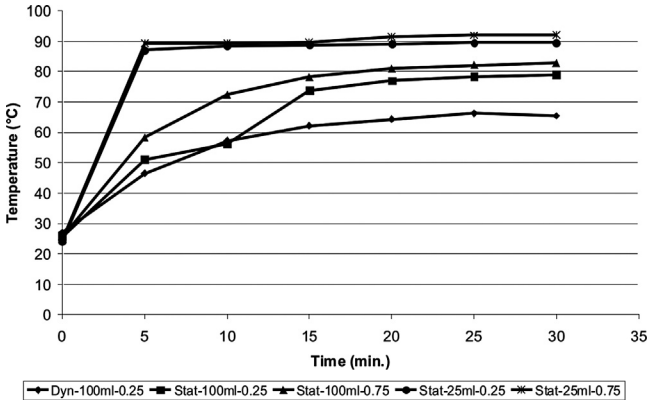

Fig. 2. Results of the adiabatic investigations for appropriate volume of 0.5% PVP solution without the presence of MEL.

The specific surface area was derived from the particle size distribution data. The assumption was made that all the particles measured were spherical.

2.2.4. Image analysis

The shape and surface characteristics of the samples were visualized by using a scanning electron microscope (Hitachi S4700, Hitachi Scientific Ltd. Tokyo, Japan). The samples were sputter-coated with gold–palladium under an argon atmosphere, using a gold sputter module in a high-vacuum evaporator and the samples were examined at 15 kV and 10 μA. The air pressure was 1.3–13 MPa. In suspensions prepared with the most effective parameters PVP was washed out and the crystals were dried in order to obtain solid particles for SEM analyses.

2.2.5. Design of experiments

Six parameters were screened in the static sonication experiments, using a two-level fractional factorial design of resolution III. Here, the main effects are not confounded with each other, whereas they are confounded with two-factor interactions. This design is typically used for the rapid identification of the main effects governing the behavior of a multi-parameter system. High and low values for each parameter were set on the basis of our prior experience with similar tasks (reported in Table 1). Dynamic sonication experiments were run by screening five parameters, using the same experimental design type. High and low parameter values for the dynamic sonication experiments are presented in Table 1, as well. All the experiments were run as triplicates.

2.2.6. Further investigations of the products

2.2.6.1. X-ray powder diffraction analysis (XRPD). The physical state of the MEL in the samples was evaluated by XRPD. XRPD patterns were produced with an X-ray Diffractometer Miniflex II (Rigaku Co. Tokyo, Japan), where the tube anode was Cu with Kα = 1.5405 Å. The pattern was collected with a tube voltage of 30 kV and a tube current of 15 mA in step scan mode (4° min^{-1}). The instrument was calibrated by using Si.

2.2.6.2. Differential scanning calorimetry (DSC). DSC measurements were carried out with a Mettler Toledo DSC 821^e thermal analysis system with the STAR^e thermal analysis program V9.0 (Mettler Inc. Schwerzenbach, Switzerland). Approximately 2–5 mg of pure drug or product was examined in the temperature range between 25 °C and 300 °C. The heating rate was 5 °C min^{-1}. Argon was used as carrier gas at a flow rate of 10 Lh^{-1} during the DSC investigations.

2.2.6.3. Fourier transform infrared (FT-IR) spectroscopy. FT-IR spectra were recorded with a Bio-Rad Digilab Division FTS-65A/896 FTIR spectrometer (Bio-Rad Digilab Division FTS-65A/869, Philadelphia, USA) between 4000 and 400 cm^{-1}, at an optical resolution of 4 cm^{-1}, operating conditions: Harrick's Meridian SplitPea single reflection, diamond, ATR accessory. Thermo Scientific GRAMS/AI Suite software (Thermo Fisher Sciencific Inc. Waltham, USA) was used for the spectral analysis.

For all of these investigations PVP was washed out and the crystals were dried.

3. Results and discussion

3.1. Effects of process parameters on particle size distribution

3.1.1. Static sonication

An analysis of the results measured by laser diffraction revealed that the static sonication under the various sonication parameters resulted in a roughly 25–70% decrease in average MEL particle size. The D10, D50 and D90 values are reported in Table 2.

Their relationship with the sonication variables was analyzed quantitatively on the basis of the D50 data in the main effects plots (Fig. 3.) and interaction plots (Fig. 4.). The D10 and D90 data furnished similar results. A main effect plot for a given parameter is obtained by averaging the results of each run where this parameter was set to low or to high, and connecting these averages with a line. If the studied parameters are independent, the plot gives a clear indication of the response of the system to the selected variable. The main effects plots for the MEL particle size distribution indicated that the small sample volume, the high amplitude and the long sonication time were preferred for efficient particle size reduction whereas the position of the sonotrode, the concentration of the solution and the temperature influenced the particle size less (Fig. 3.). It can be seen that small sample volume, high ultrasound amplitude and the long sonication time were preferred for efficient particle size reduction.

Interaction plots show the effects between variables, which are not necessarily independent, by showing the means of the responses for each level of a factor for each level of a second factor pairwise for all factors involved in the study. The interaction plots presented in Fig. 4 for D50 can be used to gain insight into the complex interactions between the sonication parameters. Longer sonication time resulted in a particle size reduction, independently of the other process parameters. The connection between the physical parameters of sonication (amplitude, position and volume) was unequivocal. The high amplitude resulted in a particle size decrease independently of the sonotrode position and sample volume. The connection between concentration, temperature and amplitude demonstrated that the particle size reduction effect of the increased amplitude occurred at low concentration and high temperature. The relationships between temperature and concentration, and temperature and volume, were unidirectional, in contrast with the temperature position relationship: increase of the temperature was useful in the lower position. At the high concentration the upper, while at the low concentration the lower position resulted in smaller particles.

To summarize the results, the appropriate parameters found for static sonication were the long time sonication (30 min), the high amplitude (70%), the small sample volume (25 mL), the high temperature (36 °C), the lower position of the sonotrode (0.75) and the low MEL concentration (2 mg/mL). In the sample at rest, the distribution of the sonication effect was inhomogeneous; the region near the sonotrode (therefore in a small volume) was the most effective. Because of the large energy input and long sonication, increased amplitude was required to achieve small particles. The larger energy investment resulted in increased cavitation activities. When the temperature was raised, the kinetic energy of the particles increased, which adverse affected the cohesive forces. When the low concentration of MEL was used, the amount of energy per particle was greater.

3.1.2. Dynamic sonication

Analysis of the produced MEL measured by laser diffraction revealed that the dynamic sonication under the various sonication parameters resulted in a roughly 15–60% decrease in the average particle size. The size distribution function is reported in Table 3.

The relationship between the sonication variables were analyzed quantitatively on the basis of the D50 data in the main effects plots (Fig. 5.) and interaction plots (Fig. 6). The D10 and D90 data furnished similar results. The main effects plots for the MEL particle size distribution indicated that the circulation of the sample at the low rpm, the high amplitude and the long sonication time resulted in the most significant particle size reduction, whereas the concentration of the suspension influenced the particle size less. The high temperature had a more significant effect on the particle size under dynamic sonication than under static sonication.

The interaction plots presented in Fig. 6. for D50 can be used to gain insight into the complex interactions between the sonication parameters. The increased amplitude and the higher temperature resulted in significant particle size reduction. The longer sonication time had no appreciable effect in the case of the low temperature and the low amplitude. The increase of the concentration had an adverse effect on the particle size at the low circulation rate.

As a conclusion, it may be stated that the most effective process parameters for dynamic sonication were the long sonication time (30 min.), the high amplitude (70%) and temperature (36 °C), the low rotation rate (50 rpm) and the low concentration of the samples (2 mg/mL). Due to the continuous circulation of the samples, the distribution of the sonication effect was homogeneous. The cavitation reduced the particle size efficiently at the low circulation rate. The sample was resident in the cavitation space for a longer period during one sonication cycle. The explanation of the effects of the other parameters is the same as in the case of the static method.

Table 2
Results of static sonication (suspension).

Volume (mL)	Position of sonotrode	Conc (mg/mL)	Temp (°C)	Amplitude (%)	Time (min)	D10 (μm)	D50 (μm)	D90 (μm)
–	–	–	–	–	–	10.82	34.03	75.81
25	0.75	2	36	70	30	1.51	10.16	19.53
100	0.75	2	0	30	30	4.81	23.07	46.88
25	0.25	2	0	70	10	2.75	18.45	42.87
100	0.25	2	36	30	10	5.92	26.52	53.39
25	0.75	18	36	30	10	3.95	19.62	41.51
100	0.75	18	0	70	10	5.19	24.16	46.98
25	0.25	18	0	30	30	3.53	17.12	29.22
100	0.25	18	36	70	30	7.19	20.83	36.62

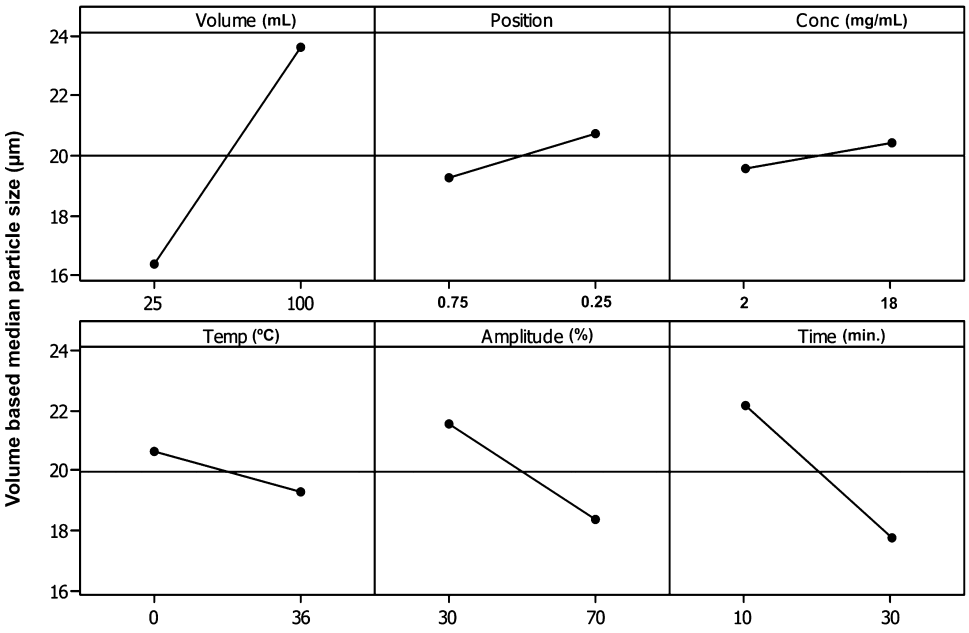

Fig. 3. The main effect plots for the case of static sonication.

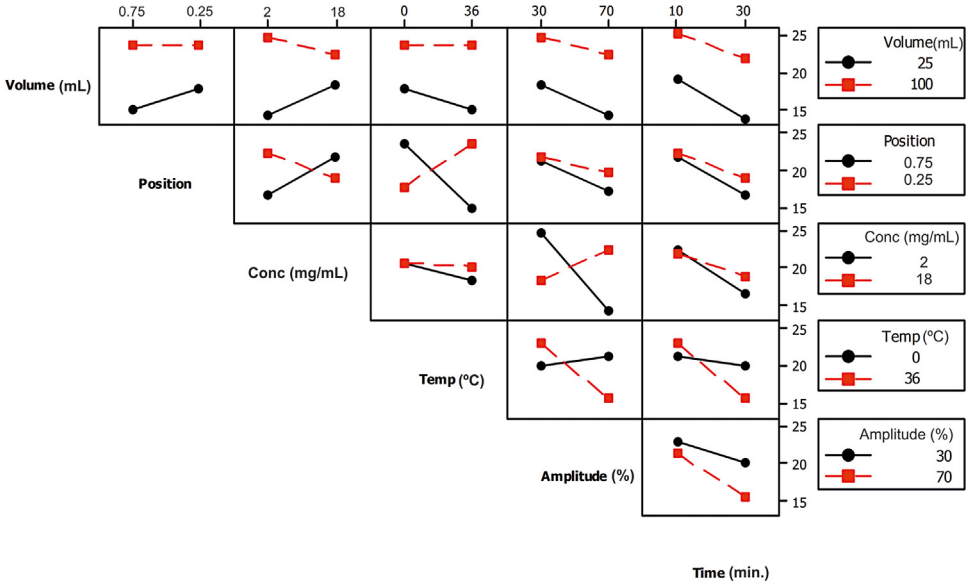

Fig. 4. Interaction plots of the main effects for the static sonication.

3.2. Particle size distribution and specific surface area

The particle size distribution of MEL (Fig. 7) was determined in the suspensions after sonications. During the dynamic sonication the sample is circulated continuously by a pump, which ensures the homogeneous sonication effect. In case of the static sonication a sample at rest is sonicated, so the cavitation effect distribution can be inhomogeneous. The raw MEL had a broad size distribution.

Table 3
Results of dynamic sonication (suspension).

Pump (rpm)	Conc (mg/mL)	Temp (°C)	Amplitude (%)	Time (min)	D10 (µm)	D50 (µm)	D90 (µm)
–	–	–	–	–	10.82	34.03	75.81
50	2	36	70	30	2.20	14.60	35.02
50	2	0	30	30	4.56	24.22	47.05
100	2	0	70	10	5.70	26.90	51.92
100	2	36	30	10	5.90	26.15	52.20
50	18	36	30	10	4.40	22.69	53.54
50	18	0	70	10	6.27	23.54	46.77
100	18	0	30	30	9.06	29.31	45.58
100	18	36	70	30	2.87	16.73	38.03

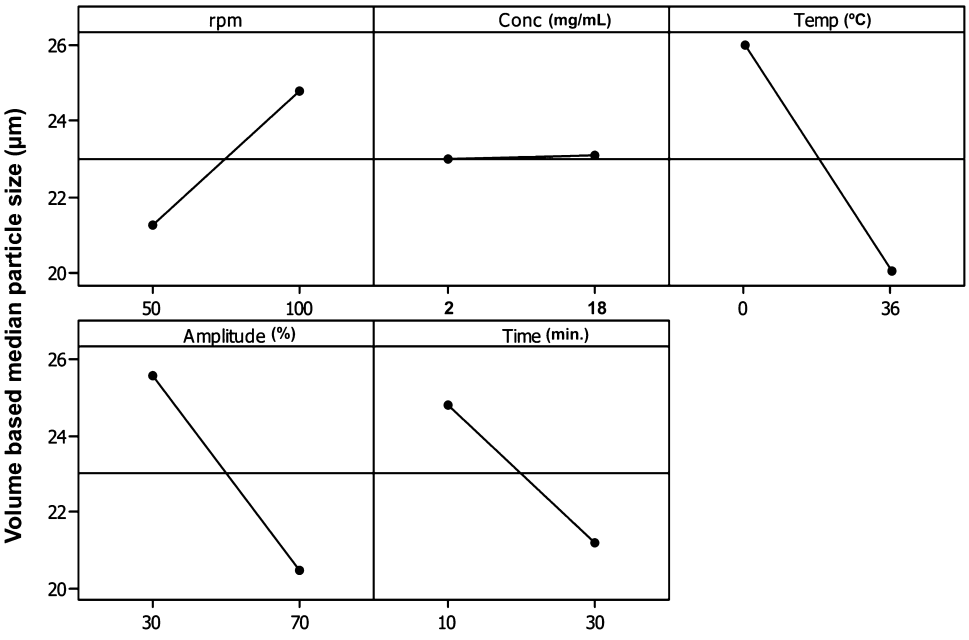

Fig. 5. The main effect plots for the case of dynamic sonication.

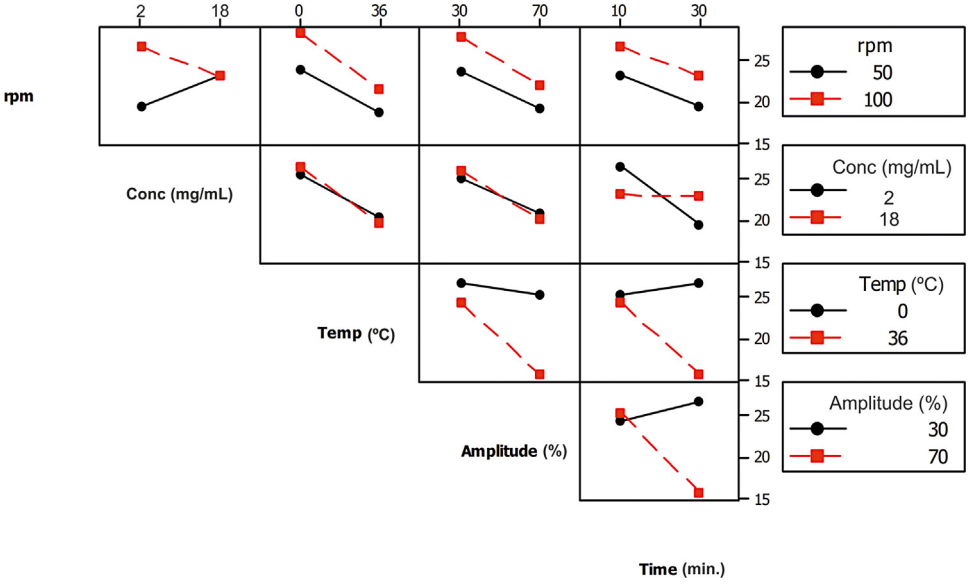

Fig. 6. Interaction plots for the dynamic sonication.

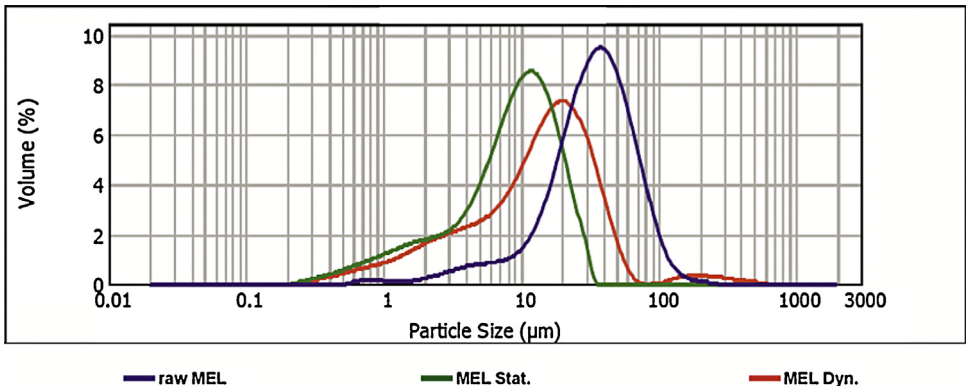

Fig. 7. Particle size distribution of raw MEL and sonicated MEL from suspensions.

Table 4
The specific surface area and size distribution of the raw MEL and the two suspensions from sonication.

	Specific surface area (m^2/g)	D10 (μm)	D50 (μm)	D90 (μm)
raw MEL	0.340	10.82	34.03	75.81
Static sonicated sample (suspension)	2.040	1.51	10.16	19.53
Dynamic sonicated sample (suspension)	1.140	2.20	14.60	35.02

The sonication methods resulted in decreased particles size. The specific surface area of the MEL increased as a consequence of acoustic cavitation in both sonication methods and for both suspensions relative to the raw MEL. The static sonication produced smaller particle sizes compared to the dynamic sonication (Table 4).

3.3. Characterization of the dried products

3.3.1. Particle shape and size

The SEM images (Fig. 8) provided an indication of the morphology of the modified particles. PVP was washed out to check how the surface and shape changed after the sonications compare with raw MEL. The crystal habit of the pure MEL has changed significantly after the procedure. The raw MEL consisted mainly of angular, prismatic crystals with a broad size distribution. The crystal lattice presumably demonstrated defects and cracks. Along them the crystals disintegrated due to the energy input of acoustic cavitation. Probably this factor is responsible for the presence of the broken pieces, which are found on the surface of the larger particles. The drying of the samples could also cause cracks and widen the PSD. The endurance during the treatment is accounted for the roundness and smooth surfaces of the crystals. The yields of the samples were 95% at 0 °C and 90% at 36 °C by both methods. The average size of the dried product was approximately 10 μm in the case of static and 15 μm in the case of dynamic sonication. Due to the high specific surface area of the dried product and since PVP is washed out, agglomeration might occur. Furthermore, aging or washing might also change the crystal size and shape.

3.3.2. X-ray diffraction

The XRPD pattern of pure MEL demonstrated its crystalline structure, as expected. The raw MEL and the sonicated dried MEL composite in both cases displayed the same X-ray diffraction patterns (see supporting information, Fig. S1.). This means that the crystalline form of the micronized MEL was not changed by the sonication and drying procedure.

3.3.3. Differential scanning calorimetry (DSC)

DSC was employed to investigate the crystallinity and the melting of MEL in the pure form and in the sonicated dried products. The DSC curve (Fig. 9) of the raw MEL revealed a sharp endothermic peak at 259.11 °C, reflecting its melting point and confirming its crystalline structure. After drying, the DSC curves exhibited the sharp endothermic peak of the MEL at 258.62 °C in the static case, and at 259.81 °C in the dynamic case, indicating that the crystallinity of the drug was retained. The value of the enthalpy and the onset-endset interval were not changed significantly for the sonicated products as compared with the values for raw MEL, and it can therefore be concluded, that the degree of crystallinity was not decreased by the treatment.

3.3.4. Chemical stability

To determine whether any decomposition occurred during the sonication process, FT-IR spectroscopy was carried out. This proved that no disintegration took place in the samples (Fig. 10). Also the contamination of solution with titanium particles by the cavitational erosion could not be detected. The applied energy did not cause chemical changes in the MEL in aqueous medium during sonication (30 min) at 36 °C. The characteristic bands of MEL were

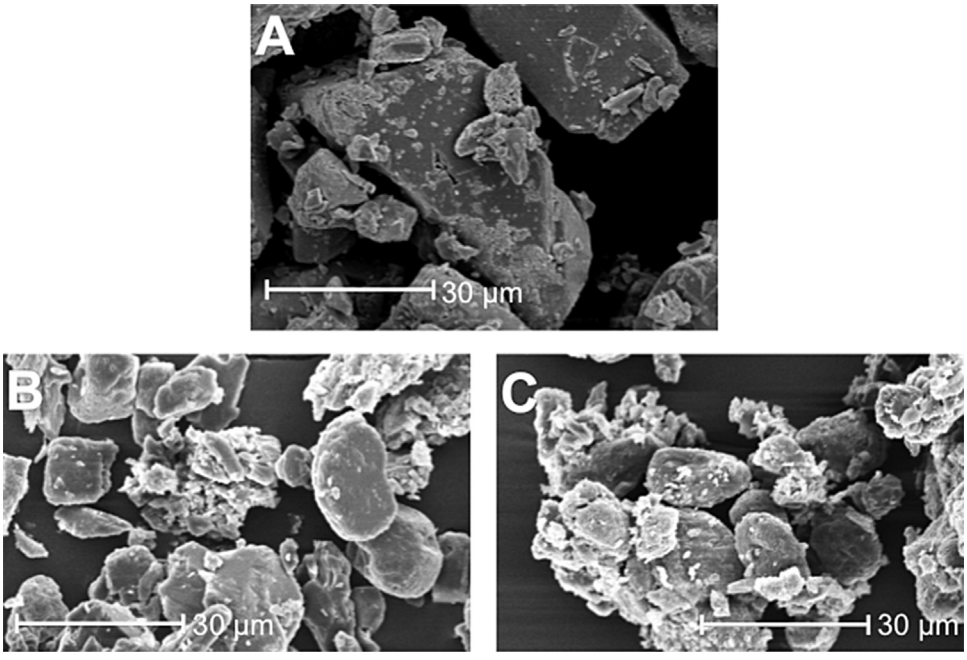

Fig. 8. SEM pictures of raw MEL (A) and the dried products after static (B) and dynamic (C) sonication after 30 min treatment (PVP was washed out).

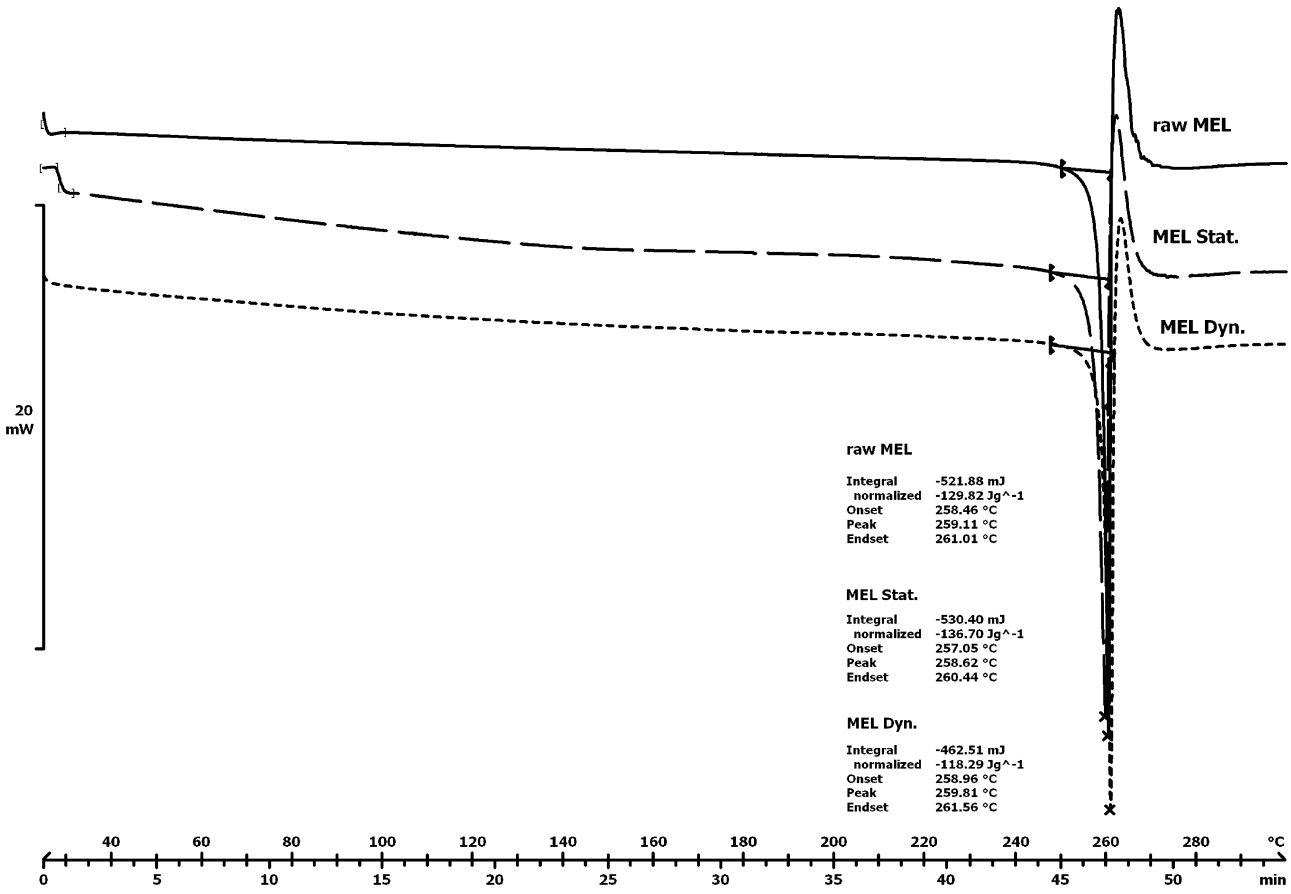

Fig. 9. DSC curves of the raw MEL and the dried sonicated products.

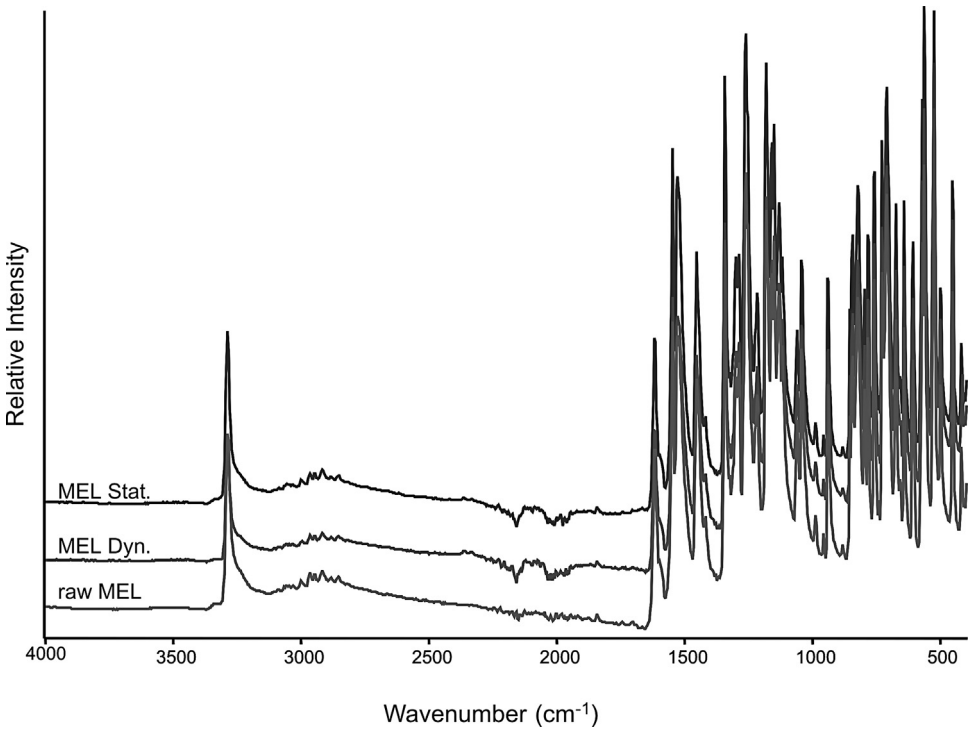

Fig. 10. FT-IR curves of raw MEL and dried sonicated products.

seen in all of the curves of the raw MEL and sonicated products, at 3289.76, 1550.04, 1530.36, 1346.73, 1265.88 and 1184.90 cm^{-1}, denoting the stretching vibration of -NH, the thiazole ring (together with that at 1184.90 cm^{-1}), the amide II band of–CO–NH–C, the asymmetric stretching vibration of the sulfone and the amide III band of–CO–NH–C, respectively.

4. Conclusions

Acoustic cavitation, as a wet-grinding procedure, can be applied to decrease the particle size and change the crystal morphology of drugs. High-intensity ultrasound equipment is easy to clean because of the few moving parts. The parameters can be set precisely and reproduced. Sonication in aqueous medium adheres to green technology: the product does not contain organic solvent residues.

This study applied a two-level factorial design plan to compare the process parameters of static and dynamic sonication methods based on their particle size reduction effects. A long sonication, a high amplitude, a high temperature and a low concentration of MEL proved to play important roles in the sonication procedures. Both of these disintegration methods with adequate process parameters involving a change in crystal habit, may decrease the particle size of MEL significantly in the presence of PVP as additive.

The investigation of the dried products showed that in both cases the crystallinity of the MEL was retained during the sonication and the process did not cause chemical degradation.

The static method is applicable for the preparation of preclinical samples with a reduced particle size of the drug candidate, for which a small sample volume is sufficient.

Dynamic sonication is suitable for preformulation of a micro-suspension, because a larger volume of sample can be used in this method. Standardization is possible, which is important for industry.

These two methods are also appropriate for particle size reduction of materials with different physico-chemical properties, applying a short-term energy input, and for the production of intermediate (in suspension form) and (after drying) dried products for additional pharmaceutical formulations.

Acknowledgements

The financial support of the projects TÁMOP-4.2.2.A-11/1/KONV-2012-0047 and TÁMOP-4.2.2.A-11/1/KONV-2012-0060 is acknowledged.

Appendix A. Supplementary data

Supplementary data associated with this article can be found, in the online version, at http://dx.doi.org/10.1016/j.cep.2014.10.015.

References

[1] M. Maghsoodi, O. Taghizadeh, G.P. Martin, A. Nokhodchi, Particle design of naproxen-disintegrant agglomerates for direct compression by a crystallo-co-agglomeration technique, Int. J. Pharm. 351 (2008) 45–54.
[2] A. Pomázi, R. Ambrus, P. Sipos, P. Szabó-Révész, Analysis of co-spray-dried meloxicam-mannitol systems containing crystalline microcomposites, J. Pharm. Biomed. Anal. 56 (2011) 183–190.
[3] H. Kublik, M.T. Vidgren, Nasal delivery systems and their effect on deposition and absorption, Adv. Drug Deliv. Rev. 29 (1998) 157–177.
[4] H.K. Chan, Dry powder aerosol drug delivery-opportunities for colloid and surface scientists, Colloids Surf. A: Physicochem. Eng. Aspects 284–285 (2006) 50–55.
[5] A. Van Gerven, T. Stankiewicz, Structure, energy synergy, time the fundamentals of process intensification, Ind. Eng. Chem. Res. 48 (2009) 2465–2474.
[6] A. Stankiewicz, Reactive separations for process intensification: an industrial perspective, Chem. Eng. Process.: Process Intensif. 42 (2003) 137–144.
[7] M.N. Patil, A.B. Pandit, Cavitation – a novel technique for making stable nano-suspensions, Ultrason. Sonochem. 14 (2007) 519–530.
[8] V. Raman, A. Abbas, Experimental investigations on ultrasound mediated particle breakage, Ultrason. Sonochem. 15 (2008) 55–64.
[9] D.K. Sandilya, A. Kannan, Effect of ultrasound on the solubility limit of sparingly soluble solid, Ultrason. Sonochem. 17 (2010) 427–434.
[10] K.S. Suslick, Sonochemistry, in: Kirk-Othmer Encyclopedia of Chemical Technology, (4th ed.) J. Wiley and Sons, New York (1998) pp. 517–541.
[11] P. Braeutigam, M. Franke, R.J. Schneider, A. Lehmann, A. Stolle, B. Ondruschka, Water Res, Degradation of carbamazepine in environmentally relevant concentrations 46 (2012) 2469–2477.
[12] T. Hielscher, Ultrasonic production of nano-size dispersions and emulsions, http://www.hielscher.com
[13] P. Cs. Bartos, Szabó-Révész, R. Ambrus, Optimization of technological parameters by acoustic cavitation to achieve particle size reduction, Farmacia 62 (2014) 34–46.
[14] D. Chen, D. Li, Y. Zhang, Z. Kang, Preparation of magnesium ferrite nanoparticles by ultrasonic wave-assisted aqueous solution ball milling, Ultrason. Sonochem. 20 (2013) 1337–1340.
[15] R. Patil, P. Bhoir, P. Deshpande, T. Wattamwar, M. Shirude, P. Chaskar, Relevance of sonochemistry or ultrasound (US) as a proficient means for the synthesis of fused heterocycles, Ultrason. Sonochem. 20 (2013) 1327–1336.
[16] O. Behrend, K. Ax, H. Schubert, Influence of continuous phase viscosity on emulsification by ultrasound, Ultrason. Sonochem. 7 (2000) 77–85.
[17] E. Benes, M. Grösschl, B. Handl, F. Trampler, H. Nowotny, Das europaische TMR-Netzwerk Ultrasonic Separation of Suspended Particles, Proc. Joint Symposium AAA and ÖPG TC Acoustics Graz, Austria 2 (1998) 14–15.
[18] U.N. Hatkar, P.R. Gogate, Process intensification of anti-solvent crystallization of salicylic acid using ultrasonic irradiation, Chem. Eng. Process. 57–58 (2012) 16–24.
[19] R. Ambrus, N.N. Amirzadi, Z. Aigner, P. Szabó-Révész, Formulation of poorly water-soluble Gemfibrozil applying power ultrasound, Ultrason. Sonochem. 19 (2012) 286–291.
[20] R. Ambrus, P. Kocbek, J. Kristl, R. Šibanc, R. Rajkó, P. Szabó-Révész, Investigation of preparation parameters to improve the dissolution of poorly water-soluble meloxicam, Int. J. Pharm. 381 (2009) 153–159.
[21] J.R. Hughey, J.M. Keen, C. Brough, S. Saeger, J.W. McGinity, Thermal processing of a poorly water-soluble drug substance exhibiting a high melting point: the utility of KinetiSol® Dispersing, Int. J. Pharm. 419 (2011) 222–230.

PUBLICATION III.

Acta Pharmaceutica Hungarica 84. 1-5 2014.

Szónikus kavitáció alkalmazása hatóanyag szemcseméretének csökkentésére[1*]

BARTOS CSILLA[1,2], AMBRUS RITA[1], SZABÓNÉ RÉVÉSZ PIROSKA[1*]

[1]*Szegedi Tudományegyetem, Gyógyszertechnológiai Intézet, Szeged, Eötvös u. 6-6720*
[2]*Richter Gedeon Nyrt., Budapest, Gyömrői út 19-21-1103*
**Levelezési cím: revesz@pharm.u-szeged.hu*

Summary

Bartos, Cs., Ambrus, R., Szabó-Révész, P.: ***Particle size reduction using acoustic cavitation***

Different pharmaceutical technological processes have been used for modification of the physico-chemical and biopharmaceutical properties of drugs. Changes of crystal size, distribution and morphology can open up new, alternative administration routes, e.g. intranasally and the pulmonary route, where the particle size is a determining factor. A wet grinding method based on acoustic cavitation (the collapse of bubbles or voids formed by sound waves) is a novel possibility for modification of the properties of particles. During our work this wet grinding technique was studied. The effect of this method was investigated on particle size reduction. The samples were treated with extreme sonication parameters. The effect of the concentration of the polymer was examined on the particle size reduction. Meloxicam was chosen as a model crystalline drug because of its poor aqueous solubility. The structural characterization and the morphological analysis of the dried products were carried out by DSC, XRPD and SEM. It was found that the acoustic cavitation resulted in crystalline micronized product.

Keywords: *meloxicam, particle size reduction, acoustic cavitation, extreme sonication parameters*

Összefoglaló

A hatóanyagok fizikai-kémiai és biofarmáciai sajátságainak változtatására számos gyógyszertechnológiai megoldás ismeretes. A részecskeméret csökkentés és a morfológia módosítása egy hatóanyag esetében új, alternatív beviteli kapukat nyithat meg, mint pl. a nazális vagy a pulmonáris bevitelt. Ilyen gyógyszerformák esetében a szemcseméret, szemcseméret megoszlás meghatározó paraméter. A szónikus kavitáción alapuló őrlés új lehetőséget nyújt a hatóanyagszemcsék sajátságainak megváltoztatására. Munkánk során akusztikus kavitáción alapuló ultrahangos nedves őrlést alkalmaztunk szemcseméret csökkentés céljából. Adott szonikációs paraméterek mellett az alkalmazott polimer koncentrációjának hatását vizsgáltuk a szemcseméret csökkentésre. Modellanyagként meloxikámot, mint rossz vízoldékonyságú, nem szteroid gyulladásgátlót alkalmaztunk. A szilárd fázis kinyerését követően vizsgáltuk a termékek fizikai-kémiai és morfológiai sajátságait (DSC, XRPD, SEM). Megállapítottuk, hogy kristályos szerkezetű, mikronizált hatóanyagot tartalmazó termék állítható elő.

Kulcsszavak: *meloxikám, szemcseméret csökkentés, akusztikus kavitáció, szélsőséges szonikációs paraméterek*

1. Bevezetés

A nedves őrlés jól ismert eljárás különböző hatóanyagok pre-szuszpenziójának előállítására, amelyek közti termékként felhasználhatók gyógyszerforma előállítására (kapszula, tabletta, injekció, orrspray, orrgél stb.) [1]. Mint ismeretes, a nedves őrlés a száraz őrléshez képest kevesebb energiát és időt vesz igénybe. A zárt rendszer miatt nincs kiporzás, továbbá csökken az anyag felmelegedése is [2]. Nedves őrlés golyós malmok, kolloid malmok és kavitáción alapuló eljárások segítségével valósítható meg.

Az ultrahangos szonotróddal generált kavitáción alapuló homogenizálás széles körben használt a gyógyszertechnológia területén [3]. Alkalmazható emulziók [4], szuszpenziók [5] előállítására, valamint kristályosításnál alkalmas a szemcseméret csökkentésére (bottom up- integráló eljárás) [6]. A szónikus kavitáción alapuló ultrahangos nedves őrlés, mint dezintegráló művelet (top down) új irányvonalként jelenik meg ebben a témában. Az akusztikus kavitáció fizikai jelenség, amely akkor következik be, amikor az ultrahang hullámok által keltett buborékok, üregek összeroppannak, az egymásnak csattanó folyadékfelületek lökéshullámot keltenek, ami rezgéssel és a környező szilárd testek eróziójával jár [7]. A méretcsökkentés – dezintegráció révén – a kavitáció eredménye; az általa generált nagy nyíróerő képes szétszakítani a részecskéket, legyőzve az azokat összetartó erőket. A részecskék elsősorban a rácshibák, repedések mentén dezintegrálódnak [8]. Szemcseméret csökkentésre az ultrahangos energiát 20-100 kHz közötti frekvencia tartományban alkalmazzák [9]. A statikus szonikáció esetében a nyugalomban lévő mintát ultrahangozzuk, így a kavitáció hatása

[1] A szerzők a cikket *Kata Mihály* emeritus professzornak ajánlják 80. születésnapja alkalmából, tiszteletük jeléül.

a szonotródtól távolodva csökken (a rendszerre nézve inhomogén).

Az ultrahangos folyadékkezelést számos paraméter befolyásolja (amplitúdó, nyomás, hőmérséklet, a kezelendő mintában lévő komponensek koncentrációja). A szonikálás hatékonysága az egységnyi térfogatra (V) jutó energiamennyiség (E) függvénnyel (f) fejezhető ki:

$$\text{hatás} = f\,(E/V),$$

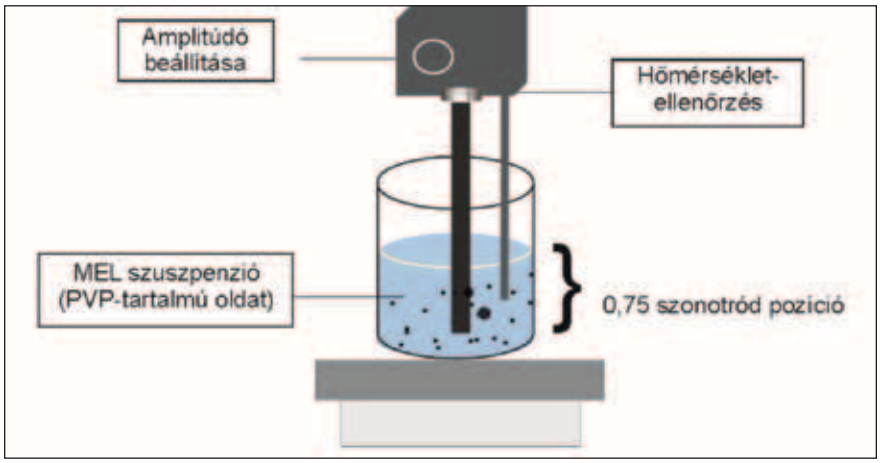

1. ábra: Az ultrahangos homogenizálás sematikus ábrája

ahol az energia (E) a teljesítményből (P) és a kezelés időtartamából (t) tevődik össze:

$$E[J] = P[W] * t[s]$$

A függvény az egyes paraméterek változtatásával módosul [10].

Jelen kísérletes munka előzményeként ultrahangos nedves őrlést alkalmaztunk. Faktoriális kísérleti tervet készítettünk és meghatároztuk az eljárási paramétereket. Az optimalizálás a termék szemcseméretére történt [11]. Munkánk során az optimalizált paraméterekhez képest olyan „szélsőséges" paramétereket alkalmazva készítettünk mintákat, amelyekkel tovább kívántuk csökkenteni a szemcseméretet. Modellanyagként rossz vízoldékonyságú hatóanyagot, a meloxikámot (MEL) választottuk. Célunk volt annak vizsgálata, hogy az így előállított termékben a MEL szemcseméret csökkenthetőségén kívül, a kavitáció milyen változásokat idéz elő a termék fizikai-kémiai és morfológiai sajátságaiban.

2. Anyagok és termék előállítása ultrahangos technikával

Anyagok

Felhasznált anyagok: meloxikám (MEL) – EGIS Gyógyszergyár (Budapest, Magyarország); PVP K-25 (PVP) (polivinilpirrolidon) – ISP Customer Service GmBH (Köln, Németország).

Szemcseméret-csökkentés ultrahangos eljárás alkalmazásával

A MEL szemcseméretét nagy intenzitású ultrahanggal (Hielscher UP 200S, 200W, Németország), statikus szonikációval csökkentettük. A korábban optimalizált paraméterekhez képest (70%-os amplitúdó, 36 ºC, 30 perc) „szélsőséges" paramétereket alkalmaztunk. A mintákat 90%-os amplitúdóval, 50 ºC-on (Julabo, Németország), 60 percen át ultrahangoztuk, a szonotród minden minta esetében a teljes folyadéktest 75%-áig merült a rendszerbe (***1. ábra***). A MEL koncentrációja 20 mg/10 ml volt. Az eljárás során minden minta esetében diszperziós közegként 25 ml térfogatú, különböző koncentrációjú PVP K-25-oldatot (0,1, 0,5 és 2,0%) alkalmaztunk. A PVP, mint polimer a gyógyszeriparban is széles körben alkalmazott diszpergálószer. A MEL karboxil-csoportja és a PVP között kialakuló gyenge másodlagos kötés segít egymástól távol tartani a hatóanyag-részecskéket csökkentve ezzel az aggregáció veszélyét [12].

3. Vizsgálati módszerek

3.1 Szemcseméret megoszlás, morfológia

A MEL szemcseméretét és méreteloszlását Malvern Mastersizer 2000 készülékkel (Malvern Instruments, Worcestershire, UK) határoztuk meg, Hydro 2000 SM kis térfogatú diszpergáló egységgel. A D0,1, D0,5, D0,9 értékeket térfogat szerinti méretanalízissel határoztuk meg.

A kiindulási hatóanyag és a szilárd minta morfológiai jellemzése pásztázó elektronmikroszkóppal történt (Hitachi S4700, Hitachi Scientific Ltd., Japan). A minta töltődésének megakadályozása céljából arany-palládium bevonó anyagot használtunk, 18 mA plazmaáram alkalmazásával. A felvételek 15 kV nagyfeszültség, 10 μA elektronáram és 0,1 Pa élővákuum beállításával készültek.

3.2 Szerkezeti sajátságok

A termékek termoanalitikai sajátságait Mettler Toledo STAR® termoanalitikai készülékkel (Mettler Inc., Schwerzenbach, Svájc) határoztuk meg. A DSC (differenciál pásztázó kalorimetria) méréseket argon gáz átáramoltatásával (10l/óra) végeztük (2-5 mg-os minta, 25-300 ºC, 5 ºC/perc fűtési sebesség).

A hatóanyag kristályos jellegét porröntgen diffrakciós vizsgálatokkal határoztuk meg (Miniflex II Rigaku porröntgen diffraktométer, Rigaku Co. Tokyo, Japan). Mérési paraméterek: Cu (Kα=1,5405 Å), 30 kV, 15 mA.

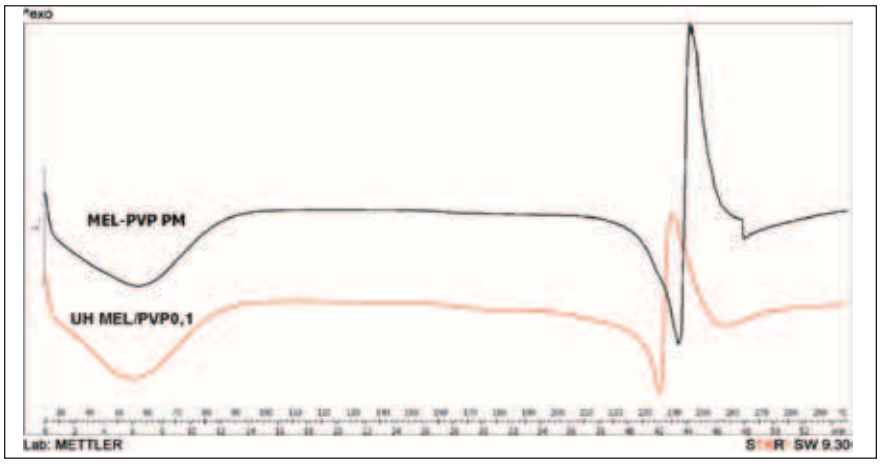

2. ábra: A MEL PVP-vel alkotott fizikai keverékének (MEL-PVP PM) és a 0,1% PVP-tartalmú szuszpenzióból nyert szilárd fázisú termék (UH MEL/PVP$_{0,1}$) DSC görbéje

4. Eredmények értékelése

4.1 MEL szemcseméret csökkentése különböző PVP-koncentráció mellett

A minták szemcseméret megoszlását ultrahangozott pre-diszperzióban határoztuk meg. Az eredmények az ***1. táblázatban*** láthatók, amelyek alapján elmondható, hogy a kiindulási mérethez képest mindhárom minta esetében jelentős mértékben lecsökkent a MEL szemcsemérete. Mivel a PVP mennyisége nem befolyásolta lényegesen a szemcseméret-megoszlást, egymáshoz viszonyítva a három termékben, ezért a legkisebb PVP-tartalmú mintát vizsgáltuk tovább. Az alacsony segédanyag-koncentráció mellett végzett mikronizálás mind gazdasági, mind citotoxicitás szempontjából is előnyösebb.

4.2 Szilárd fázisú termék jellemzése

A 0,1% PVP-tartalmú szuszpenzióból (UH MEL/PVP$_{0,1}$) 40 ºC-on vákuum szárítóban távolítottuk el a vizet (Binder, Németország) abból a célból, hogy szilárd fázisú terméket nyerjünk. A szárítást követően a termék fizikai-kémiai sajátságait vizsgáltuk és annak fizikai keverékével (MEL-PVP PM) hasonlítottuk össze. A kezelt minta hőmérséklete szonikálás során 53 ºC-ig emelkedett, tehát hő hatására bomlás nem következett be.

DSC felvételek

A kezeletlen MEL-nek 259,27 ºC-on jól definiálható olvadáspontja van. A PVP amorf sajátságú segédanyag, olvadásponttal nem rendelkezik. A MEL-PVP fizikai keverékében és a szilárd fázisú minta görbéjén is megfigyelhető a hatóanyag kristályok olvadáspontja, amivel a MEL kezelés és szárítás utáni kristályos jellegét bizonyítottuk (***2. ábra***). A fizikai keverék esetében az olvadáspont-csökkenés annak köszönhető, hogy a PVP az üvegesedési hőmérsékletén (T_g = 34 ºC) meglágyul, ennek következtében a MEL olvadása alacsonyabb hőmérsékleten következik be (242 ºC). A kezelt, szárított mintában megfigyelhető további olvadáspont-csökkenés (236 ºC) azzal magyarázható, hogy a kisebb kristályok megolvadásához kevesebb energiára van szükség.

XRPD eredmények

A porröntgen-diffrakciós eredmények ugyancsak a minta kristályos jellegét bizonyítják. A ka-

1. táblázat

Szonikált termékek szemcseméret-megoszlása különböző PVP-koncentráció mellett

	PVP-oldat (%)	**D0,1**	**D0,5**	**D0,9**
MEL$_{kiindulási}$	-	10,82	34,03	75,81
UH MEL/PVP$_{0,1}$	0,1	0,16	3,08	16,80
UH MEL/PVP$_{0,5}$	0,5	0,14	2,79	19,09
UH MEL/PVP$_{2,0}$	2,0	0,28	3,93	12,91

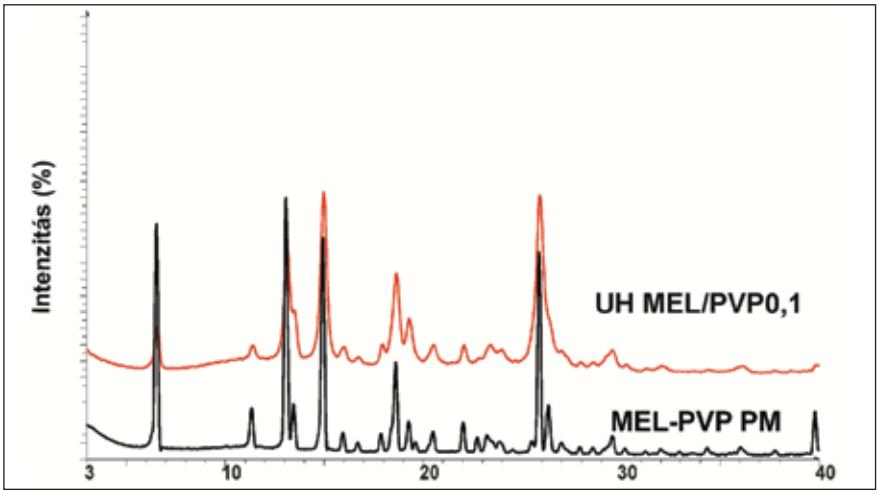

3. ábra: A MEL PVP-vel alkotott fizikai keverékének (MEL-PVP PM) és a 0,1% PVP-tartalmú szuszpenzióból nyert szilárd fázisú termék (UH MEL/PVP$_{0,1}$) porröntgen felvétele

rakterisztikus csúcsok a fizikai keverék és a szilárd fázisú minta esetében is megjelennek. A MEL-re jellemző csúcsok 13,22, 15,06, 26,46 és 26,67 2θ értékeknél olvashatók le (***3. ábra***). Mivel a fizikai keverék és a termék jellemző csúcsai egybeesnek – azon túl, hogy a MEL kristályos maradt – az is megállapítható, hogy polimorf módosulat a kezelés hatására nem keletkezett. A szonikációval előállított mintában a csúcsok intenzitása kisebb a fizikai keverékben található MEL csúcsaihoz képest, ami a méretcsökkenéssel magyarázható.

Elektronmikroszkópos felvételek

Az elektronmikroszkópos képek alapján látható, hogy a kiindulási MEL kristályai nagy, oszlopos kristályok. A szilárd fázisú termék hatóanyag kristályai szabálytalan alakúak, egyenetlen felszínűek. A MEL kristályok a felvételeken is látható, nagyméretű, amorf PVP-részecskék között detektálhatók (***4. ábra***).

5. Összegzés

Közleményünk összefoglalót adott a kavitáció jelenségéről, az ultrahangos nedves őrléses eljárásról. Munkánk során statikus szonikációt alkalmaztunk a MEL szemcseméretének csökkentése céljából, s vizsgáltuk a különböző PVP-koncentráció szemcseméretre gyakorolt hatását. Megállapítottuk, hogy az alkalmazott eljárási paraméterekkel (90%-os amplitúdó, 50 ºC, 60 perc, 75% szonotród pozíció) mikronizált MEL-t tartalmazó pre-szuszpenzió állítható elő, amely alkalmas közvetlenül szuszpenziós orrspray és orrgél fejlesztésére. A 0,1% PVP-t tartalmazó minták szárítását követően, fizikai-kémiai vizsgálatokat végeztünk. Megállapítottuk, hogy kristályos szerkezetű, mikronizált hatóanyagot tartalmazó termék állítható elő. Terveink között szerepel nátrium-hialuronát, mint mukoadhezív segédanyag, továbbá Cremophor RH 40, illetve kitozán, mint permeabilitást fokozó segédanyagok alkalmazásával nazális gyógyszerforma fejlesztése.

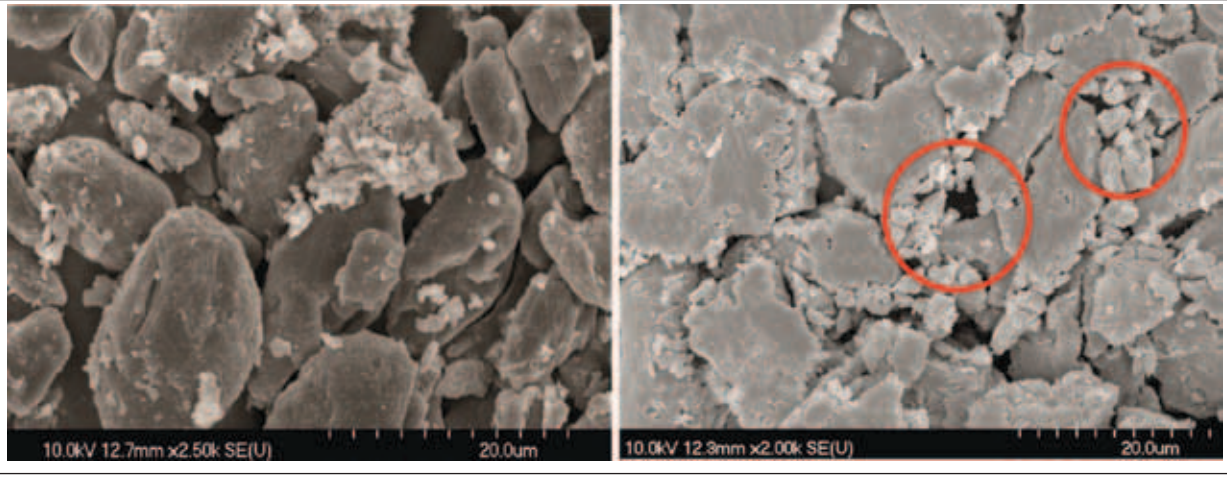

4. ábra: A kiindulási MEL és a 0,1% PVP-tartalmú szuszpenzióból nyert szilárd fázisú termék (UH MEL/PVP$_{0,1}$) elektronmikroszkópos felvétele

Irodalom

[1] *Juhnke, M., Märtin, D., John, E.*: Eur. J. Pharm. Biopharm. *81*, 214-222 (*2012*).

[2] *Sipos P.*: Gyógyszertechnológiai műveletek középüzemi méretben, Galenusi gyógyszerkészítmények előállítása és vizsgálata. JATEPress, Szeged, 2005. 71-104. old.

[3] *Mettin, R., Cairós, C., Troia, A.*: Ultrason. Sonochem. http://dx.doi.org/10.1016/ j.ultsonch.2014.08.015 (2014).

[4] *Behrend, O., Ax. K., Schubert, H.*: Ultrason. Sonochem. *7*, 77-85 (*2000*).

[5] *Benes, E., Grösschl, M., Handl, B., Trampler, F., Nowotny, H.*: *Das europaische TMR-Netzwerk Ultrasonic Separation of Suspended Particles*. Proc. Joint Symposium AAA and ÖPG TC Acoustics, Graz, Austria. 2, 1998, pp. 14-15.

[6] *Hatkar, U. N., Gogate, P. R.*: Chem. Eng. Process. *57-58*, 16-24 (*2012*).

[7] *Caupin, F., Herbert, E.*: Comptes Rendus Physique. *7*, 1000-1017 (*2006*).

[8] *Patil, N.M., Pandit, B.A.*:Ultrason. Sonochem. *14*, 519-530 (*2007*).

[9] *Sandilya D. K., Kannan A.*: Ultrason. Sonochem. *17*, 427-434 (*2010*).

[10] http://www.hielscher.com [2013. 10. 10.] *Hielscher T.*: Ultrasonic production of nano-size dispersions and emulsions

[11] *Bartos, Cs., Kukovecz, Á., Ambrus, R., Farkas, G., Radacsi, N., Szabó-Révész, P.*: Chem. Eng. Process. *87*, 26-34 (2015).

[12] *Mártha, Cs., Kürti, L., Farkas,G., Jójárt-Laczkovich, O., Szalontai, B., Glässer, E., Deli, M. A., Szabó-Révész, P.*: Eur. Polym. J. *49*, 2426-2432 (*2013*).

Érkezett: 2014. december 5.

PUBLICATION IV.

OPTIMIZATION OF TECHNOLOGICAL PARAMETERS BY ACOUSTIC CAVITATION TO ACHIEVE PARTICLE SIZE REDUCTION

CSILLA BARTOS, PIROSKA SZABÓ-RÉVÉSZ, RITA AMBRUS*

Department of Pharmaceutical Technology, University of Szeged, Eötvös u. 6, H-6725 Szeged, Hungary
**Corresponding author: arita@pharm.u-szeged.hu*

Abstract

This article reports on particle engineering by a top-down method involving the organic solvent-free acoustic cavitation of ibuprofen (IBU). The process parameters (temperature, amplitude, sonication period and stabilizers) were optimized. The particle size distribution of IBU was measured after sonication and compared with the raw IBU (D 0.5=153 μm). Due to acoustic cavitation, the particle size decreased (D 0.5=25 μm), but the use of a stabilizer was needed for further decrease (D 0.5=11 μm). Samples sonicated with optimized process parameters, containing the most efficient stabilizer, were dried, their morphology was characterized by scanning electron microscopy and the structure was determined by differential scanning calorimetery and X-ray powder diffraction (XRPD). During the thermoanalytical and XRPD characterization, the crystalline structure of IBU was detected after the sonication procedure.

Rezumat

Prezentul articol se încadrează în domeniul ingineriei particulelor prezentând o metodă de cavitare acustică fără solvent organic a ibuprofenului (IBU). Parametrii procedeului (temperatură, amplitudine, timp de sonicare şi stabilizatori) au fost optimizaţi. După sonicare s-a măsurat distribuţia mărimii particulelor de IBU. Datorită cavitării acustice, dimensiunea particulelor a scăzut (D = 0.5=25 μm), dar a fost necesară utilizarea unui stabilizator pentru o scădere mai pronunţată (D 0.5=11 μm). Probele sonicate, cu parametrii de proces optimizaţi, conţinând cel mai eficient stabilizator, au fost uscate şi caracterizate morfologic prin microscopie de scanare electronică, precum şi structural, prin calorimetrie de scanare diferenţială şi difracţie de raze X (XRPD). În timpul analizei termice şi XRPD, structura cristalină a IBU a fost identificată după sonicare.

Keywords: Acoustic cavitation, Particle engineering, Particle size reduction

Introduction

Particle engineering techniques have been developed to produce drug particles with modified physico-chemical and biopharmaceutical properties. Different procedures are employed in order to optimize the habit of the particles [17, 15, 21]. The procedures involve either particle size reduction of larger crystals (top-down approach - disintegration) or the building-up of particles (bottom-up approach-integration) [4, 5, 3, 2].

Energy input may be important for the particle size reduction of active substances, and is possible by cavitation [20]. Cavitation is the formation and immediate implosion of cavities in a liquid. Cavitation is usually divided into two classes: inertial and non-inertial cavitation. Inertial cavitation is the process where a void or bubble in a liquid rapidly collapses, producing a shock wave. Non-inertial cavitation is the process in which a bubble in a fluid is forced to oscillate in size or shape due to some form of energy input. In pharmaceutical technology, hydrodynamic (high-pressure homogenization) and acoustic (power ultrasound) cavitation, are generally used, which are of non-inertial cavitation type. Acoustic cavitation, a novel possibility to decrease particle size [2, 8, 22], has the ability to erode and break down particles [13]. Particle engineering uses ultrasound power in the frequency range 20-100 kHz to induce particle size reduction [23].

Power ultrasound is used for the processing of liquids, e. g. mixing, emulsifying, dispersing and de-agglomeration or milling. During sonication, the sound waves that propagate into the liquid media result in alternating high-pressure and low-pressure cycles, with rates depending on the frequency. During the low-pressure cycle, high-intensity ultrasonic waves create small vacuum bubbles or voids in the liquid. If the acoustic intensity is sufficiently high, the bubbles will first grow in size and then rapidly collapse during a high-pressure cycle. This phenomenon is termed ultrasonic cavitation [24]. Ultrasonic liquid processing is described by a number of parameters (amplitude, pressure, temperature and concentrations of compounds). The effect of the process may be determined as a function of the energy *per* processed volume:

$$\text{effect} = f\,(E/V)$$

where the energy (E) is the product of the power output (P) and the duration of exposure (t):

$$E[Ws] = P[W] * t[s]$$

The function alters with changes in the individual parameters. Additionally, the actual power output *per* surface area of the sonotrode of an ultrasonic unit depends on the parameters [10].

Ibuprofen is a non-steroidal anti-inflammatory drug, which is often used for the relief of symptoms of arthritis or fever, and as an analgesic [26, 16]. We chose IBU as a model crystalline drug because of its large particle size (D 0.5=153.73 μm) and low melting point (approximately 75 °C) [12]. Formulation of the IBU-β-cyclodextrin complex [6] and amorphization of this drug are known as feasible ways to increase its solubility [25]. The rapid expansion of supercritical solutions (supercritical fluid technology)

[11, 19], melt emulsification [14] and the solvent diffusion method [12] are well known to decrease the particle size of IBU through use of an organic solvent, but the residual organic solvent may be a problem in the pharmaceutical formulation.

In the present work, the use of acoustic cavitation, as a novel organic solvent-free, static wet grinding technique in pharmaceutical technology is reported. The aims of our work were to reduce the particle size of IBU to the micrometer range by using power ultrasound, with optimization of the process parameters (temperature, amplitude and sonication period) and excipients, and to study the effects of power ultrasound on the physico-chemical properties of IBU.

Materials and Methods

Materials

IBU 2-[4-(2-methylpropyl)phenyl]propanoic acid, was purchased from Aldrich Chemie, Deisenhofen, Germany; PVP K-25 (polyvinylpyrrolidone) was purchased from ISP Customer Service GmBH, Köln, Germany; Poloxamer 188 (polyethylene-polypropylene-glycol) was from BASF, Ludwigshafen, Germany; Tween 80 (Polysorbat 80; polyoxyethylenesorbitan-monooleate) was from Hungaropharma, Budapest, Hungary; and Solutol HS 15 (polyethylene glycol 15-hydroxystearate) was from BASF, Ludwigshafen, Germany.

Methods

Optimization of process parameters

A power ultrasound device (Hielscher UP 200S Ultrasonic processor with 200 W, Germany) was applied for energy input in the sample preparation. The samples (suspensions containing 300 mg of pure IBU in 30 mL of water) were sonicated at room temperature without cooling (the initial suspension temperature was 25°C) and using an ice bath with standardized temperature at around 18°C (the initial suspension temperature was 18°C, the temperature of the cooling water was monitored continuously). A range of ultrasonic amplitudes (30%, 50% and 70%) were tested in order to determine the optimum amplitude *via* a 200 W model ultrasound device for 10, 20 or 30 min during the procedures (Table I) (Figure 1).

Table I
Parameters applied during sonication

Temperature (°C)	room temperature, ice cooling
Amplitude (%)	30, 50, 70
Time (min)	10, 20, 30

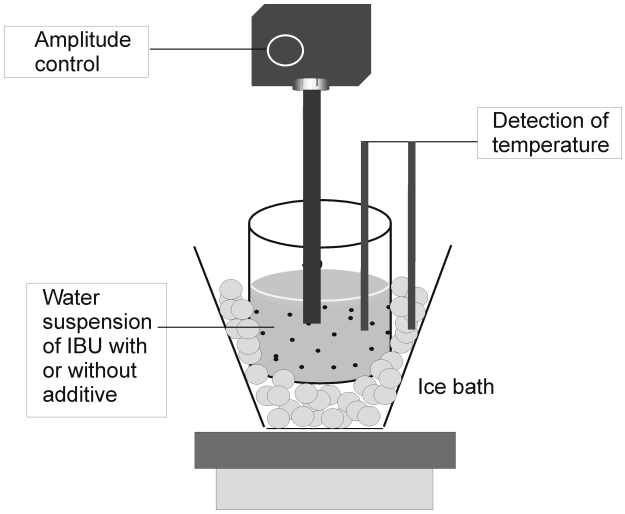

Figure 1
Scheme of preparation

Effects of stabilizers on particle size distribution

During the content optimization, different additives were applied: PVP K-25, Poloxamer 188, Tween 80 and Solutol HS 15. PVP K-25 is a stabilizer, Poloxamer 188 is a non-ionic surfactant, Tween 80 is an emulsifier and solubilizer, and Solutol HS 15 is a non-ionic solubilizer. These may promote particle size reduction and prevent agglomeration by stabilizing the particles against inter-particle forces [9, 8]. When the influence of these stabilizers was investigated, the stabilizer was dissolved in water and a fixed concentration of IBU was suspended in an aqueous solution of the excipient. The effects of the concentration of IBU (1 and 0.25 m/v %) on the particle size decrease were also studied (Table II). The concentrations of the stabilizers were determined as in previous studies: 0.5 and 0.25 m/v % of excipients were tested [12].

Table II
Applied additives, concentration of IBU and additives

Additives	PVP K-25, Poloxamer 188, Tween 80, Solutol HS 15
Concentration (m/v %)	1, 0.25 (IBU) 0.5, 0.25 (additive)

Preparation of solid products

Suspensions prepared with the optimized parameters with efficient stabilizer were dried in a static bed dryer (Memmert, Germany) at 50 °C in order to obtain solid products. 50 °C was chosen because of the low melting point of IBU, which could fuse at higher temperature. The yield of IBU was approximately 90%. After drying, the physico-chemical properties of the products were investigated.

Particle size distribution and morphology

The volume particle size distribution of raw IBU was measured by laser diffraction (Mastersizer 2000, Malvern Instruments Ltd, Worcestershire, UK) with the following parameters: 300RF lens; small volume dispersion unit (3000 rpm); refractive index for dispersed particles 1.4364; refractive index for dispersion medium 1.330. Water was used as dispersant and the obscuration was in the range 11-16% for each measurement. The IBU particle size was determined immediately on the initial water suspension. After drying, the solid product was resuspended in water using an ultrasonic bath for 5 min. Water was applied as dispersion phase, in which the additives were dissolved, and therefore only IBU particles could be detected. In all cases the average size volume distribution, D 0.1, D 0.5, and D 0.9 were determined and evaluated.

The shape and surface characteristics of the various samples were visualized by using a scanning electron microscope (Hitachi S4700, Hitachi Scientific Ltd., Tokyo, Japan). Briefly, the samples were sputter-coated with gold–palladium under an argon atmosphere, using a gold sputter module in a high-vacuum evaporator and the samples were examined at 15 kV and 10 μA. The air pressure was 1.3-13.0 mPa.

Structural analysis

DSC measurements were carried out with a Mettler Toledo DSC 821^e thermal analysis system with the STAR^e thermal analysis program V9.0 (Mettler Inc., Schwerzenbach, Switzerland). Approximately 2-5 mg of pure drug or product was examined in the temperature range between 25 °C and 300 °C. The heating rate was 5 °C min^{-1}. Argon was used as carrier gas at a flow rate of 10 L h^{-1} during the DSC investigations.

The physical state of IBU in the samples was evaluated by X-ray powder diffraction (XRPD). XRPD patterns were produced with an X-ray Diffractometer Miniflex II (Rigaku Co. Tokyo, Japan), where the tube anode was Cu with K_α = 1.5405 Å. The pattern was collected with a tube

voltage of 30 kV and a tube current of 15 mA in step scan mode (4° min^{-1}). The instrument was calibrated by using Si.

Results and Discussion

Effects of process parameters on particle size distribution

During the procedure, the experimental parameters were first investigated. The amplitude, temperature and sonication time were varied (Table III). In the starting suspensions, the concentration of IBU (with an average particle size of about 154 μm) was 300 mg in 30 mL of water. For each sample, three parallel measurements were performed to check the reproducibility.

At room temperature, the application of an amplitude of 30, 50 or 70% resulted in a 50% decrease in the average IBU particle size. During the procedure, the temperature of the suspension increased from 25 °C to 77-85 °C. We presumed that some of the invested energy was transformed to heat, and the D 0.9 value was therefore increased by amplitudes of 30 and 50% (Sample 1 and Sample 2) relative to raw IBU (Figure 2 on the left). The reason for these phenomena is the melting of IBU, due to the temperature of the system increasing to above the melting point of IBU (75°C). After the impaction, therefore, the sample presented large precipitated IBU crystals.

For Samples 4-6, continuous ice cooling ($T_{cooling\ water}$ = 18 °C) was applied. After the procedure, the temperature of the suspension was decreased to approximately 35 °C, which prevented the melting of IBU. Furthermore, the cohesive forces (which promote the aggregation of the particles) were lower at low temperature, and this helped achieve smaller particles. Sonication with an amplitude of 30% caused a further 50% decrease in the average particle size. The smallest particles were produced by the application of an amplitude of 70%, with the largest energy investment, on use of an ice bath (Sample 6).

Increase of the amplitude of sonication did not cause a significant alteration in the temperatures of the suspensions relative to one another at 18 °C on ice cooling. Increasing of the duration of sonication to 20 min resulted in a lower size reduction than with a combination of increased amplitude and cooling (Figure 2). No difference in particle size was observed when the sonication time was increased from 20 min to 30 min. A sonication time of 20 min was therefore, considered to be optimum (Sample 7 and Sample 8).

Consequently, the increased amplitude-due to the largest energy investment and decreased temperature-due to lower cohesive forces and less energy-transformation to heat-jointly resulted in the most effective particle size reduction; the best combination was sonication with an amplitude of 70% for 20 min with ice cooling, which resulted in an average IBU particle size of more than 25 μm because of grinding resistance (Figure 2).

The use of a lower concentration of active substance might be predicted to yield a smaller particle size after the sonication, energy is directed to less material and the cohesive forces are weaker. Decrease of the concentration of IBU (0.25 m/v%) did not cause a further particle size reduction (Sample 9) as compared with the results at a higher concentration of IBU (Figure 2), which allows formulation with a larger quantity of active substance.

Table III

Effects of acoustic cavitation on particle size distribution at different parameters

Batch code	Investi-gated factor	Amp-litude %	Starting temperature of suspension (°C)	Temperature of suspension after sonication (°C)	Time (min)	Conc. of IBU (mg/30 mL water)	Particle size distribution (μm) D 0.5
Raw IBU		-------	-------	-------	-------	-------	153.73
Sample 1		30	25	77.7	10	300	85.16±9.14
Sample 2	Amp.	50	25	73.7	10	300	85.35±3.85
Sample 3		70	25	85.0	10	300	84.49±1.63
Sample 4		30	18	32.3	10	300	39.44±2.10
Sample 5	Temp.	50	18	34.5	10	300	31.92±2.63
Sample 6		70	18	40.0	10	300	28.19±2.30
Sample 6		70	18	40.0	10	300	28.19±2.30
Sample 7	Time	70	18	40.0	20	300	25.78±2.20
Sample 8		70	18	37.6	30	300	24.88±2.87
Sample 7		70	18	40.0	20	300	25.78±2.20
Sample 9	Conc.	70	18	37.8	20	75	22.24±5.82

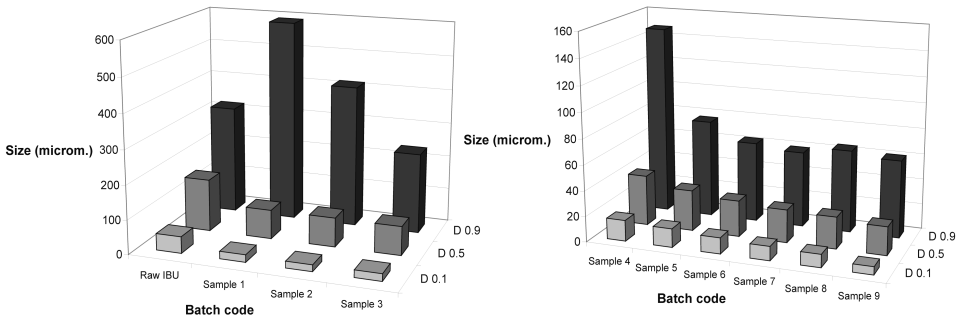

Figure 2
Particle size distribution of IBU after sonication under different conditions (Samples 1-9)

Effect of stabilizers

The choice of stabilizer is specific for each drug candidate and each formulation procedure. The stabilizer should exhibit sufficient affinity for the particle surface in order to stabilize the suspension. When the influence of different stabilizers was investigated, the suspensions were prepared with a fixed concentration of the drug and optimized parameters (see Sample 7). The type of compound employed for stabilization has a pronounced effect on the particle size and distribution (Table IV). Four different stabilizers were tested to check the effect of the nature of the surfactant on the IBU particle size. Micronized drugs have a tendency to agglomerate as a result of their hydrophobicity, thus reducing their available surface area [8, 1]. One of the most common methods to reduce the tendency to drug agglomeration is a steric technique. Steric stabilization is achieved by adsorbing polymers onto the drug particle surface [9], forming a protective layer on the surface of the particles and overcoming the cohesive forces. Solutol was least effective, followed by PVP and Tween 80. The smallest particle size was achieved with Poloxamer: the average size was approximately 11 μm. When Poloxamer was used, this stabilizer exerted a strong steric stabilization effect preventing aggregation of the particles. An important function of polymers (e. g. Poloxamer) is that they can form a substantial mechanical and thermodynamic barrier at the interface, which retards the approach and coalescence of individual emulsion droplets [7]. Non-ionic non-polymeric surfactants (e.g. Tween) offer an advantage over polymers in that they have a higher adsorption potential than an equal-chain-length polymer [18].

The use of a lower concentration of Poloxamer might be expected to lead to a large IBU particle size because it could well be less effective as

regards overcoming the cohesive forces. However, a decreased concentration of Poloxamer did not cause a particle size reduction: no significant change in average particle size occurred.

Table IV

Effects of additives on IBU particle size distribution

Sample	Type of additive	Size		
		D 0.1 (μm)	D 0.5 (μm)	D 0.9 (μm)
Sample 7	-------	10.97±1.65	25.78±2.20	59.18±1.73
Sample 10	0.5% PVP	5.82±0.08	12.56±0.11	24.55±1.09
Sample 11	0.5% Tween	5.29±0.03	11.14±0.11	23.64±2.33
Sample 12	0.5% Solutol	6.71±0.11	14.57±0.28	27.74±0.63
Sample 13	0.5% Polox	5.13±0.23	11.09±0.03	21.47±0.62
Sample 14	0.25% Polox	5.26±0.43	11.53±0.40	22.49±0.23

Table V lists the optimum experimental factors for the most efficient IBU particle size reduction. The batch containing 0.25% Poloxamer as stabilizer and sonicated with an amplitude of 70% for 20 min under ice cooling was dried in a static bed dryer at 50 °C in order to obtain a solid product.

Table V

Sample produced with optimized parameters using the most appropriate additive

	Additive	Amp/T (%)/(°)	T (Susp) (°)	Time (min)	Conc. (mg/30 mL)	Size D 0.5 (μm)
Dried Sample 14	0.25% Polox.	70/ 18	35.5	20	300	11.5

Characterization of dried product

Particle size distribution and morphology

The change in average particle size on drying was not significant as compared with the suspension of Sample 14: aggregation did not occur. The specific surface area of IBU increased 10-fold due to acoustic cavitation and was not altered after drying (Table VI).

Table VI

Specific surface and size distribution of pure IBU and two samples

	Spec. surface (m^2/g)	D 0.1 (μm)	D 0.5 (μm)	D 0.9 (μm)
Raw IBU	0.062	48.50	153.73	319.36
Sample 14 (suspension)	0.598	5.26	11.53	22.49
Dried Sample 14	0.614	5.52	12.44	25.38

The SEM pictures (Figure 3) provided an indication of the morphology of the modified particles. The crystal habit of pure IBU changed significantly. The raw IBU consisted mainly of roundish crystals with a broad focal size distribution. The dried product comprised irregular-shaped crystals with an average size of 10-15 μm. Poloxamer adsorbed strongly onto the surfaces of IBU particles *via* its poly(ethylene oxide) central block and formed a layer on the IBU surface after drying. The crystal lattice of IBU demonstrated defects and cracks, along which the crystals were disintegrated due to acoustic cavitation. These two factors accounted for the relatively rough surface.

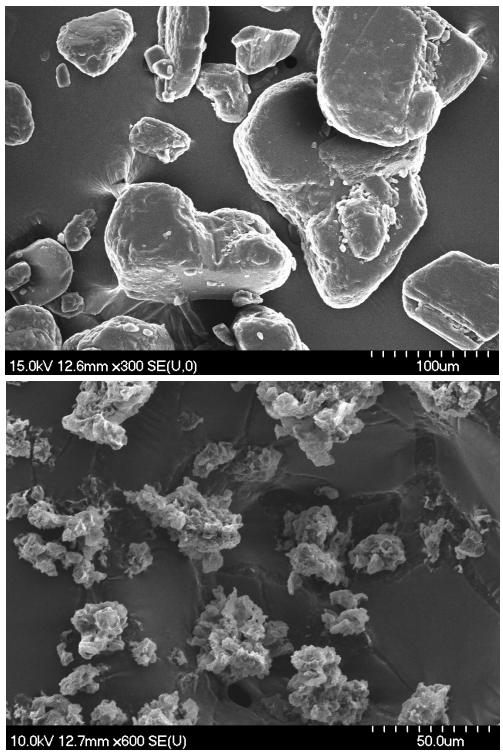

Figure 3
SEM picture of raw IBU (A), and dried Sample 14 (B)

Structure (DSC and XRPD)

DSC was employed in order to investigate the crystallinity and the melting of IBU and Poloxamer in the pure forms and in the sonicated dried product. The DSC curve (Figure 4) of pure IBU revealed a sharp endothermic peak at 76.93^{o}C, which is its melting point, confirming its crystalline structure. Poloxamer is a semi-crystalline additive (melting point:

55.84°C). The DSC curves exhibited sharp endothermic peaks of the two materials at 72.80°C (IBU) and 42.18°C (Poloxamer), indicating that the crystallinity of the drug was retained in the product. The IBU crystals in the product melted at a lower temperature than the melting point of pure IBU. This is due to the smaller particle size of IBU and the fact that the Poloxamer melted at a lower temperature, which promoted the melting of IBU. Both components melted at lower temperature in the product compared with melting point of pure materials. Several different materials alongside each other are present such as impurity of other components, which causes the melting of substances at lower melting points.

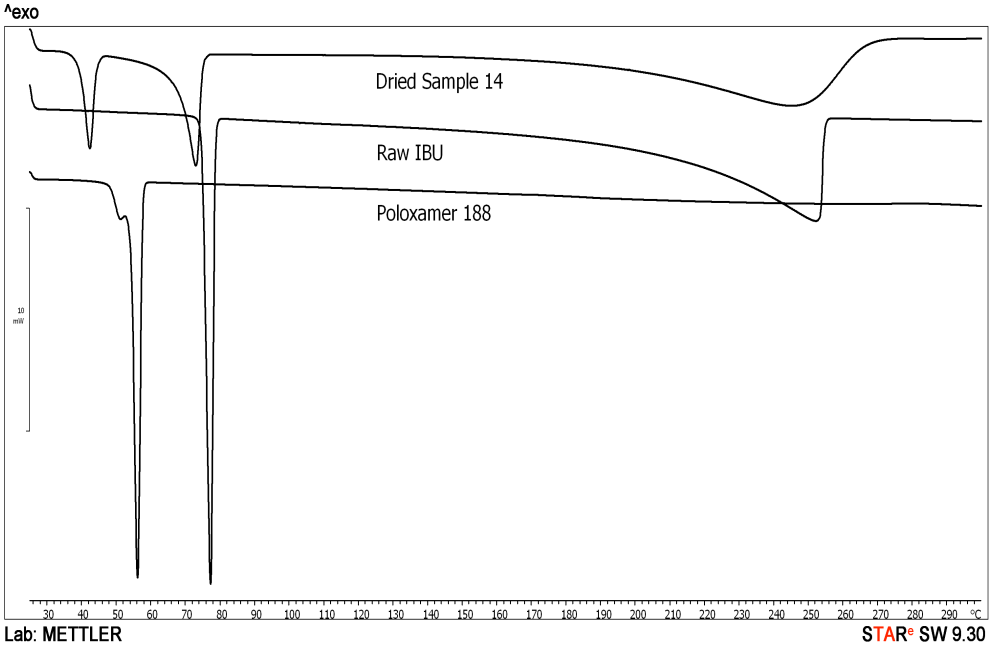

Figure 4
DSC curves of raw materials and of the product

The XRPD pattern of pure IBU demonstrated its crystalline structure, as expected. The characteristic 2θ data: 6.50, 17.00 20.20 and 22.00. The XRPD pattern of pure Poloxamer exhibited peaks at 2θ values of 19.50 and 22.00. The raw IBU and the sonicated dried IBU composite displayed similar X-ray diffraction patterns (Figure 5). This means that the crystalline form of the micronized IBU was not changed by the sonication and drying procedure.The differences in intensity of the IBU diffractogram peaks in the product as compared with raw IBU are due to the Poloxamer, a semi-crystalline additive with a crystallization inhibitory effect besides its stabilizer effect.

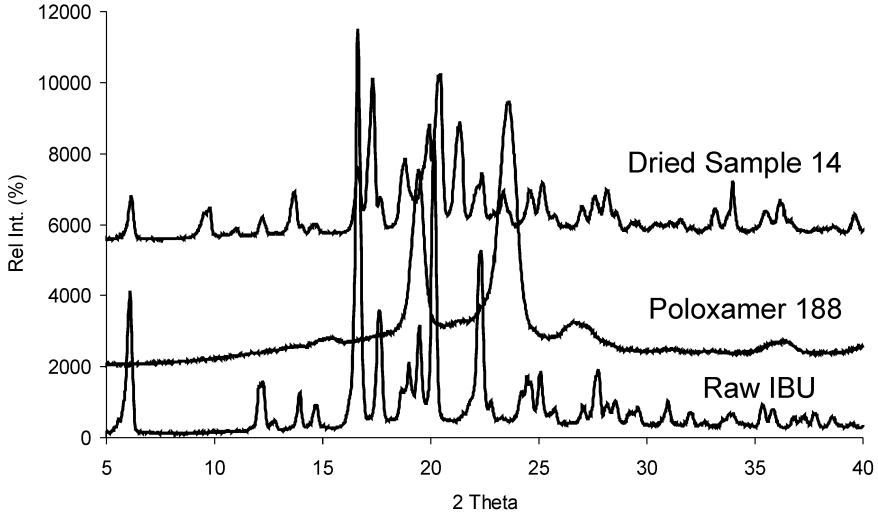

Figure 5
XRPD examination of IBU, Poloxamer and dried Sample 14

Conclusions

The top-down method can be applied to decrease the particle size and change the crystal habit, and in this way may it be useful for the formulation of original preparations and also to facilitate generic formulation.

Our study has illustrated the important role of power ultrasound in drug formulation. Because of the small amount of the samples, this method is recommended in preformulation studies. Acoustic cavitation, a static disintegration method with optimized process parameters, involving a change in crystal habit, may decrease the IBU particle size to the micrometer range. For further particle size reduction, additives are needed. The most efficient combination proved to be sonication with an amplitude of 70% for 20 min under ice cooling, with Poloxamer 188 as a stabilizer, which resulted in an average particle size of approximately 11.5 μm. The specific surface area of IBU increased 10-fold compared to the initial particle size of pure drug due to the treatment. The crystallinity of the drug was retained in the product after the sonication and drying procedure.

Wet grinding at a controlled temperature may be favourable in the grinding of materials with low melting points: the melting of the materials may be avoided.

In the future, we plan to compare static sonication with dynamic sonication in a double-walled flow cell, which allows a continuous flow of the sample during sonication.

Acknowledgements

The publication/presentation is supported by the European Union and co-funded by the European Social Fund. Project number: TÁMOP-4.2.2/B-10/1-2010-2012

Project title: "Broadening the knowledge base and supporting the long term professional sustainability of the Research University Centre of Excellence at the University of Szeged by ensuring the rising generation of excellent scientists."

References

1. Aguiar A. J., Zelmer J. E., Kinkel A. W., Deaggregation behavior of a relatively insoluble substituted benzoic acid and its sodium salt, *J. Pharm. Sci*. 1967, 56, 1243-1252.
2. Ambrus R., Amirzadi N. N., Aigner Z., Szabó-Révész P., Formulation of poorly water-soluble Gemfibrozil applying power ultrasound, *Ultrason. Sonochem*. 2012, 19, 286-291.
3. Bakar M. R. A., Nagy Z. K., Saleemi A. N., Rielly C. D., The impact of direct nucleation control on crystal size distribution in pharmaceutical crystallization processes, *Cryst. Growth and Des*. 2009, 9, 1378-1384.
4. Blagden N., M. de Matas, Gavan P. T., York P., Crystal engineering of active pharmaceutical ingredients to improve solubility and dissolution rates, *Adv. Drug Deliver. Rev*. 2007, 59, 617-630.
5. Bund R. K., Pandit A. B., Sonocrystallization: Effect on lactose recovery and crystal habit, *Ultrason. Sonochem*. 2007, 14, 143-152.
6. Chow D. D., Karara A. H., Characterization, dissolution and bioavailability in rats of ibuprofen- β -cyclodextrin complex system, *Int. J. Pharm*. 1986, 28, 95-101.
7. D. Myers, Surfaces, Interfaces and Colloids: Principles and Applications (second ed.), in: Wiley-VCH, Weinheim, 1999, pp. 253–294.
8. Friedrich H., Fussnegger B., Kolter K., Bodmeier R., Dissolution rate improvement of poorly water-soluble drugs obtained by adsorbing solutions of drugs in hydrophilic solvents onto high surface area carriers, *Eur. J. Pharm. Biopharm*. 2006, 62, 171-177.
9. Ghosh I., Bose S., Vippagunta R., Harmon F., Nanosuspension for improving the bioavailability of a poorly soluble drug and screening of stabilizing agents to inhibit crystal growth, *Int. J. Pharm*. 2011, 409, 260-268.
10. Ghica MV, Albu MG, Titorencu I, Albu L, Popa L, Collagen-doxycycline topical hydrogels: rheological, kinetic and biocompatibility studies, *Farmacia*, 2012, 60(6), 866-876
11. Kayrak D., Akman U., Hortaçsu Ö., Micronization of Ibuprofen by RESS, *J. Supercrit. Fluid* 2003, 26, 17-31.
12. Kocbek P., Baumgartner S., Kristl J., Preparation and evaluation of nanosuspensions for enhancing the dissolution of poorly soluble drugs, *Int. J. Pharm*. 2006, 312, 179-186.
13. Kuldiloke J., Effect of Ultrasound, Temperature and Pressure Treatments on Enzyme Activity an Quality Indicators of Fruit and Vegetable Juices, Ph. D. Thesis at Technische Universität Berlin 2002; http://opus.kobv.de/tuberlin/volltexte/2002/440/pdf/kuldiloke_jarupan.pdf
14. Manish M., Harshal J., Anant P., Melt sonocrystallization of ibuprofen: Effect on crystal properties, *Eur. J. Pharm. Sci*. 2005, 25, 41-48.
15. Miclea L. M., Vlaia L., Vlaia V., Hădărugă D. I., Mircioiu C., Preparation and characterization of inclusion complexes of meloxicam and α-cyclodextrin and β-cyclodextrin, *Farmacia* 2010, 58, 5, 583-593.
16. Miles S., Ibuprofen, xPharm: The comprehensive pharmacology Reference, 2007, pp. 1-7.
17. Nandiyanto A. B. D., Okuyama K., Progress in developing spray-drying methods for the production of controlled morphology particles: From the nanometer to submicrometer size ranges, *Adv. Powder Technol*. 2011, 22, 1-19.

18. Palla B. J., Shah D. O., Stabilization of high ionic strength slurries using surfactant mixtures: molecular factors that determine optimal stability, *J. Colloid Interf. Sci*. 2002, 256, 143–152.
19. Pathak P., Meziani M. J., Desai T., Sun Y. P., Formation and stabilization of ibuprofen nanoparticles in supercritical fluid processing, *J. Supercrit. Fluid* 2006, 37, 279-286.
20. Patil M. N., Pandit A. B., Cavitation-A novel technique for making stable nano-suspensions, *Ultrason. Sonochem*. 2007, 14, 519-530.
21. Popa L, Ghica MV, Ibuprofen pediatric suspension designed and optimized by response surface methodology, *Farmacia*, 2011, 59(4), 500-506
22. Raman V., Abbas A., Experimental investigations on ultrasound mediated particle breakage, *Ultrason. Sonochem*. 2008, 15, 55-64.
23. Sandilya D. K., Kannan A., Effect of ultrasound on the solubility limit of sparingly soluble solid, *Ultrason. Sonochem*. 2010, 17, 427-434.
24. Suslick K. S., Sonochemistry, in: J. Wiley & Sons (4th Ed), Kirk-Othmer Encyclopedia of Chemical Technology, New York, 1998, pp. 517-541.
25. Szabó-Révész P., Laczkovich O., Ambrus R., Szűts A., Aigner Z., Protocols for amorphization of crystalline solids through the application of pharmaceutical technological processes, *Eur. J. Pharm. Sci*. 2007, 32, S18.
26. Troullos E. S., Hargreaves K. M., Butler D. P., Dionne R. A., Comparison of nonsteroidal anti-inflammatory drugs, ibuprofen and flurbiprofen, with methylprednisolone and placebo for acute pain, swelling, and trismus, *J. Oral Maxil. Surg*. 1999, 48, 945-952.

Manuscript received: January 15th 2013

PUBLICATION V.

European Journal of Pharmaceutical Sciences 50 (2013) 86–92

Contents lists available at SciVerse ScienceDirect

European Journal of Pharmaceutical Sciences

journal homepage: www.elsevier.com/locate/ejps

In vitro and *in vivo* characterization of meloxicam nanoparticles designed for nasal administration

Levente Kürti [a,b], Róbert Gáspár [c], Árpád Márki [c], Emese Kápolna [d], Alexandra Bocsik [a,b], Szilvia Veszelka [b], Csilla Bartos [a], Rita Ambrus [a], Monika Vastag [d], Mária A. Deli [b], Piroska Szabó-Révész [a,*]

[a] Department of Pharmaceutical Technology, University of Szeged, Szeged, Hungary
[b] Institute of Biophysics, Biological Research Centre of the Hungarian Academy of Sciences, Szeged, Hungary
[c] Department of Pharmacodynamics and Biopharmacy, Faculty of Pharmacy, University of Szeged, Szeged, Hungary
[d] Gedeon Richter Ltd., Budapest, Hungary

ARTICLE INFO

Article history:
Received 30 December 2012
Received in revised form 7 March 2013
Accepted 16 March 2013
Available online 28 March 2013

Keywords:
Intranasal
Meloxicam
Nanoparticle
RPMI 2650
Nasal permeability
Pharmacokinetics

ABSTRACT

The nasal pathway represents a non-invasive route for delivery of drugs to the systemic circulation. Nanonization of poorly soluble drugs offers a possibility to increase dissolution properties, epithelial permeability or even bioavailability. The aim of the present study was to use *in vitro* methods to screen formulations which were intended for nasal application, and to perform animal experiments for recognizing the differences in plasmakinetics of intranasal- and oral-administered meloxicam nanoparticles. Due to nanonization the solubility of meloxicam elevated up to 1.2 mg/mL, additionally the extent of dissolution also increased, complete dissolution was observed in 15 min. Favorable *in vitro* diffusion profile of meloxicam nanoparticles was observed and their epithelial permeability through human RPMI 2650 cells was elevated. The pharmacokinetic parameters were significantly increased when meloxicam was administered as nanoparticles to rats either nasally (increase of C_{max} 2.7-fold, AUC 1.5-fold) or orally (increase of C_{max} 2.4-fold, AUC 2-fold) as compared to physical mixture of the drug and the excipients.

1. Introduction

Alternative sites of drug administration for systemic delivery and novel solutions of pharmaceutical technology offer numerous opportunities for the development of innovative pharmaceutical compositions (Mäder and Weidenauer, 2010). The nasal pathway represents a non-invasive drug administration route (Illum, 2003), although the nasal epithelium forms a restricting barrier (Wolburg et al., 2008). The tightness of the intercellular junctional complex is low in the nasal mucosa, it is considered as a leaky epithelial tissue, while brain capillaries and the skin epithelial cells form very tight barriers (Deli, 2009).

During the formulation of a pharmaceutical dosage form intended for intranasal application, several factors should be taken into consideration (Ugwoke et al., 2005). The poor aqueous solubility of a drug and the low rate of dissolution can lead to insufficient absorption or delayed pharmacological effect. Indeed the nasally administered pharmaceutical preparations will be cleared rapidly from the nasal mucosa into the gastrointestinal tract by the mucociliary clearance (Chien et al., 2008).

Nanonization is a way to increase drug solubility (Müller et al., 2011) and permeability through mucosal barriers (Morgen et al., 2012). Two basic technologies are involved in the production of nanoparticles, the integration techniques (controlled precipitation, crystallization) and the disintegration methods (high pressure homogenization, wet milling, co-grinding).

A possible approach to augment drug absorption is the application of different types of polymers. Polymer additives of the grinding process enhance the efficacy of size reduction and particle agglomeration can be prevented by steric stabilization (Rabinow, 2004). Mucoadhesive polymers increase residence time of the pharmaceutical formulation on the nasal epithelium (Schiller et al., 2011). Sodium hyaluronate, a naturally occurring anionic linear polysaccharide has an excellent mucoadhesive capacity and is used in many bioadhesive drug delivery systems. In our previous work sodium hyaluronate was selected as a component of an intranasal formulation (Horvát et al., 2009). This study further confirmed that viscosity and mucoadhesion are key factors in nasal drug delivery.

For successful formulation of a nasal delivery system, testing with reliably established *in vitro*, cell culture, *ex vivo* tissue and *in vivo* animal models are crucial. Vertical Franz cell diffusion model is a valid *in vitro* model for evaluating drug penetration (Siewert et al., 2003). Basically, donor and acceptor compartments are

* Corresponding author. Address: H-6720 Eötvös utca 6, Szeged, Hungary. Tel.: +36 62 545 572; fax: +36 62 545 571.
E-mail address: revesz@pharm.u-szeged.hu (P. Szabó-Révész).

0928-0987/$ - see front matter © 2013 Elsevier B.V. All rights reserved.
http://dx.doi.org/10.1016/j.ejps.2013.03.012

separated by a membrane of artificial-, animal- or human-origin (Östh et al., 2002; Schmidt et al., 1998). Several *in vivo* models were reported to deliver pharmacons via the nasal route (Chien et al., 2008; Costantino et al., 2007). Although there are drawbacks of the *ex vivo* tissue and *in vivo* animal models, including differences between the species, specialities in many anatomical and physiological features in various animal nasal cavities (Chien et al., 2008).

A cell culture model based on human RPMI 2650 cell line has been mostly used for nasal metabolism studies and toxicity assays but it can provide information on nasal permeability as well (Bai et al., 2008; Wengst and Reichl, 2010; Kürti et al., 2013).

Undoubtedly animal experiments are unavoidable in preclinical studies, but the number of animals can be reduced by the use of proper *in vitro* screening techniques. Based on the *in vitro* results, the most promising pharmaceutical formulations will further undergo *in vivo* pharmacokinetic verifications in animals.

In an earlier study the preparation of meloxicam (MEL) nanoparticles was investigated, the influence of different parameters on MEL particle size reduction was discussed and the optimization of the co-grinding process was performed by using a three-level full factorial design (Kürti et al., 2011).

The aim of the present study was to investigate MEL nanoparticles, intended for nasal and oral drug delivery, by *in vitro* and *in vivo* methods to verify their potential relevance helping to consider their further use in therapy.

2. Materials and methods

2.1. Preparation of meloxicam nanoparticles and the nasal formulations

MEL was obtained from Egis Ltd. (Hungary). The grinding additive, polyvinylpyrrolidone C30 (PVP) was purchased from BASF (Germany). Sodium hyaluronate (HA; Mw = 1400 kDa) was obtained as a gift from Gedeon Richter Ltd. (Hungary).

MEL was co-ground with PVP in a planetary monomill (Fritsch Pulverisette 6, Fritsch GmbH, Germany) in 1:1 drug–carrier ratio (Kürti et al., 2011). All experiments were carried out with two MEL formulations: (i) physical mixture of MEL and PVP and (ii) co-ground product of MEL and PVP. The nasal formulations contained MEL in 1 mg/mL concentration and HA in 5 mg/mL concentration, the vehicle was phosphate buffer (PBS; pH 7.4) or cell culture medium (pH 7.4). All samples were prepared freshly 1 day prior the *in vitro* and *in vivo* experiments.

2.2. Meloxicam thermodynamic solubility and extent of dissolution

The thermodynamic solubility of MEL was determined in PBS at pH 7.4, 37 °C, and the content of dissolved drug was measured spectrophotometrically at 362 nm (Unicam UV/vis spectrophotometer, Germany).

The extent of MEL dissolution was studied in 50 mL PBS at pH 7.4, 37 °C with Pharma test equipment (Germany) at a paddle speed of 100 rpm. At predetermined time points, 1 mL samples were withdrawn and immediately filtered (cut-off 0.2 μm, Minisart SRP 25, Sartorius, Germany) and the amount of dissolved drug was determined spectrophotometrically. Withdrawn samples were replaced with 1 mL of fresh medium.

2.3. In vitro permeability of meloxicam

In vitro permeability studies were performed on a vertical Franz-diffusion cell system (Microette Topical and Transdermal Diffusion Cell System, Hanson Research, USA) containing six cells (Makai et al., 2003; Csóka et al., 2005) in PBS at pH 7.4, 37 °C. The donor phase contained MEL at 1 mg/mL and sodium hyaluronate at 5 mg/mL concentration, which were placed on the synthetic membrane impregnated with isopropyl myristate. The effective diffusion surface was 1.8 cm^2. PBS (pH 7.4, 37 °C) was used as an acceptor phase. The rotation of the stir-bar was set to 100 rpm. At predefined time points, samples of 0.8 mL were taken from the acceptor phase by the autosampler (Microette Autosampling System, Hanson Research, USA) and were replaced with fresh receiving medium. The diffused amount of MEL was determined spectrophotometrically.

2.4. Nasal epithelial toxicity and permeability of meloxicam nanoparticles

MEL nanoparticles were tested on a cell culture model of the nasal epithelium (Kürti et al., 2013), RPMI 2650 human nasal epithelial cell line (ATCC, USA) was applied for toxicity and permeability assays. Cells were grown in Eagle's minimal essential medium (Invitrogen, USA) supplemented with 10% foetal bovine serum (Lonza, Switzerland). For all assays confluent RPMI 2650 layers were used. Cell confluency was checked by phase contrast microscopy and measurement of transepithelial electrical resistance. The resistance of RPMI 2650 layers varied between 50 and 100 Ω cm^2, in accordance with our previous data (Kürti et al., 2012, 2013).

To study the effects and toxicity of MEL nanoparticles on the human nasal epithelial cells a colorimetric viability assay was performed. Living cells convert the yellow dye 3-(4,5-dimethyltiazol-2-yl)-2,5-diphenyltetrazolium bromide (MTT) to purple, insoluble formazan crystals. RPMI 2650 cells were cultured on sterile, collagen-coated 96-well plates. After 1-h treatment the cells were incubated with 0.5 mg/mL MTT solution for 3 h in CO_2 incubator. The amount of formazan crystals was dissolved in dimethyl-sulfoxide and determined by measuring absorbance at 570 nm with a microplate reader (Fluostar Optima, BMG Labtechnologies, Germany).

To measure the flux of MEL across the cell layers, RPMI 2650 cells were seeded onto Transwell filter inserts (polycarbonate membrane, 0.4 μm pore size, 1.1 cm^2 surface area, Corning Costar Co., USA) and grown for 2 days (Kürti et al., 2013). The inserts were transferred to 12-well plates containing 1.5 mL Ringer–Hepes solution in the basolateral compartments. In apical chambers culture medium was replaced by 500 μL formulations containing 1 mg/mL MEL prepared in Ringer–Hepes buffer. The plates were kept for 1 h in a 37 °C incubator containing 5% CO_2 on a rocking platform. After incubation, the concentration of MEL was determined spectrophotometrically from the basolateral compartments. The flux of the drug was calculated from the quantity of MEL, which permeated through the RPMI 2650 cells, divided by the surface of the filter insert and the duration of time.

Real-time cell microelectronic sensing (RT-CES) was used (xCELLigence, Roche, Switzerland) to measure changes in the impedance of individual microelectronic wells. Electric impedance correlates linearly with cell index reflecting cell number, adherence and cell growth (Solly et al., 2004; Kürti et al., 2012). The cells were seeded into a special 96-well E-plate (Roche, Hungary), which was coated with gelatine-PBS solution. Culture media was added to each well for background readings, than cell suspension was dispensed at the density of 6×10^3 cells per well. The cells were kept in an incubator at 37 °C for 24 h and monitored every 5 min. The cell index at each time point was defined as $(R_n - R_b)/15$, where R_n is the cell-electrode impedance of the well when it contains cells and R_b is the background impedance of the well with the medium alone. After cells grew to confluency and the cell index reached a plateau level, nasal formulation containing MEL nanoparticles and sodium hyaluronate was added to the wells. The control group

Table 1
Instrumental operating conditions for UHPLC-ESI-MS/MS.

RP-UHPLC					
Column		Kinetex C18 (100 mm × 2.1 mm × 2.6 μm)			
Mobile phases		(A): 20 mM ammonium-acetate (B): methanol 0–1 min: 80% A–20% B 1.1–3 min: 0% A–100% B 3.1–6 min: 80% A–20% B			
Flow rate		400 μL min^{-1}			
Injection volume		15 μL			
Column heating		40 °C			
ESI-MS/MS					
CAD		4			
CUR		25			
GS1		40			
GS2		50			
IS		5500			
TEM		400 °C			
MRM transitions	Compound	MRM (m/z)	DP	CE	CXP
	Meloxicam	352/115	81	25	8
	Piroxicam	332/95	76	31	8

received cell culture medium and the toxicity control group was treated with 10 mg/mL TritonX-100 detergent.

2.5. In vivo pharmacokinetics of meloxicam nanopartices in rats

For nasal delivery, MEL was dispersed in PBS (pH 7.4) containing 5 mg/mL sodium hyaruronate to reach a final concentration of 1 mg/mL. A dose of 60 μg per animal was administered to the right nostril of male Sprague–Dawley rats ($n = 5$) via a polyethylene tube by using a syringe. During drug administration the animals were narcotised by isoflurane. Blood samples were withdrawn from the tail vein before and at 5, 15, 30, 60, 120, 360 and 1440 min post-dosing, respectively.

For oral delivery, the formulation, which was diluted 10 times with PBS (pH 7.4) from that prepared for nasal delivery, was given at a dose of 60 μg MEL per animal to male Sprague–Dawley rats ($n = 5$) by gastric gavages. During drug administration the animals were narcotised by isoflurane. Blood samples were withdrawn from the tail vein before and at 5, 15, 30, 60, 120, 360 and 1440 min post-dosing, respectively.

The experiments performed conform to European Communities "Council directive for the care and use of laboratory animals" and were approved by the Hungarian Ethical Committee for Animal Research (permission number: IV/01758-0/2008).

2.6. Determination of meloxicam from biological samples

The blood samples were centrifuged (4000 rpm, 10 min) in CR 132 centrifuge (Jouan, France) to obtain blood plasma for further analysis. The biological samples were stored at −20 °C, protected from light.

An LC–MS/MS system was applied to the analysis of MEL in biological samples. For sample introduction an Agilent 1260 chromatographic system with an HTS autosampler was used (Agilent Technologies, Japan). A triple-quadrupole mass spectrometer (API 4000 MS/MS AB Sciex) equipped with a TurboV ion source in positive mode.

Multiple-reaction-monitoring (MRM) mode was used for quantification by monitoring the transitions: m/z 352 → 115 for MEL and m/z 332 → 95 for piroxicam (internal standard).

Gradient chromatographic separation was performed on a Kinetex C18 column (100 mm × 2.1 mm × 2.6 μm) (Phenomenex, Torrance, USA) using ammonium acetate and methanol as mobile phases. Supplementary information is listed in Table 1. The method had a detection limit of 0.2 ng/mL. The calibration curve was demonstrated to be linear over the concentration range of 1–1000 ng/mL.

2.7. Materials and reagents for analytical procedures

MEL (purity; 99.2%) and piroxicam (purity; 98.4%) were purchased from Egis Ltd. (Hungary) and Sigma–Aldrich (USA). Ammonium acetate, acetonitrile and methanol of analytical grade were obtained from Merck KGaA (Germany).

2.8. Sample preparation before analytical procedures

To a 50 μL of plasma sample, 100 μL acetonitrile containing piroxicam (internal standard at 30 ng/mL concentration) was added and the mixture was vortex-mixed for 30 s. Supernatant was obtained by centrifugation of the mixture for 25 min at 16,100 g at 4 °C. The resulted supernatant was injected into the LC–MS/MS system for analysis.

Rat plasma calibration standards and quality control samples of MEL were prepared by spiking the working standard solutions (2–1000 ng/mL) into a pool of drug-free rat plasma and the procedure described above was followed.

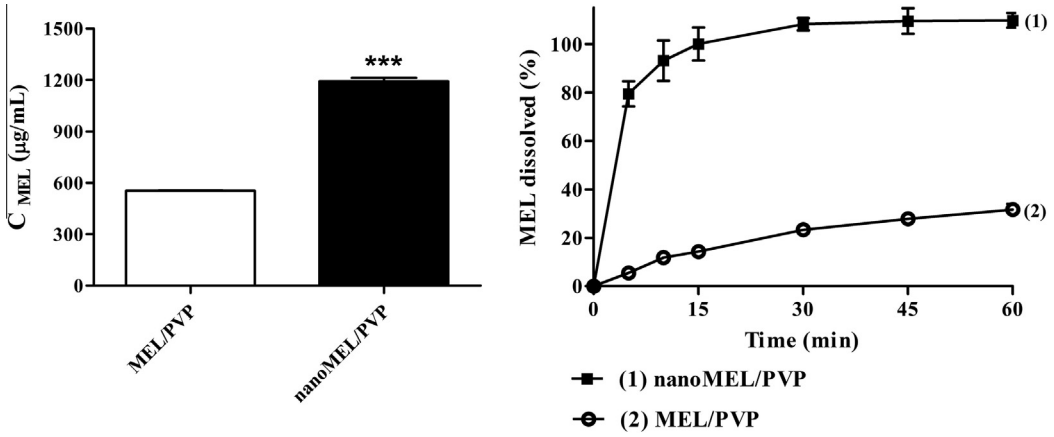

Fig. 1. (A) Thermodynamic solubility of meloxicam in case of the physical mixture (MEL/PVP) and the co-ground product (nanoMEL/PVP) in phosphate buffer (pH 7.4, 37 °C). (B) The extent of dissolution of meloxicam in case of the MEL/PVP and the nanoMEL/PVP in phosphate buffer (pH 7.4, 37 °C). MEL/PVP, meloxicam and polyvinylpyrrolidone C30 mass ratio 1:1. Data are presented as mean ± S.D., $n = 3$. Statistically significant differences between groups are indicated as $^{*}P < 0.05$; $^{**}P < 0.01$ and $^{***}P < 0.001$.

2.9. Calculations of the pharmacokinetic parameters and statistical analysis

Pharmacokinetic parameters were analyzed by PK. Solver 2.0 software. In case of oral data the analysis was made with one compartment extravascular model, while the nasal data were analyzed with non-compartmental extravascular model. The statistical analysis was performed with Prism 4.0 (Graphpad Software Inc., USA) software through unpaired *t*-test.

All data presented are means ± S.D. The values were compared using the analysis of variance followed by Dunnett tests using GraphPad Prism 5.0 software. Changes were considered statistically significant at $P < 0.05$.

3. Results

3.1. Meloxicam thermodynamic solubility and extent of dissolution

Our earlier study described and characterized binary mixtures of MEL and PVP-C30 which were co-ground for 2 h in a planetary monomill. The optimum co-grinding parameter set was a MEL to carrier ratio 1:1, and a rotation frequency of 400 rpm. The nanonized MEL particles displayed an uniform size distribution and an average particle size of 140.4 (±69.2) nm. Due to the co-grinding process the crystallinity of MEL was decreased, the typical characteristic peaks of MEL disappeared (Kürti et al., 2011).

In the present work amorphous MEL nanoparticles showed favorable dissolution properties at 37 °C, pH 7.4. In one hand the thermodynamic solubility of MEL elevated up to 1.2 mg/mL (Fig. 1A), on the other hand the extent of dissolution also increased, complete dissolution of MEL was observed in 15 min (Fig. 1B). In lower, acidic pH the thermodynamic solubility of MEL remained poor in artificial gastric fluid (37 °C, pH 1.2), 3.6 μg/mL in the case of MEL nanoparticles vs. 1.1 μg/mL in the case of MEL with PVP.

3.2. In vitro permeability experiments through an artificial membrane

The cumulative amount of MEL that diffused through a synthetic membrane from the different pharmaceutical formulations was measured against time on a Franz cell diffusion system. The diffusion from the formulation containing MEL nanoparticles and sodium hyaluronate was quicker, 25% of MEL was diffused from the formulation containing MEL in nanonized form vs. 10% in case of the physical mixture after the first 2 h (Fig.2).

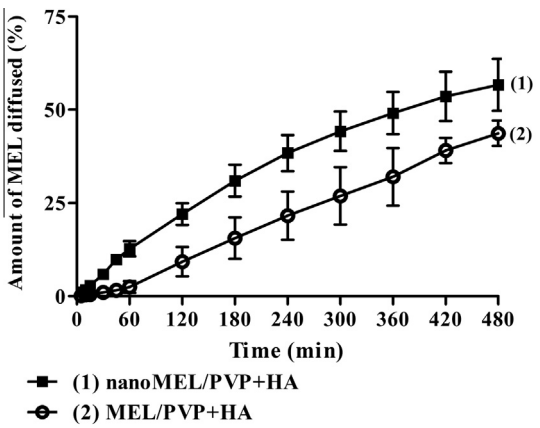

Fig. 2. *In vitro* permeability of meloxicam through an artificial membrane in case of the physical mixture (MEL/PVP) and the co-ground product (nanoMEL/PVP) in phosphate buffer (pH 7.4, 37 °C). MEL/PVP, meloxicam and polyvinylpyrrolidone C30 mass ratio 1:1; HA, sodium hyaluronate (5 mg/mL). Data are presented as mean ± S.D., $n = 6$.

3.3. In vitro cell culture experiments on human RPMI 2650 cells

To test the biological effects of the MEL nanoparticles a cell culture model of the nasal barrier, human RPMI 2650 cells were used. The effect of the pharmaceutical formulations, which contained MEL in nanonized form or the pure drug, was studied by MTT cell viability assay. The viability of human RPMI 2650 cells did not

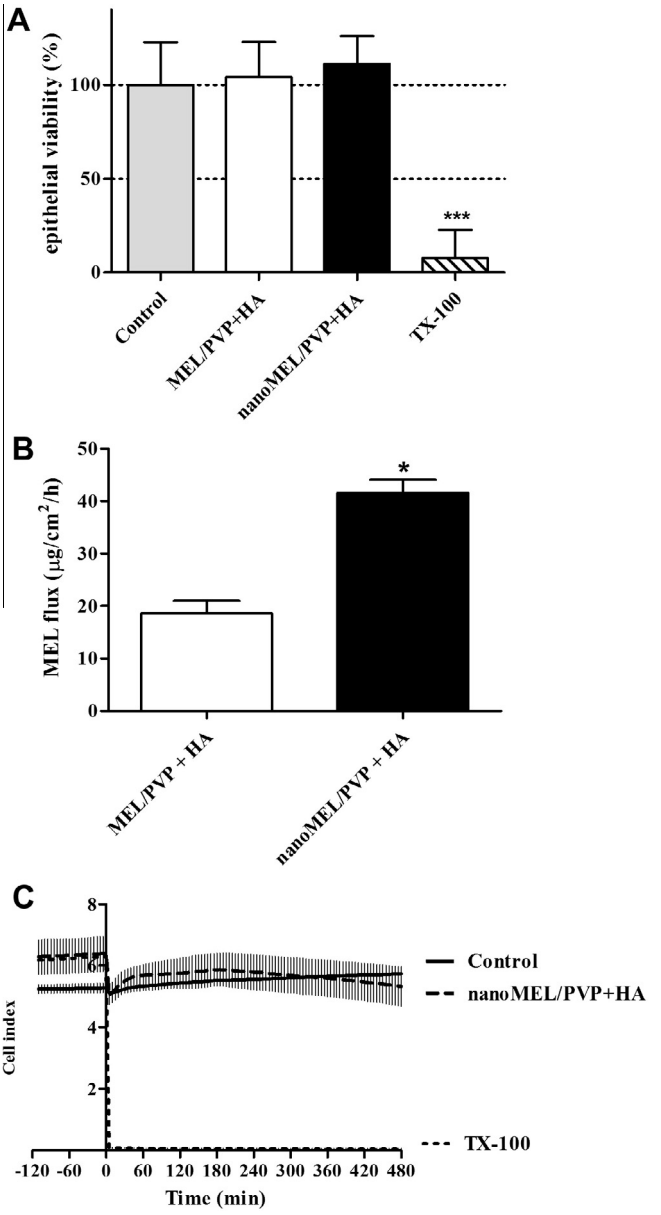

Fig. 3. (A) MTT dye conversion cytotoxicity assay provides information from the nasal epithelial cell viability after 1-h treatment with the physical mixture (MEL/PVP) and the co-ground product (nanoMEL/PVP) as compared to vehicle-treated cells (control). Data are presented as mean ± S.D., $n = 8$. (B) Flux of meloxicam in case of MEL/PVP + HA and nanoMEL/PVP + HA across human RPMI 2650 nasal epithelial cell layers. Data are presented as mean ± S.D., $n = 3$. C: Real-time cell microelectronic sensing measurement of cell viability and integrity of human RPMI 2650 nasal epithelial cells treated by vehicle and the nanoMEL/PVP + HA. Data are presented as mean ± S.D., $n = 4$. MEL/PVP, meloxicam and polyvinylpyrrolidone C30 mass ratio 1:1; HA, sodium hyaluronate (5 mg/mL); MTT, 3-(4,5-dimethyltiazol-2-yl)-2,5- diphenyltetrazolium bromide; TX-100, TritonX-100 (10 mg/mL). Statistically significant differences between groups are indicated as $^{*}P < 0.05$; $^{**}P < 0.01$ and $^{***}P < 0.001$.

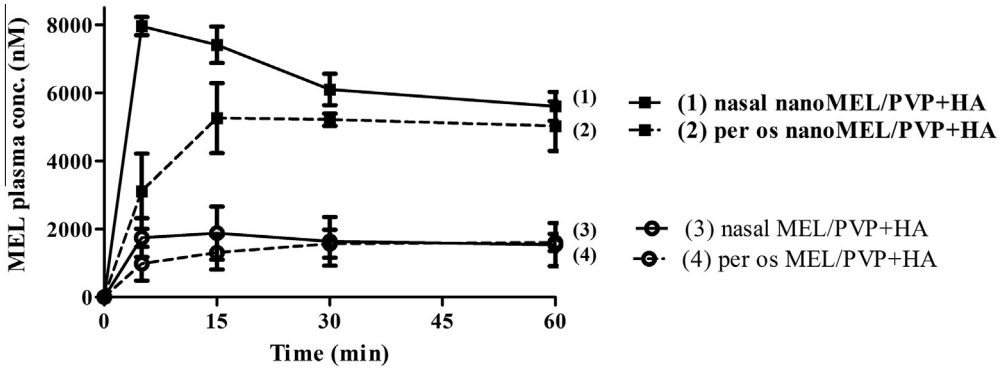

Fig. 4. Plasma drug concentrations vs. time profile in rats after nasal and oral administration of 60 μg meloxicam. MEL/PVP, meloxicam and polyvinylpyrrolidone C30 mass ratio 1:1; HA, sodium hyaluronate (5 mg/mL). Data are presented as mean ± S.D., $n = 5$.

Table 2
Pharmacokinetic parameters after nasal and oral administration of 60 μg meloxicam in rats.

	Per os MEL/PVP + HA (±S.D.)	Per os nanoMEL/PVP + HA (±S.D.)	Nasal MEL/PVP + HA (±S.D.)	Nasal nanoMEL/PVP + HA (±S.D.)	*P* p.os	*P* nas	*P* p.os/nas	*P* nano p.os/nas
k_a (1/min)	0.13 ± 0.12	0.12 ± 0.10	NA	NA	ns	NA	NA	NA
k_e (1/min)	5.3 (±2.0) × 10^{-4}	8.3 (±1.9) × 10^{-4}	5.6 (±3.6) × 10^{-4}	8.8 (±0.7) × 10^{-4}	*	ns	ns	ns
t_{max} (min)	110.6 (±140.8)	88.0 (±90.2)	312.0 (±107.3)	5.0 (±0.0)	ns	***	*	ns
C_{max} (μM)	2.15 (±0.32)	5.03 (±0.59)	2.92 (±0.96)	7.95 (±0.23)	***	***	ns	***
AUC 0-t (μmol * min/L)	2.287.0 (±466.7)	4.478.0 ± (412.1)	3,342.0 (±1,236.0)	4,838.0 (±384.4)	***	*	ns	ns
AUMC (μmol * min^2/L)	1.42 (±1.65) × 10^7	0.89 (±0.39) × 10^7	3.24 (± 3.69) × 10^7	7.17 (±1.32) × 10^7	ns	ns	ns	ns
MRT (min)	2.292 (±1.346)	1.277 (±293)	2.882 (±2.298)	1.064 (±98)	ns	ns	ns	ns

Statistically significant differences between groups are indicated as $^{*}P < 0.05$; $^{**}P < 0.01$ and $^{***}P < 0.001$. Abbreviations: AUC, area under the curve; AUMC, area under the first moment curve; C_{max}, the peak plasma concentration; k_a, absorption rate constant; k_e, elimination rate constant; MEL/PVP + HA, meloxicam and polyvinylpyrrolidone C30 mass ratio 1:1 with sodium hyaluronate (5 mg/mL); MRT, mean residence time; NA, not applicable; nanoMEL/PVP + HA, nanonized meloxicam and polyvinylpyrrolidone C30 mass ratio 1:1 with sodium hyaluronate (5 mg/mL); ns, not significant; p.os, per os drug administration; S.D., standard deviation; t_{max}, time to reach C_{max}.

decrease after 1-h treatment with various MEL-containing liquid formulations in the applied concentrations as compared to the control group which was treated with culture medium used as the vehicle of the formulations. These results indicate that nasal formulations do not influence nasal epithelial cell viability (Fig. 3A).

The flux of MEL through human RPMI 2650 cell layers was significantly increased in the case of the nasal formulation which contained nanoparticles and sodium hyaluronate (Fig. 3B).

Impedance measured by RT-CES non-invasively quantifies adherens cell proliferation, viability and cell layer integrity. The RT-CES results indicated no sign of disruption in the integrity of the human RPMI 2650 cell layers, which could be observed in the toxicity control group (Fig. 3C).

3.4. In vivo experiments on rats to study nasal and oral delivery of meloxicam

Nasal and oral administration of MEL nanoparticles to Sprague–Dawley rats led to completely different pharmacokinetic profile of MEL. During the first 60 mins after intranasal and oral treatment with 60 μg MEL/animal, the drug concentration in blood plasma vs. time is shown in Fig. 4. The differences in maximum plasma concentration (C_{max}), time to reach the maximum plasma concentration (t_{max}) and other important pharmacokinetic parameters were summarized by the plasma concentration–time profile (Table 2).

In the case of nasal administration of MEL nanoparticles extremely high, about 8 μM plasma level of MEL was observed in the first time point, after 5 min. The differences between the nasal and oral drug administration route almost disappeared after 30 min, but the two formulations remained entirely different, the average plasma level of MEL was 6 μM vs. 2 μM.

The absorption coefficients (k_a), the t_{max} values were not significantly different in case of the oral administration route, nor the mean residence time (MRT) of MEL, although the C_{max} and AUC were doubled in case of oral delivery of nanoparticles. Concerning nasal administration of both the formulations, there was no statistical difference in MRT but almost 5 μmol × min/L AUC could be reached with the nanonized drug. The AUC and C_{max} were found to be significantly elevated when meloxicam was administered nasally to rats as drug nanoparticles compared to orally given physical mixture of the drug and the excipients (2-fold higher AUC, 4-fold higher C_{max}).

4. Discussion

MEL, a non-steroidal anti-inflammatory drug (NSAID) with analgesic properties, is an enolic acid oxicam derivative (Hanft et al., 2001; Fahmy, 2006). The aqueous thermodynamic solubility of MEL is poor (4.4 μg/mL in water) and the rate of dissolution is low (15% in 5 min). MEL has low molecular mass (351.4 kDa) and relatively well-permeable. The poor dissolution property of the drug is a limiting factor for its absorption rate and its onset of action, although its bioavailability is 89% after dissolution (Del Tacca et al., 2002; Ambrus et al., 2009). The usual recommended oral dose is 7.5–15 mg/day; a dose as high as 30 mg/day may also be applied (Euller-Ziegler et al., 2001). A parenteral formulation of MEL (15 mg/1.5 mL) has been developed for situations requiring rapid analgesia, such as acute mechanical lower back pain, sciatica and acute flares of osteoarthritis (Davies and Skjodt, 1999).

However the mean C_{max} value was achieved within 4–5 h after oral administration of MEL incorporated to a solid dosage form, indicating elongated drug absorption (Busch et al., 1998). According to our results with MEL nanoparticles the C_{max} was reached

within 90 min in the case of oral liquid formulation and 5 min in the case of the nasal formulation. However Illum et al. (2001) and Wang et al. (2011) described that very short t_{max} values (15–20 min) could be achieved by nasal administration of hydrophilic and lipophilic active agents as well. Considerably the plasmakinetics of MEL in the case of nasally applied drug nanoparticles was similar to an intravenous injection, the C_{max} was reached in the first time point (5 min).

The relationship between solubility and permeability was investigated by other research groups (Frank et al., 2012a,b). Solubility enhancement is not always accompanied by increase in permeability; it depends on the chosen method. Of all the strategies to increase the apparent solubility of poorly soluble drugs, enhancement of the molecularly dissolved drug concentration (induction of true supersaturation) would lead to better permeation though membranes as demonstrated by di Cagno and Luppi (2013).

Nanonization of MEL led to significant increase in thermodynamic solubility and subsequent permeability. Several factors may contribute to the significantly better dissolution properties of MEL nanoparticles, namely (i) the particle size reduction, (ii) the increase in specific surface area, (iii) the presence of hydrophilic polymers, (iv) the amorphization of MEL and (v) the interaction between the drug and the polymer additive. These differences in the dissolution properties of MEL were more remarkable in case of nasal conditions (pH 5.6; 30 °C; Kürti et al., 2011), while the thermodynamic solubility of MEL is pH-dependent (Seedher and Bhatia, 2003).

NSAIDs, including MEL, can cause serious gastrointestinal adverse events including inflammation, bleeding, ulceration, and perforation of the stomach, small intestine, or large intestine, which can be fatal (Hanft et al., 2001). Therefore nasal pathway of drug administration is preferable to reduce gastrointestinal side-effects and to circumvent the first-pass metabolism in the liver (Illum et al., 2001).

Information on epithelial toxicity is crucial for pharmaceutical use of nanoparticles. *In vitro* cell culture assays are useful tools to investigate the toxicity of nanonized drugs. In comparison to animal models, cell viability assays allow for a simpler, faster and more cost-efficient assessment of toxicity. Limitation of *in vitro* test systems is the lack of the complexity of animal models or the human body. Nanoparticles can interfere with conventional end-point colorimetric *in vitro* toxicity assays (Kroll et al., 2009). Therefore novel technologies such as marker-free, real-time assays greatly help to reveal the interaction of nanoparticles with cells. Furthermore the continuous monitoring of the biological status of the cells can be integrated in conventional medium or high-throughput plate formats (Ressler et al., 2004; Ózsvári et al., 2010).

By using a MTT test and a real-time assay we demonstrated for the first time that the liquid pharmaceutical formulation containing MEL nanoparticles and sodium hyaluronate is not toxic for human nasal epithelial cells. By comparing the results of RT-CES on nasal epithelial cells with other data from the epithelial toxicity of sucrose esters (Kürti et al., 2012), the lack of change in cell index indicates that MEL nanoparticles are not toxic and do not influence the paracellular pathway.

The *in vitro* permeability results on a synthetic membrane and the cell-based assays suggest the potential usefulness of the pharmaceutical formulation containing nanoMEL/PVP + HA for nasal delivery. In animal experiments the MEL drug nanoparticles administered nasally or orally to rats as compared to physical mixture of the drug and the excipients showed better pharmacokinetic parameters. In the case of drug nanoparticles administered either by the nasal or oral route the individual differences in plasma drug levels were smaller indicating a more uniform absorption.

Based on our results it can be concluded that the pharmacokinetic parameters were significantly increased when MEL was administered as nanoparticles to rats either nasally or orally as compared to physical mixture of the drug and the excipients. Drug nanoparticles administered intranasally show a very quick and high plasma peak. Further experiments are necessary to prove the therapeutic relevance of this innovative pharmaceutical formulation.

Acknowledgements

Dr. Ákos Kukovecz and Gábor Kozma for the co-grinding process; Dr. László Puskás and dr. Béla Ózsvári for the real-time cell microelectronic sensing; Dr. Erzsébet Csányi and Dr. Eszter Csizmazia for the Franz cell diffusion experiment; Dr. Adrienn Seres, Dr. Beáta Deák, Zoltánné Csiszár and Lászlóné Horváth for the *in vivo* experiments.

The Project named, TÁMOP-4.2.2/B-10/1-2010-2012 – Broadening the knowledge base and supporting the long term professional sustainability of the Research University Centre of Excellence at the University of Szeged by ensuring the rising generation of excellent scientists" is supported by the European Union and co-financed by the European Regional Development Fund.

References

Ambrus, R., Kocbek, P., Kristl, J., Sibanc, R., Rajkó, R., Szabó-Révész, P., 2009. Investigation of preparation parameters to improve the dissolution of poorly water-soluble meloxicam. Int. J. Pharm. 381, 153–159.

Bai, S., Yang, T., Abbruscato, T.J., Ahsan, F., 2008. Evaluation of human nasal RPMI 2650 cells grown at an air–liquid interface as a model for nasal drug transport studies. J. Pharm. Sci. 97, 1165–1178.

Busch, U., Schmid, J., Heinzel, G., Schmaus, H., Baierl, J., Huber, C., Roth, W., 1998. Pharmacokinetics of meloxicam in animals and the relevance to humans. Drug Metab. Dispos. 26, 576–584.

Chien, Y.W., Su, K.S.E., Chang, S., 2008. Nasal Systemic Drug Delivery. Informa Healthcare Inc., New York.

Costantino, H.R., Illum, L., Brandt, G., Johnson, P.H., Quay, S.C., 2007. Intranasal delivery: physicochemical and therapeutic aspects. Int. J. Pharm. 337, 1–24.

Csóka, I., Csányi, E., Zapantis, G., Nagy, E., Féher-Kiss, A., Horváth, G., Blazsó, G., Erős, I., 2005. In vitro and in vivo percutaneous absorption of topical dosage forms: case studies. Int. J. Pharm. 291, 11–19.

Davies, N.M., Skjodt, N.M., 1999. Clinical pharmacokinetics of meloxicam. A cyclo-oxygenase-2 preferential nonsteroidal anti-inflammatory drug. Clin. Pharmacokinet. 36, 115–126.

Del Tacca, M., Colucci, R., Fornai, M., Blandizzi, C., 2002. Efficacy and tolerability of meloxicam, a COX-2 preferential nonsteroidal antiinflammatory drug: a review. Clin. Drug Investig. 22, 799–818.

Deli, M.A., 2009. Potential use of tight junction modulators to reversibly open membranous barriers and improve drug delivery. Biochim. Biophys. Acta 1788, 892–910.

di Cagno, M., Luppi, B., 2013. Drug "supersaturation" states induced by polymeric micelles and liposomes: a mechanistic investigation into permeability enhancements. Eur. J. Pharm. Sci. 48, 775–780.

Euller-Ziegler, L., Velicitat, P., Bluhmki, E., Türck, D., Scheuerer, S., Combe, B., 2001. Meloxicam: a review of its pharmacokinetics, efficacy and tolerability following intramuscular administration. Inflamm. Res. 50, 5–9.

Fahmy, M., 2006. Ca-alginate beads loaded with meloxicam: effect of alginate chemical composition on the properties of the beads and ulcerogenicity of the drug. J. Drug Deliv. Sci. Technol. 16, 183–189.

Frank, K.J., Rosenblatt, K.M., Westedt, U., Hölig, P., Rosenberg, J., Mägerlein, M., Fricker, G., Brandl, M., 2012a. Amorphous solid dispersion enhances permeation of poorly soluble ABT-102: true supersaturation vs. apparent solubility enhancement. Int. J. Pharm. 437, 288–293.

Frank, K.J., Westedt, U., Rosenblatt, K.M., Hölig, P., Rosenberg, J., Mägerlein, M., Brandl, M., Fricker, G., 2012b. Impact of FaSSIF on the solubility and dissolution-/permeation rate of a poorly water-soluble compound. Eur. J. Pharm. Sci. 47, 16–20.

Hanft, G., Turck, D., Scheuerer, S., Sigmund, R., 2001. Meloxicam oral suspension: a treatment alternative to solid meloxicam formulations. Inflamm. Res. 50, 35–37.

Horvát, S., Fehér, A., Wolburg, H., Sipos, P., Veszelka, S., Tóth, A., Kis, L., Kurunczi, A., Balogh, G., Kürti, L., Erős, I., Szabó-Révész, P., Deli, M.A., 2009. Sodium hyaluronate as a mucoadhesive component in nasal formulation enhances delivery of molecules to brain tissue. Eur. J. Pharm. Biopharm. 72, 252–259.

Illum, L., 2003. Nasal drug delivery: possibilities, problems and solutions. J. Control. Release 87, 187–198.

Illum, L., Watts, P., Fisher, A.N., Hinchcliffe, M., Norbury, Jabbal-Gill, H.I., Nankervis, R., Davis, S.S., 2001. Intranasal delivery of morphine. J. Pharmacol. Exp. Ther. 301, 391–400.

Kroll, A., Pillukat, M.H., Hahn, D., Schnekenburger, J., 2009. Current in vitro methods in nanoparticle risk assessment: limitations and challenges. Eur. J. Pharm. Biopharm. 72, 370–377.

Kürti, L., Kukovecz, Á., Kozma, G., Ambrus, R., Deli, M.A., Szabó-Révész, P., 2011. Study of the parameters influencing the co-grinding process for the production of meloxicam nanoparticles. Powder Technol. 212, 210–217.

Kürti, L., Veszelka, S., Bocsik, A., Dung, N.T.K., Ózsvári, B., Puskás, L.G., Kittel, Á., Szabó-Révész, P., Deli, M.A., 2012. The effect of sucrose esters on a culture model of the nasal barrier. Toxicol. In Vitro 26, 445–454.

Kürti, L., Veszelka, S., Bocsik, A., Ózsvári, B., Puskás, L.G., Kittel, Á., Szabó-Révész, P., Deli, M.A., 2013. Retinoic acid and hydrocortisone strengthen the barrier function of human RPMI 2650 cells, a model for nasal epithelial permeability. Cytotechnology 65, 395–406.

Mäder, K., Weidenauer, U., 2010. Innovative Arzneiformen -Ein Lehrbuch für Studium und Praxis. Wissenschaftliche Verlagsgesellschaft mbH, Stuttgart, pp. 340–344.

Makai, A., Csányi, E., Németh, Z., Pálinkás, J., Erős, I., 2003. Structure and drug release of lamellar liquid crystals containing glycerol. Int. J. Pharm. 256, 95–107.

Morgen, M., Bloom, C., Beyerinck, R., Bello, A., Song, W., Wilkinson, K., Steenwyk, R., Shamblin, S., 2012. Polymeric nanoparticles for increased oral bioavailability and rapid absorption using celecoxib as a model of a low-solubility, high-permeability drug. Pharm. Res. 29, 427–440.

Müller, R.H., Gohla, S., Keck, C.M., 2011. State of the art of nanocrystals – Special features, production, nanotoxicology aspects and intracellular delivery. Eur. J. Pharm. Biopharm. 78, 1–9.

Östh, K., Paulsson, M., Björk, E., Edsman, K., 2002. Evaluation of drug release from gels on pig nasal mucosa in a horizontal Ussing chamber. J. Control. Release 83, 377–388.

Ózsvári, B., Puskás, G.L., Nagy, L.I., Kanizsai, I., Gyuris, M., Madácsi, R., Fehér, L.Z., Gerö, D., Szabó, Cs., 2010. A cell-microelectronic sensing technique for the screening of cytoprotective compounds. Int. J. Mol. Med. 25, 525–530.

Rabinow, B.E., 2004. Nanosuspensions in drug delivery. Nat. Rev. Drug Discovery 3, 785–796.

Ressler, J., Grothe, H., Motrescu, E., Wolf, B., 2004. New concepts for chip-supported multi-well-plates: realization of a 24-well-plate with integrated impedance sensors for functional cellular screening applications and automated microscope aided cell-based assays. Conf Proc. IEEE Eng. Med. Biol. Soc. 3, 2074–2077.

Schiller, J., Volpi, N., Hrabárová, E., Soltés, L., 2011. Hyaluronic acid: a natural biopolymer. In: Kalia, S., Avérous, L. (Eds.), Biopolymers: Biomedical and Environmental Applications. Scrivener Publishing LLC, Massachusetts, pp. 3–34.

Schmidt, M.C., Peter, H., Lang, S.R., Ditzinger, G., Merkle, H.P., 1998. In vitro cell models to study nasal mucosal permeability and metabolism. Adv. Drug Deliv. Rev. 29, 51–79.

Seedher, N., Bhatia, S., 2003. Solubility enhancement of Cox-2 inhibitors using various solvent systems. AAPS PharmSciTech 4, 1–9.

Siewert, M., Dressman, J., Brown, C.K., Shah, V.P., 2003. FIP/AAPS Guidelines to dissolution/in vitro release testing of novel/special dosage forms. AAPS PharmSciTech 4, 1–10.

Solly, K., Wang, X., Xu, X., Strulovici, B., Zheng, W., 2004. Application of real-time cell electronic sensing (RT-CES) technology to cell-based assays. Assay Drug Dev. Technol. 4, 363–372.

Ugwoke, M.I., Agu, R.U., Verbeke, N., Kinget, R., 2005. Nasal mucoadhesive drug delivery: background, applications, trends and future perspectives. Adv. Drug Deliv. Rev. 57, 1640–1665.

Wang, S., Chow, M.S.S., Zuo, Z., 2011. An approach for rapid development of nasal delivery of analgesics – identification of relevant features, in vitro screening and in vivo verification. Int. J. Pharm. 420, 43–50.

Wengst, A., Reichl, S., 2010. RPMI 2650 epithelial model and three-dimensional reconstructed human nasal mucosa as in vitro models for nasal permeation studies. Eur. J. Pharm. Biopharm. 74, 290–297.

Wolburg, H., Wolburg-Buchholz, K., ·Sam, K., Horvát, S., Deli, M.A., Mack, A.F., 2008. Epithelial and endothelial barriers in the olfactory region of the nasal cavity of the rat. Histochem. Cell Biol. 130, 127–140.

PUBLICATION VI.

Acta Pharmaceutica Hungarica 81. 1-8 2011.

Eljárási paraméterek optimalizálása szónikus kavitáció alkalmazásával, hatóanyag szemcseméret csökkentése céljából

AMBRUS RITA, BARTOS CSILLA, SZABÓNÉ RÉVÉSZ PIROSKA*

Szegedi Tudományegyetem, Gyógyszertechnológiai Intézet, Szeged, Eötvös u. 6 – 6720

Levelezési cím: revesz@pharm.u-szeged.hu

Summary

Ambrus, R., Bartos, Cs., Szabó-Révész, P.: ***Optimization of technological parameters using acustic cavitation to reach particle size reduction of pharmacon***

The main aspect in the field of pharmaceutical technology is the preformulation of the poorly water soluble drugs. The habit of particles can effect the physico-chemical properties which are important factors by drug administration. In the past years the role of the procedures by acustic cavitation increased in the field of particle engineering. Application of high power ultrasound by integration and dezintegration can lead to particle size decreasing. Meloxicam as a nonsteroid anti-inflammatory model drug was used to study the effect of power ultrasound on the particle size decreasing. During our work technological parameters, as amplitude, temperature, time, excipients and concentration were optimized based on particle size distribution. Physico-chemical stability tests were also performed (XRPD, DSC, SEM, particle size). With optimized parameters (70% amplitude, 20 min, 47 °C) using excipients, crystalline micronized product was produced.

Key-words: *meloxicam, particle size decreasing, acustic cavitation, optimization.*

Összefoglaló

Napjainkban az egyik legnagyobb kihívást a gyógyszertechnológus számára a rossz vízoldékonyságú hatóanyagok preformulálása jelenti. A szemcsék habitusa, morfológiai sajátságai nagy befolyással vannak a hatóanyagok fizikai-kémiai sajátságaira, ezen kívül meg kell felelniük egyes formulálási és alkalmazási követelményeknek. Az utóbbi években a szemcseméret csökkentés területén az akusztikus kavitáción alapuló eljárások előretörése figyelhető meg. Aktív ultrahanggal integráláson vagy dezintegráláson alapuló szemcseméret csökkentés érhető el.

Modellanyagként a meloxikámot, nem szteroid gyulladáscsökkentőt választottuk a szónikus kavitáció szemcseméret csökkentésre gyakorolt hatásának tanulmányozása céljából. Vizsgálataink során technológiai paraméterek, mint amplitúdó, hőmérséklet, idő, segédanyag és koncentráció optimalizálását végeztük el. Az eljárási paraméterek optimalizálásánál a minták szemcseméret megoszlását vettük alapul. Munkánk során fizikai-kémiai stabilitási vizsgálatokat (XRPD, DSC, SEM, szemcseméret) végeztünk. Optimalizált paraméterekkel (70% amplitúdó, 20 perc, 47 °C) segédanyag jelenlétében kristályos, mikronizált terméket kaptunk.

Kulcsszavak: *meloxikám, szemcseméret csökkentés, szónikus kavitáció, optimalizálás.*

1. A kavitáció jelensége és csoportosítása

A kavitáció (***1. ábra***) fizikai jelenség, amely akkor következik be, ha egy anyag folyadék fázisból hirtelen gáz fázisba megy át a nyomás esése következtében. Ha a folyadék sebessége hirtelen megnő, akkor az energia-megmaradás törvénye értelmében (Bernoulli törvénye) a nyomása leesik. Ha a keletkező gőzbuborék, az áramlás mentén olyan helyre ér, ahol a nyomás nagyobb az ottani hőmérséklethez tartozó telített gőz nyomásnál, akkor a buborék hirtelen összeroskad, az egymásnak csattanó folyadékfelületek erős akusztikus lökéshullámot keltenek, ami egyrészt erős zajjal, rezgéssel, másrészt a környező szilárd testek eróziójával jár [1].

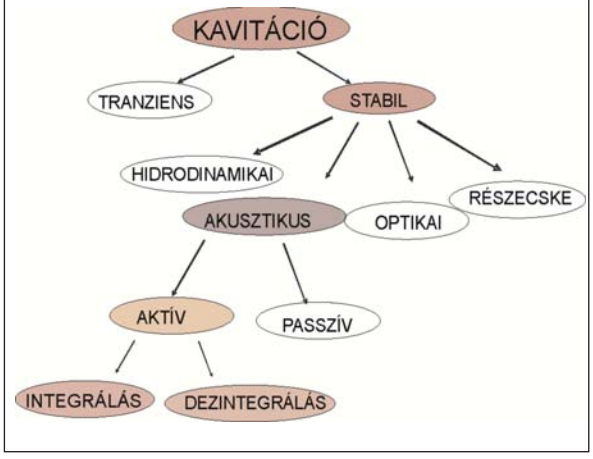

1. ábra: A kavitáció jelensége és csoportosítása

Tranziens kavitáció során a kavitációs üreg egy ciklus során megnövekszik, majd hevesen összeomlik. A folyamat során a molekulák széttöredezése is megfigyelhető, a vele szemben elhelyezkedő szilárd falat, így például sejteket, készüléket erőteljesen erodálja [2]. *Stabil kavitáció* akkor történik, ha a buborék számos cikluson keresztül oszcillál, a térből való távozás, vagyis felszínre vándorlás, illetve összeomlás nélkül, és a depresszió alatt mérete csökken, majd az ellenkező fázisban újra kitágul, mivel gőzt tartalmaz. Bizonyos esetekben a depressziós akusztikai/mechanikai ciklus alatt tágul, az ellenkező fázisban pedig zsugorodik a buborék, amelynek erőteljes több ezer kelvines hőképződés lehet az eredménye. A stabil kavitációs buborék az oszcilláló akusztikai tér miatt saját frekvenciával rendelkezik, illetve általában további felületi rezgések is kialakulhatnak rajta, amelyek a buborék környezetében erőteljes turbulenciákat indukálnak. Ezeket a turbulenciákat nevezzük mikroáramlásoknak, amelyekre nagy nyíróerő a jellemző [3].

Az ultrahang 16 kHz frekvencia feletti mechanikai hullámokat jelent. Az ultrahangot aktív és passzív tartományra oszthatjuk, vagyis megállapodás szerint az 1 W/cm^2 vagyis a 10000 W/m^2 teljesítmény alatt passzív, míg felette aktív ultrahangról beszélünk. A passzív ultrahangot leginkább az anyagtulajdonságok vizsgálatára, míg az aktív ultrahangot az anyag tulajdonságainak megváltoztatására alkalmazzuk. Tipikusan nemlineáris jelenség az állandó folyadékmozgás, amit az intenzív ultrahang okoz. Ennek során a folyadékban szemmel látható keveredés, turbulencia tapasztalható. A keverés mellett megvalósítható a diszpergálás is (pl. emulzió és szuszpenzió előállítás). Az ultrahangot rezgéskeltőkkel állítjuk elő. Legelterjedtebbek az elektromechanikus átalakítók. Az adszorpció miatt az ultrahang intenzitása a távolsággal exponenciálisan csökken. A modern ultrahang-berendezések aktív elemei legtöbbször ólom cirkonát titanát (PZT) kerámiák [4-7].

Munkánk során célul tűztük ki a nagyintenzitású ultrahang alkalmazhatóságának tanulmányozását a gyógyszerformulálás területén, továbbá kísérletes eredményekkel mutatjuk be a szemcseméret csökkentésben betöltött szerepét.

2. Aktív ultrahang a gyógyszerészet területén

A nagyintenzitású ultrahang alkalmazása a gyógyszertechnológiai preformulációban új irányvonalként jelent meg az utóbbi időben, ahol az akusztikus kavitáció szemcseméretre és morfológiára gyakorolt hatását mind integráló, mind dezintegráló műveleteknél hasznosíthatjuk [8].

2.1. Emulgeálás és szuszpendálás ultrahanggal, szonokémia

Az aktív ultrahang, emulzióképző berendezésben vagy szuszpenziók akusztikai ülepítésére alkalmas szeparáló készülékben és szonokémiai generátorban funkcionálhat a gyógyszerészet területén. Az emulzióképzés elvi sémája alapján az olajos és vizes fázis egymással szembe lép be a rendszerbe, majd a középvonalon, az addigi áramlással merőleges ultrahangsugárban képződik az emulzió. Több ultrahangos emulzió-előállító berendezéssel szemben előnyt jelenthet, hogy az ultrahangsugár hosszabb távon érheti az anyagokat, így sokkal stabilabb emulziók készíthetőek [9]. További felhasználási lehetősége az ultrahangnak az emulziók és szuszpenziók ülepítésének gyorsítása. A technika lényege az, hogy speciálisan tervezett akusztikai kamrában állóhullámot kialakítva történik meg az eltérő fizikai tulajdonságú közegek szétválasztása, a vivőközeghez képest sűrűség, fajsúly, kompresszibilitásbeli különbség, alaki részecskejellemzők stb. alapján. Meghatározható, hogy milyen szemcsekoncentráció szükséges egy adott intenzitás mellett, vagy milyen intenzitás szükséges egy adott szemcsekoncentrációhoz az ultrahangtérben, hogy akusztikai állóhullám, vagy akusztikai kavitáció alakulhasson ki. Amennyiben a rendszerben állóhullám kerül kialakításra, akkor a szeparáció és szedimentáció, amikor viszont kavitáció dominál a hangtérben, akkor a diszpergálás, az emulgeálás és a szuszpendálás valósítható meg az ultrahang segítségével [10]. A kémia speciális területe a szonokémia, melyben speciális reakciókat, új reakció utakat és reakciótermékeket nyerhetünk ultrahang hatására, és az eljárásokat pedig szónikus reaktorokban folytatjuk. Az ultrahang fő kémiai szerepe a kavitációs buborékon kialakuló katalízis, vagyis a reakciók aktiválási energiájának csökkentése, szonokemikáliák kialakítása, reakciók gyorsítása, reakciópartnerek diszpergálása, diffúziós felület növelése és az enzimaktivitás szabályozása, preparatív termékek előállítása stb. [11].

2.2. Ultrahang alkalmazása a szemcsék habitusának változtatása céljából

Az ultrahangos homogenizálás egy mechanikai

I. táblázat

Az ultrahang szemcseméretre gyakorolt hatása

Anyagok	Módszer	Méret	Eljárás jellemző paraméterei
Cefuroxim [14]	Ultrahangos kristályosítás	80-130 nm (amorf)	Oldószer: aceton Antiszolvens: izopropil-éter T~5 °C; t = 1 perc
Kaolinit [15]	Ultrahang	360 nm	Diszpergálószer: ioncserélt víz T: 20 °C; t = 20 h 20 kHz; 750 W
Glicin [16]	Ultrahangos hűtéses kristályosítás	100 μm	Diszpergálószer: ioncserélt víz 20 kHz
Dipiridamol [17]	Szuperkritikus antiszolvens eljárás ultrahanggal kombinálva	300-600 nm	Oldószer: metilén-klorid T: 37 °C Amplitúdó: 20-40%
Nitrendipin [18]	Ultrahangos kristályosítás	209 nm	Oldószer: PEG 200 + aceton (30 mg/ml nitrendipin konc.) Antiszolvens: PVA + víz T: 3 °C alatt t= 15 perc; 400 W
Cellulóz [19]	Hidrodinamikai kavitáció kombinálva ultrahanggal	301 nm (amorf és kristályos)	Diszpergálószer: ioncserélt víz 22 kHz
Nátrium-klorid [20]	Szonokristályosítás	1,23 μm	Diszpergálószer: ioncserélt víz T: 5 °C alatt; 20 kHz; 35 W
Ibuprofen [21]	Olvadék-kristályosítás	13,01 μm	Minta: ibuprofen olvadék + ionmentes víz T: 25 °C; t = 2 perc; Amplitúdó: 80%
Meloxicam [22]	Emulzió-diffúzió módszer	165 nm	Oldószer: benzil-alkohol + 3 perc ultrahang + (Tween 80 + víz) + újabb 3perc ultrahang Amplitúdó: 30%; 500 W
Gemfibrozil [23]	Emulzió-diffúzió módszer	2,89 μm	Oldószer: etil-acetát, az oldat 0,5% PVP K-25 oldatba lett csepegtetve t = 7,5 perc; Amplitúdó: 30%

II. táblázat

Szonikáció során változó paraméterek

Hőmérséklet (°C)	szobahő, jeges hűtés
Amplitudó (%)	30, 50, 70
Idő (perc)	10, 20, 30

folyamat, amely a részecskeméret csökkentésére, egyenletes méreteloszlás elérésére irányul, javítva ezáltal az egységességet és a stabilitást, növelve a részecskeszámot és a fajlagos felületet, csökkentve a részecskék közötti átlagos távolságot. A részecskék (diszpergált rész) lehetnek szilárd vagy folyékony halmazállapotúak. További nagy előny, hogy a paraméterek (amplitúdó, pulzáció, idő, hőmérséklet) pontosan beállíthatók és ellenőrizhetők, az ultrahangos homogenizálás reprodukálható. Az ultrahangnak két fő része van, a szonotród és az áramlási cella, mindkettő egyszerű geometriai felépítésű, nem rendelkeznek kicsi, rejtett nyílásokkal. Az ultrahangos homogenizálás egyik nagy előnye, hogy kevés a mozgó alkatrész, így megbízhatóbb, kevésbé kopik és a tisztítási idő is rövidebb [12].

A méretcsökkentés, dezintegráció révén, a kavitáció eredménye. Az ultrahangos kavitáció nagy nyíróerőt generál, ami képes szétszakítani a részecske-aggregátumot, legyőzve a részecskék közötti vonzóerőket. Az ultrahangos kezelés által elérhető a részecskék homogén eloszlatása is. A részecskeméret akár 500 μm-ről 10 nm-re csökkenthető, ahol a nagy fajlagos felületű részecskék méretének egységességét lehet elérni [13].

Az ***I. táblázat*** az ultrahang alkalmazásának lehetőségeit szemlélteti különböző hatóanyagok szemcseméret csökkentése céljából.

3. Anyagok és eljárás

Felhasznált anyagok: *meloxikám* (MEL) – EGIS Gyógyszergyár (Budapest, Magyarország); *Tween 80* (Tween) – Hungaropharma (Budapest, Magyarország); *Poloxamer 188* (polox) (polietilén-polipropilén glikol) – Fluka (Ljubljana, Szlovénia); *Solutol HS 15* – BASF (Ludwigshafen, Németország); *PVP K25* (PVP) (polivinilpirrolidon) – ISP Customer Service GmBH (Köln, Németország).

Ultrahangos eljárás

Az eljárás során a mintákat (vizes szuszpenzió – 300 mg hatóanyag / 30 ml víz) szobahőmérsékleten (25 °C), illetve jeges hűtés (a mintát kezelés közben 18 °C-os jéggel hűtött fürdőbe helyeztük) mellett ultrahangoztuk (Hielscher 200 W Ultrasound system, Németország), az amplitúdót 30 és 70% között változtattuk. A megjelölt paraméterekkel 10, 20, illetve 30 perces szonikációt végeztünk (***II. táblázat***).

4. Vizsgálati módszerek

4.1. Szemcseméret megoszlás, morfológia

A MEL *szemcsék méretét* és méreteloszlását Malvern Mastersizer 2000 készülékkel (Malvern Instruments, Worcestershire, UK) határoztuk meg (Hydro 2000 SM kis térfogatú diszpergáló egység). A hatóanyag és szilárd minta *morfológiai jellemzése* pásztázó elektronmikroszkóppal történt (Hitachi S4700, Hitachi Scientific Ltd., Japan). A minta töltődésének megakadályozása céljából arany-palládium bevonó anyagot használtunk 18 mA plazmaáram alkalmazásával. A felvételek 15 kV nagyfeszültség, 10 μA elektronáram és 0,1 Pa élővákuum beállításával készültek. A D 0,1, D 0,5, D 0,9 értékeket térfogat szerinti méretanalízissel határoztuk meg. A D 0,1, D 0,5, D 0,9 azok a méretek mikrométerben, amelyeknél a minta 10, 50 illetve 90%-a kisebb [24].

4.2. Szerkezeti jellemzők

A termékek *termoanalitikai viselkedését* Mettler Toledo STAR® termoanalitikai készülékkel (Mettler Inc., Schwerzenbach, Svájc) határoztuk meg. A *DSC (differenciál pásztázó kalorimetria)* és *TG (termogravimetria)* méréseket argon gáz átáramoltatásával (10 l/óra) végeztük (2–5 mg-os minta, 25–300 °C, 5 °C/perc fűtési sebesség).

A hatóanyag *kristályos jellegét* porröntgen diffraktométerrel határoztuk meg (Miniflex II Rigaku por-röntgen diffraktométer, Rigaku Co. Tokyo, Japan). Mérési paraméterek: Cu (Kα = 1,5405 Å), 30 kV, 15 mA.

5. Eredmények értékelése

5.1. Eljárási paraméterek és az összetétel optimalizálása

Munkánk során először az eljárás paramétereit vizsgáltuk, változtatva a hőmérsékletet, a szonikáció amplitúdóját, illetve az ultrahangozás idejét.

III. táblázat

A MEL kiindulási D 0,1, D 0,5, D 0,9 értékei

D 0,1 (μm)	D 0,5 (μm)	D 0,9 (μm)
24,80	85,39	237,92

Ezután segédanyagok alkalmazásával, a minta összetételét optimalizáltuk.

Az összetétel optimalizálásánál különböző stabilizáló segédanyagokat használtunk, mint a PVP K-25 (kristályosodást gátló, stabilizáló szer), Poloxamer 188 (nemionos felületaktív anyag), Tween 80 (nemionos szolubilizáló szer), Solutol HS 15 (nemionos szolubilizáló szer), illetve tanulmányoztuk a ható- és segédanyagok koncentrációjának szemcseméretre gyakorolt hatását. A hatóanyag koncentrációja 1 m/v %, a segédanyagé pedig 0,5 illetve 0,25 m/v % volt. A ***III. táblázatban*** a MEL kiindulási méretmegoszlása látható, amelyre jellemző a heterodiszperzitás.

30%-os amplitúdóval 10 perces ultrahangozás után megállapítottuk, hogy a szemcseméret a kiindulásihoz képest a felére csökkent. 50%-os amplitúdó esetében a méret tovább csökkent, de az amplitúdó további növelése (70%) jelentős változást nem okozott, a D 0,5 érték körülbelül 26 μm maradt (***2. ábra bal***). A kezelés során a minta hőmérséklete kb. 85 °C-ra emelkedett, ami a hatóanyag olvadáspontja (260 °C) alá esik, így az végig szilárd formában volt jelen.

Jéggel történő hűtéssel ($T_{hűtővíz}$ = 18 °C) és 30%-os amplitudóval történő szonikációval ugyanazt a méretet értük el, amit szobahőmérsékleten az 50 és 70%-os amplitúdóval sikerült megvalósítani (26 μm). A minta kezelést követő hőmérséklete kb. 47 °C volt, azaz felére csökkent a hűtés nélküli eljáráshoz viszonyítva, ezzel segítve a kisebb méret elérését, mérsékelve a szemcsék közötti kohézió nagyságát. A legjobb eredményt – mind a D 0,1, D 0,5, D 0,9 értékek esetében – a 70%-os amplitúdóval történő kezelés biztosította, a szemcsék átlagosan 22 μm-esek lettek (***2. ábra jobb***).

A következőkben azt vizsgáltuk, hogy a kezelési idő 20 illetve 30 percre növelése eredményez-e további szemcseméret csökkenést. 20 perces kezelést követően a méret 14 μm-re csökkenthető, a 30 perces szonikáció azonban ezen jelentősen nem változtatott (ábra nem látható).

Az eddigiek alapján tehát a következő eljárási paramétereket választottuk a további vizsgálatokhoz: jeges fürdőt ($T_{hűtővíz}$ = 18 °C), 70%-os amplitúdót és 20 perces kezelést. Az összetétel optimalizálása céljából különböző segédanyagok hatását

IV. táblázat

Segédanyagok MEL szemcseméretére gyakorolt hatása

	-	0,5% PVP	0,5% Tween	0,5% Polox.	0,5% Solutol	0,25% PVP
D 0,1	3,71	0,25	1,27	1,27	0,46	**0,75**
D 0,5	14,65	4,07	11,79	11,09	7,70	**5,60**
D 0,9	36,34	20,73	30,03	40,21	25,71	**17,11**

V. táblázat

Optimalizált paraméterekkel előállított megfelelő összetételű minta

Szárítás (°C)	Segédanyag	Amp/T (70%)/(°C)	T (Szuszp) (°C)	Idő (perc)	Konc. (mg/30 ml)	Kiindulási méret D 0,5 (μm)
50	0,25% PVP	Jeges fürdő, 18	46,20	20	300	5,60

vizsgáltuk a MEL szemcseméret megoszlására. A segédanyagokat, illetve azok koncentrációját korábbi tanulmányok alapján választottuk meg [14-23]. Eredményeinket összevetve a segédanyag nélküli kísérletek eredményeivel (D 0,5: 14 μm), a legkevésbé hatékonynak a Tween 80 bizonyult, ezt követte a Poloxamer és a Solutol (***IV. táblázat***). A legkisebb szemcseméretet, átlagosan 5 μm-t PVP-vel értük el. Ez az érték a PVP koncentrációjának csökkentésekor sem változott. Látható, hogy a PVP, mint stabilizáló és kristályosodást gátló anyag mindenképpen szükséges az összetételben. A PVP koncentráció csökkentésének jelentősége az esetleges toxicitási problémák megelőzésében rejlik, hiszen különböző beviteli kapuk (pulmonális, nazális) is előtérbe kerülhetnek a kis szemcseméretű termék által, ahol az összetétel sejt toxicitására is kiemelten figyelni kell. Tehát a vizsgált rendszerek közül a 0,25% PVP tartalmú MEL szemcseméret megoszlása bizonyult optimálisnak.

5.2. Szilárd fázisú termék jellemzése (SZ-MEL-UH)

Az előkísérletek alapján az eljárási paraméterek és összetételek optimalizálását követően a kapott szuszpenzióból (***V. táblázat***) 50 °C-on, nyugvó réteges szárítóban távolítottuk el a vizet (Memmert, Németország) abból a célból, hogy szilárd terméket nyerjünk (SZ-MEL UH). A szárított termék fizikai-kémiai sajátságait az alábbiak szerint vizsgáltuk. Meg kívánjuk jegyezni, hogy a kezelt minta hőmérséklete nem haladta meg a 46,2 °C-ot, tehát hő hatására bekövetkező bomlás nem történt.

DSC felvételek

A DSC görbén a MEL-nek 259,27 °C-on jól definiálható olvadáspontja van, amit bomlás követ. A PVP amorf sajátságú segédanyag, olvadásponttal nem rendelkezik (***3. ábra***).

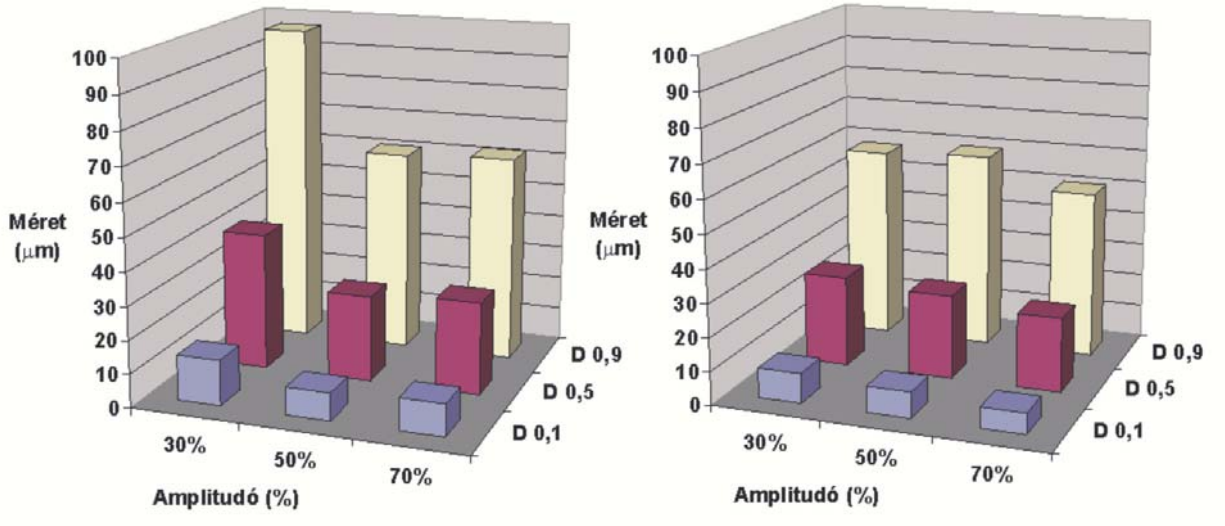

2. ábra: MEL szemcseméret megoszlása hűtés nélkül (bal) és jegesfürdő (jobb) alkalmazásával

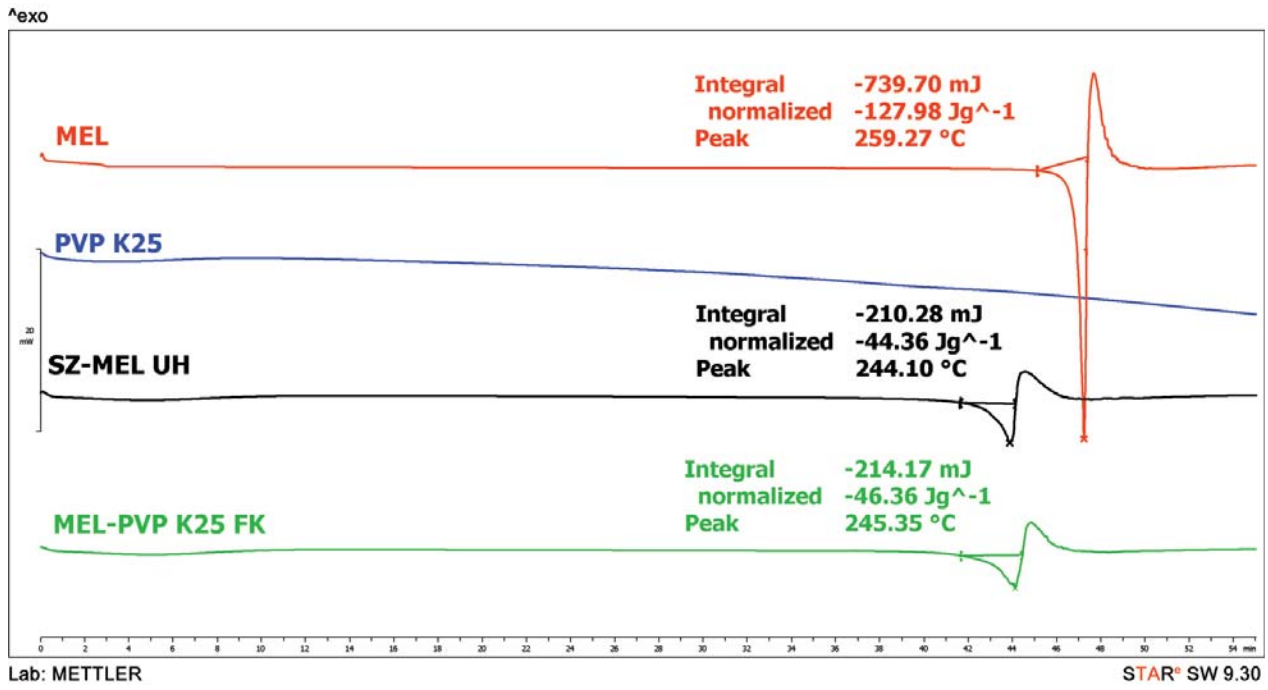

3. ábra: A kiindulási anyagok és a termék DSC görbéi

A szilárd fázisú minta (SZ-MEL-UH) görbéjén is megfigyelhető a hatóanyag kristályok olvadáspontja, amivel a MEL kezelés és szárítás utáni kristályos jellegét bizonyítottuk. A mintában látható olvadáspont-csökkenés (244,10 °C) egyrészt annak köszönhető, hogy a kisebb kristályok megolvadásához kevesebb energiára van szükség, másrészt pedig a PVP az üvegesedési hőmérsékletén (Tg = 34 °C) meglágyul, ilyen körülmények közt a MEL olvadása alacsonyabb hőmérsékleten következik be. Referenciaként a termékkel azonos arányban fizikai keveréket (MEL-PVP K25 FK) készítettünk, így összevetve a normalizált integrál értékeket az anyagok kristályossági indexét határoztuk meg. A fizikai keverékben levő MEL kristályosságát 100%-nak véve a szilárd fázisú mintában jelen levő hatóanyag kristályossága kismértékben csökkent (96%-ban kristályos frakciót detektáltunk).

XRPD eredmények

A porröntgen-diffrakciós vizsgálatok ugyancsak a minta kristályos jellegét bizonyítják, mert a karakterisztikus csúcsok a kiindulási anyagnál és a szilárd fázisú termékben is megjelennek. A MEL-re jellemző csúcsok 13,22, 15,06, 26,46 és 26,67 2Θ értékeknél olvashatóak le (***4. ábra***). A PVP amorf sajátságát bizonyítja, hogy esetében a kristályos anyagra jellemző csúcsok nem jelennek meg a diffraktogramon. Mivel a kiindulási anyagok (MEL és PVP) és a termék (SZ-MEL UH) jellemző csúcsai egybeesnek – azon kívül, hogy mintánk kristályos maradt – az is megállapítható, hogy polimorf módosulat a kezelés hatására nem jött létre.

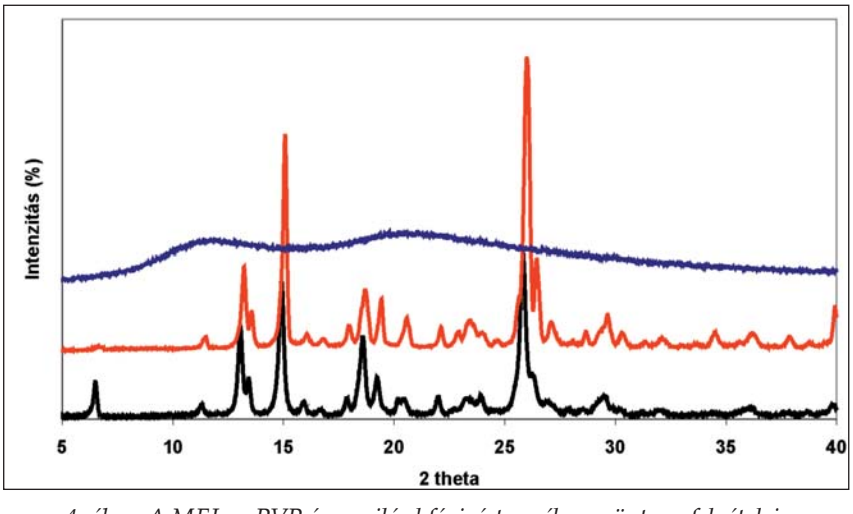

4. ábra: A MEL, a PVP és a szilárd fázisú termék porröntgen felvételei

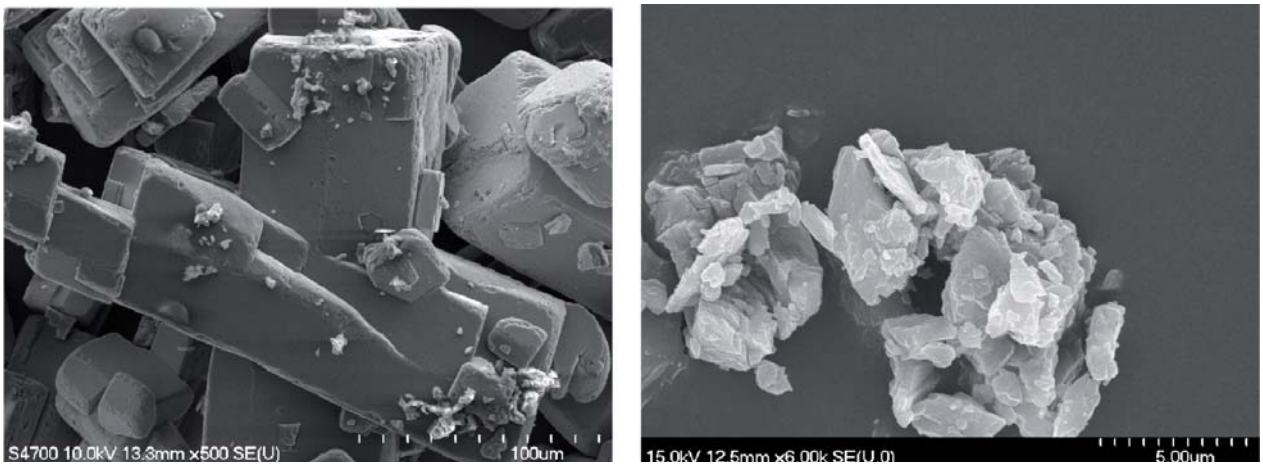

5. ábra: A kiindulási MEL (bal) és a termék (jobb) elektronmikroszkópos felvételei

VI. táblázat

A kiindulási anyag és a mintákban levő hatóanyagok fajlagos felülete és méreteloszlása

	Spec. fel (m^2/g)	D 0,1 (μm)	D 0,5 (μm)	D 0,9 (μm)
MEL	0,091	24,80	85,39	237,92
MEL UH	1,923	0,75	5,60	17,11
SZ-MEL UH	0,969	2,57	11,92	53,48

Elektronmikroszkópos felvételek

Az elektronmikroszkópos képek alapján látható, hogy a kiindulási MEL kristályai nagy, hexagonális, sima felületű kristályok, míg a MEL-t, PVP-t tartalmazó ultrahanggal kezelt termék kristályai a kezelést követően szabálytalan alakúak, egyenetlen felszínűek, a mérések alapján átlagosan 10 μm-esek (***5. ábra***).

Szemcseméret megoszlás és specifikus felület

A ***VI. táblázat*** összehasonlításban mutatja a kiindulási MEL, a szuszpenzióban levő, már ultrahangozott (MEL UH) és az abból nyert szilárd fázisú termék (SZ-MEL UH) szemcseméret megoszlását és a részecskék specifikus felületét. A szemcseméretet egy nagyságrenddel csökkentettük, ez jól látható a D 0,1, D 0,5 és D 0,9 értékek esetében is. A fajlagos felület vizes szuszpenzióban 21-szeresére növelhető. A MEL-nél szárítás hatására a stabilizáló PVP alkalmazása mellett is aggregáció következett be. A szilárd fázisú termék szemcseméretе ennek ellenére is kedvezőbb a kiindulási anyaghoz viszonyítva. Megállapítható, hogy a mikroszuszpenzió és a szilárd fázisú termék is alkalmas gyógyszerforma fejlesztéséhez.

6. Összegzés, jövőkép

Dolgozatunk összefoglalót adott a kavitáció jelenségéről és csoportosításáról, az ultrahang fizikai alapjairól és alkalmazásának lehetőségeiről a gyógyszerformulálás területén, elsősorban a kristályméret megváltoztatása céljából. Munkánk során az eljárási paramétereket és az összetételt optimalizáltuk. Megállapítottuk, hogy ultrahangozással a meloxikám kristályok mérete a mikrométer tartományba csökkenthető. A termékekben a hatóanyag kristályosságát fizikai-kémiai vizsgálatokkal bizonyítottuk. Az eredmények azt igazolták, hogy a hatóanyag fizikai-kémiai sajátsága, illetve az alkalmazott segédanyagok befolyásolják mind a szemcseméret-csökkenést, mind a szárítás során az aggregáció mértékét. Az aggregáció gátlása céljából célszerűnek tartjuk hordozó segédanyag (pl. mannit) alkalmazását is. Terveink között szerepel újabb modellanyagok vizsgálata, a kavitáció szemcseméret-csökkentő hatásának további tanulmányozása, paraméterek, összetételek optimalizálása.

7. Köszönetnyilvánítás

A TÁMOP-4.2.1/B-09/1/KONV-2010-0005 azonosító számú, „Kutatóegyetemi Kiválósági Központ létrehozása a Szegedi Tudományegyetemen” című projekt az Európai Unió támogatásával, az Európai Regionális Fejlesztési Alap társfinanszírozásával valósul meg.

IRODALOM

1. *Caupin, F., Herbert, E.*: Comptes Rendus Physique, *7*(9-10), 1000-1017 (*2006*).
2. *Church, C.C., Carstensen, L.E.*: Ultrasound Med Biol, *27*(10), 1435-1437 (*2001*).
3. *Servant, G., Caltagirone, J. P., Gérard, A., Laborde, J. L., Hita, A.*: Ultrason Sonochem, *7*(4), 217-227 (*2000*).
4. *Laborde, J.L., Bouyer, C., Caltagirone, J.P., Gérard, A.:* Ultrasonics, *36*(1-5), 581-587 (*1998*).

5. *Moholkar, V.S., Kumar, S.P., Pandit, A.B.*: Ultrason Sonochem, *6*(1-2), 53-65 (*1999*).
6. *Bunkin, N.F., Kochergin, A.V., Lobeyev, A.V., Ninham, B.W., Vinogradova, O.I.*: Colloid Surface A, *110*(2), 207-212 (*1996*).
7. *Miller, L.D., Thomas, M.R.*: J Acoust Soc Am *93*, 3475-3480 (*1993*).
8. *Franco, F., Cecila, J.A., Pérez-Maqueda, L.A., Pérez-Rodríguez, J.L., Gomes, C.S.F.*: Appl Clay Sci, *35*(1-2), 119-127 (*2007*).
9. *Behrend, O., Ax, K., Schubert, H.*: Ultrason Sonochem, *7*(2), 77-85 (*2000*).
10. *Benes, E., Grösschl, M., Handl, B., Trampler, F., Nowotny, H.*: *Das europaische TMR-Netzwerk Ultrasonic Separation of Suspended Particles*. Proc. Joint Symposium AAA and ÖPG TC Acoustics, Graz, Austria. *2*, 14-15 (*1998*).
11. *Török, B., Balázsik, K., Felföldi, K., Bartók, M.*: Ultrason Sonochem, *8*(3), 191-200 (*2001*).
12. *Dhumal, S.R., Biradar, V.S., Paradkar, R.A., York, P.*: Int J Pharm, *368*(1-2), 129-137 (*2009*).
13. *Patil, N.M.., Pandit, B.A.*: Ultrason Sonochem, *14*(5), 519-530 (*2007*).
14. *Dhumal, S.R., Biradar, V.S., Yamamura, S., Paradkar, R.A., York, P.*: Eur J Pharm Biopharm *70*, 109-115 (*2008*).
15. *Franco, F.L., Pérez-Maqueda, L.A., Pérez-Rodríguez, J.L.*: J Colloid Interf Sci *274*, 107-117 (*2004*).
16. *Louhi-Kultanen, M., Karjalainen, M., Rantanen, J., Huhtanen, M., Kallas, J.*: Int J Pharm *320*, 23-29 (*2006*).
17. *Sanganwar, P.G., Gupta, B.R.*: Powder Technol *196*, 36-49 (*2009*).
18. *Xia, D, Quan, P., Piao, H., Piao, H., Sun, S., Yin, Y., Cui, F.*: Eur J Pharm Sci *40*, 325-334 (*2010*).
19. *Pinjari, V.D., Pandit, B.A.*: Ultrason Sonochem *17*, 845-852 (*2010*).
20. *Abbas, A., Srour, M., Tang, P., Chiou, H., Hak-Kim Ch., Romagnoli, A.J.*: Chem Eng Sci *62*, 2445-2453 (*2007*).
21. *Manish, M., Harshal, J., Anant, P.*: Eur J Pharm Sci *25*, 41-48 (*2005*).
22. *Ambrus, R., Kocbek, P., Kristl, J., Šibanc, R., Rajkó, R., Révész, P.*: Int J Pharm *381*, 153-159 (*2009*).
23. *Ambrus, R., Amirzadi, N.N., Sipos, P., Révész, P.*: Chem Eng Technol *33*(5), 827-832 (*2010*).
24. *Farkas, B., Révész, P.*: Kistályosítástól a tablettázásig. Universitas Szeged Kiadó, Szeged 125-145 (*2007*).

[Érkezett: 2011. május 5.]

3. sz. melléklet: nyilatkozat az értekezés eredetiségéről

NYILATKOZAT SAJÁT MUNKÁRÓL

Név: Bartos Csilla

A doktori értekezés címe: Application of wet milling techniques to produce micronized and nanonized drug pre-dispersions for the development of intranasal formulations

Én, *Bartos Csilla* teljes felelősségem tudatában kijelentem, hogy a Szegedi Tudományegyetem Gyógyszertudományok Doktori Iskolában elkészített doktori (Ph.D.) disszertációm saját kutatási eredményeimre alapulnak. Kutatómunkám, eredményeim publikálása, valamint disszertációm megírása során a Magyar Tudományos Akadémia Tudományetikai Kódexében lefektetett alapelvek és ajánlások szerint jártam el.

Szeged, 2016. február 16.

_____